Curriculum Vitae

Jacob Matthew Smith
jacobmsmith1@gmail.com

Education:

B.A, Biology

St. Mary's College of Maryland

St. Mary's City, Maryland

Graduated May 2008

Experience:

Teaching Assistant; Fall 2006, Fall 2007

St. Mary's College of Maryland

Courses: Principles of Biology I, Genetics

Graduate Research Assistant: Fall 2008 – present

University of Maryland, Baltimore,

Program in Neuroscience

Awards and Honors:

SMCM Academic Achievement Award

Dean's list; Fall 2004 – Spring 2008

Beta Beta Beta Biological Honor Society; 2006 – 2008, Treasurer 2007-2008

Nu Rho Psi National Honor Society in Neuroscience; Vice President 2007-2008

Memberships:

Student training committee: 2010 - present

University of Maryland, Baltimore

Program in Neuroscience

Society for Neuroscience: 2009 - present

Publications:

Smith, J.M., Xu, J, and Powell, E.M., 2012. Age dependent forebrain structural changes in mice deficient in the autism associated gene *Met* tyrosine kinase. *Neuroimage: Clinical* 1, 66-74.

Smith, J.M. and Powell, E.M., 2012. Mice with impaired Met tyrosine kinase signaling demonstrate characteristics relevant to autism. *Autism* S1:002.

In preparation:

Smith, J.M., Plachez, C., Martins, G.J., Lassiter, C.A., and Powell, E.M. Loss of Met signaling in the *Emx1* lineage alters progenitor proliferation and cortical layer morphology. *in preparation*

Abstracts:

1. Smith, J.M., Martins, G.J., Plachez, C., Powell, E.M., "A role for HGF/SF-Met signaling in the developing cortex", International Meeting for Autism Research, Philadelphia, PA, May 2010.
2. Smith, J.M., Martins, G.J., Plachez, C., Powell, E.M., "A role for HGF/SF-Met signaling in the developing cortex, Society for Developmental Biology, Mid-Atlantic Regional Meeting, Baltimore, MA, June 2010.
3. Smith, J.M., Martins, G.J., Plachez, C., Xu, J., and Powell, E.M., "HGF-Met signaling in cerebral cortical development," *Soc. Neurosci. Abstr.*, Nov 2010.
4. Smith, J.M., Martins, G.J., Xu, J., Long, L.V., and Powell, E.M., "Structural effects of Met inactivation in the cerebral cortex," *Soc. Neurosci. Abstr.*, Nov 2011.
5. Smith, J.M., Xu, J., and Powell, E.M., "Neuroanatomical alterations in conditional Met mutant mice", *International Meeting for Autism Research*, Toronto, Canada, May 2012
6. Smith, J.M., Martins, G.J., and Powell, E.M., "Loss of Met signaling alters cerebral cortical structure and cellular composition", *Soc. Neurosci. Abstr.*, Oct. 2012.

7. Smith, J.M., and Powell, E.M., "Mice with reduced Met signaling in cortex show altered cortical lamination", *Soc. Neurosci. Absr*., Nov. 2013.

Abstract

Role of the Autism-Associated Met Tyrosine Kinase Receptor in Cerebral Cortical Development:

Jacob Smith, Doctor of Philosophy, 2014

Dissertation Directed by: Dr. Elizabeth Powell, Associate Professor, Department of Anatomy and Neurobiology

I study the role of Met, the hepatocyte growth factor receptor, in the development of the cerebral cortex using a conditional mutant mouse line. This line expresses a kinase-dead Met in the *Emx1* lineage of the cerebral cortex and hippocampus. Loss of Met signaling in the *Emx1* lineage leads to a number of anatomical changes in adult, but not juvenile mice, including increased size of the frontal cortex and corpus callosum. Expansion of the cortex in these mice appears to be due to an increase in cortical surface area, rather than thickness. Histological examination of the cortex in *Met* mutants revealed that the cortex is actually thinner at the level of the cortical barrel fields. Subsequent analysis of layer morphology showed that this decrease was mostly due to a reduction in the thickness of layer II/III, with no change in deep layer morphology. Furthermore, some cells expressing Cux1 - a marker of superficial layers - were found in ectopically deep layers in *Met* mutants, suggesting a possible mechanism for the reduction of layer II/III. These findings have prompted an examination of cortical progenitor proliferation by bromodeoxyuridine birth-dating. Results from these studies indicate that Met plays a role in regulating proliferation in cortical progenitors, and that this role may be temporally restricted.

Role of the Autism-Associated Met Tyrosine Kinase Receptor in Cerebral Cortical Development

by
Jacob Matthew Smith

Dissertation submitted to the faculty of the Graduate School of the
University of Maryland, Baltimore in partial fulfillment
of the requirements for the degree of
Doctor of Philosophy
2014

©Copyright 2014 by Jacob Matthew Smith

all rights Reserved

Acknowledgements

I would like to open by thanking my principal investigator, Dr. Elizabeth Powell, for her help with the design and execution of the experiments discussed here, for her help and advice with preparing several manuscripts for publication, and for serving as my mentor throughout my time here at the University of Maryland. I would also like to thank my other committee members, Doctors Mooney, Erzurumlu, Gullapalli, and Torii, for their helpful advice and comments throughout this process. I would like to thank Dr. Mooney and Dr. Erzurumlu in particular for agreeing to serve as my readers. I would like to thank our collaborators at the small animal MRI core facility, in particular Su Xu, for their help with the imaging studies. Lastly, I would be remiss if I did not mention a number of lab members, both current and former, who have helped with this work, including Gabriela Martins, Celine Plachez, Jennifer Xu, and Rolicia Martin.

Table of Contents

- Chapter 1: Introduction 1
  - 1.1 Genetic association of Autism with the Met signaling pathway 3
  - 1.2 Mouse models with disruptions in the HGF-Met signaling pathway: 6
    - 1.2.1 Anatomical consequences of altered Met signaling 6
  - 1.2.2 Behavioral consequences of altered HGF - Met signaling..... 11
  - 1.3 Summary 14
- Chapter 2: Age dependent forebrain structural changes in mice deficient in the autism associated gene *Met* tyrosine kinase..... 16
  - 2.1 Introduction 16
  - 2.2 Material and Methods..... 19
    - 2.2.1 Animals..... 19
    - 2.2.2 MRI Imaging 19
    - 2.2.3 Area and volume estimation 19
    - 2.2.4 Black-gold staining:..... 22
    - 2.2.5 Data analysis..... 23
  - 2.3 Results 23
    - 2.3.1 Alterations in gray-matter structures in adult, but not juvenile, Met-Emx1 mice 23
    - 2.3.2 Whole brain 24
    - 2.3.3 Cerebral cortex 27
    - 2.3.4 Hippocampus 32
    - 2.3.5 Striatum - 35
    - 2.3.6 Thalamus 38
    - 2.3.7 Altered white matter morphology in adult, but not juvenile, Met-Emx1 mice 40
  - 2.4 Discussion 45
- Chapter 3: Altered cortical lamination in mice deficient in Met tyrosine kinase . 50
  - 3.1 Introduction 50
  - 3.2 Material and Methods..... 53
    - 3.2.1 Animals..... 53

- 3.2.2 Immunohistochemistry and histology 53
- 3.2.3 Cell counts and analysis 53
- 3.3 Results 54
- 3.3.1 Abnormal lamination in Met mutants 54
- 3.4 Discussion 69
- Chapter 4: Loss of Met signaling alters cell proliferation in the embryonic cerebral cortex. 72
- 4.1 Introduction 72
- 4. 2 Methods 73
- 4.2.1 Animals 73
- 4.2.2 BrdU injections 73
- 4.2.3 Immunohistochemistry and histology 74
- 4.2.4 Cell counts and analysis 74
- 4.3 Results 77
- 4.3.1 BrdU incorporation: Somatosensory cortex 78
- 4.3.2. BrdU incorporation: Prelimbic cortex 93
- 4.3.3 BrdU co-labeling 101
- 4.4 Discussion 103
- Chapter 5- Altered social behavior in mice deficient in Met tyrosine kinase 107
- 5.1 Introduction: 107
- 5.2 Methods: 109
- 5.2.1. Animals and order of tests 109
- 5.2.2 Open field 110
- 5.2.3 Light-dark preference 110
- 5.2.4 Three-chamber social interaction 110
- 5.3 Results 111
- 5.3.1 Open field 111
- 5.3.2 Light-dark preference 114
- 5.3.3 Three-chamber social interaction 116
- 5.4 Discussion 118

- Chapter 6: Conclusions and Significance 121
  - 6.1 Met association with ASD..... 121
  - 6.2 Structural alterations: grey matter 122
  - 6.3 Structural alterations: white matter 122
  - 6.4 Cell number and proliferation 124
  - 6.5 Summary 126
  - 6.6 Future work 127
- Appendix 1: Common Methods..... 130
  - A.1 Animals..... 130
  - A.2 Histology and Immunohistochemistry:..... 130

List of figures

Figure 1.1. Schematic diagram showing Met protein and downstream targets. 2
Figure 2.1 Schematics representing the areas included in measurements. 21
Figure 2.2. Loss of Met function alters whole-brain cross-sectional area. 26
Figure 2.3. Structural differences in the cerebral cortex of *Met-Emx1* mice are age specific. 28
Figure 2.4. Expansion of the brain in *Met-Emx1* mice. 31
Figure 2.5. Loss of Met function alters hippocampal area in adult mice..... 33
Figure 2.6. Loss of Met signaling alters hippocampal area in adult mice. 34
Figure 2.7. The striatum of adult *Met-Emx1* mice is larger than the striatum of control mice. 37
Figure 2.8. Loss of Met function alters thalamic area in adult mice. 39
Figure 2.9. The corpus callosum is expanded at rostral levels in adult *Met-Emx1* mice.. 41
Figure 2.10. The corpus callosum is expanded at rostral levels in adult Met-Emx1 mice. 42
Figure 2.11. Loss of Met signaling alters corticostriatal fascicles. 44
Figure 3.1. Reduced cortical thickness in *Met-Emx1* mice. 55
Figure 3.2 Cell size is unaltered in *Met-Emx1* mice. 57
Figure 3.3 Altered dendritic morphology in *Met-Emx1* mice. 58
Figure 3.4 Schematic of layer marker staining in control and *Met-Emx1* mice. 60
Figure 3.5. Superficial layer neurons distribute abnormally in *Met-Emx1* mice. 63
Figure 3.6. Loss of Met signaling does not alter the distribution of $Cux1^{+}$ cells in OFC. 64
Figure 3.7. Loss of Met signaling does not impact deep layers in frontal cortex. 65
Figure 3.8. The distribution of callosal projection neurons is altered in *Met-Emx1* mice. 68
Figure 4.1. Sampling levels for BrdU counts 76
Figure 4.2. Unaltered BrdU labeling at the level of plate 5 in somatosensory cortex of *Met-Emx1* mice after BrdU injections at E12.5. 80
Figure 4.3. Increased BrdU cell density at the level of plate 6 in somatosensory cortex of *Met-Emx1* mice after injections at E12.5. 81
Figure 4.4. Increased BrdU cell density at the level of plate 7 in the somatosensory cortex of *Met-Emx1* mice after injections at E12.5..... 82
Figure 4.5. Altered BrdU labeling at the level of plate 5 in the somatosensory cortex of *Met-Emx1* mice after BrdU injections at E14.5. 84
Figure 4.6. Reduced BrdU cell density at the level of plate 6 in the somatosensory cortex of *Met-Emx1* mice after BrdU injections at E14.5. 86
Figure 4.7. Reduced BrdU cell density at the level of plate 7 in the somatosensory cortex of *Met-Emx1* mice after BrdU injections at E14.5..... 87
Figure 4.8. Reduced BrdU cell density at the level of plate 5 in the somatosensory cortex of *Met-Emx1* mice after BrdU injections at E16.5. 89

Figure 4.9. Reduced BrdU cell density at the level of plate 6 in the somatosensory cortex of *Met-Emx1* mice after BrdU injections at E16.5. 91
Figure 4.10. Reduced BrdU cell density at the level of plate 7 in the somatosensory cortex of *Met-Emx1* mice after BrdU injections at E16.5. 92
Figure 4.11. Altered BrdU labeling in prelimbic cortex of *Met-Emx1* mice after BrdU injections at E12.5. 94
Figure 4.12. Altered BrdU labeling in prelimbic cortex of *Met-Emx1* mice after BrdU injections at E14.5. 96
Figure 4.13. Altered BrdU labeling in prelimbic cortex of *Met-Emx1* mice after BrdU injections at E16.5. 97
Figure 4.14. Estimated number of BrdU cells per radial strip counted for each injection time and region. 99
Figure 4.15. Cortical thickness is unaltered at P0. 100
Figure 4.16. Ectopic Cux1^{+} cells are laregly not labeled by E12.5 BrdU injections. 102
Figure 5.1. Normal motor behavior and altered anxiety-like behavior in *Met* mutants in the open field. 113
Figure 5.2.Altered anxiety behavior in the light-dark exploration test in *Met* mutant mice. 115
Figure 5.3. Social behavior in mice with reduced Met signaling. 117

List of abbreviations

ADI-R	Autism Diagnostic Interview, Revised
ADOS	Autism Diagnostic Observation Schedule
ANOVA	analysis of variance
ASD	Autism Spectrum Disorder
bp	base pairs
CA1	Cornu Ammonis 1
CA3	Cornu Ammonis 3
CC	corpus callosum
CR	calretinin
ctx	cerebral cortex
Dlx5/6	Distal-less homeobox 5/6
EEG	Electroencephalogram
Emx1	Empty spiracles homeobox 1
EN2	Engrailed 2
EPSC	excitatory postsynaptic potential
GABA	Gamma aminobutyric acid

Gad67	Glutamic acid decarboxylase 67
GE	Ganglionic eminence
HGF	Hepatocyte growth factor
H, hipp	hippocampus
HOXA1	Homeobox A1
K-S	Komolgorov-Smirnoff
mm	millimeter
MRI	Magnetic resonance imaging
MSN	medium spiny neuron
NF1	Neurofibromin 1
NrCAM	Neuronal cell adhesion molecule
OFC	Orbital frontal cortex
P(#)	Postnatal day #
PCR	polymerase chain reaction
PV	Parvalbumin
PI3K	Phosphoinositol 3 kinase
PL	Prelimbic cortex

PLCγ	Phospholipase C gamma
RARE	rapid acquisition relaxation enhancement
RAS	Rat sarcoma
S1	Primary somatosensory cortex
SEM	standard error of the mean
Six3	Sine oculis-related homeobox 3
SNP	Single nucleotide polymorphism
SRS	Social Responsiveness Scale
SST	somatostatin
str	striatum
th, thal	thalamus
tPA	Tissue-type plasminogen activator
uPA	urokinase plasminogen activator
uPAR/*PLAUR*	urokinase plasminogen activator receptor protein/gene
WT	wild type

Chapter 1: Introduction

Met/MET is a tyrosine kinase receptor which binds the high-affinity ligand hepatocyte growth factor (HGF) (Naldini et al., 1991). Both Met and HGF are initially produced as single-chain pro-proteins, which are subsequently processed into their mature forms by proteolytic cleavage (Trusolino and Comoglio, 2002). In the case of HGF, this is accomplished by enzymes such as matriptase (Lee et al., 2000), HGF activator (Shimomura et al., 1995), tissue-type plasminogen activator (tPA, gene: *Plat*)(Mars et al., 1993) or urokinase-type plasminogen activator (uPA, gene: *Plau*) (Naldini et al., 1992). The proteolytic activity of uPA is increased upon binding to its receptor (uPAR, gene:*Plaur*) (Ellis et al., 1991). Upon binding to HGF, Met auto-phosphorylates creating a multi-substrate docking site for a number of adaptor proteins (Fig. 1.1) (Ponzetto et al., 1994). Downstream targets of HGF-Met signaling include PI3K, RAS, and PLCγ (Ponzetto et al., 1994). Potentially owing to this diverse array of downstream targets, Met signaling has been implicated in cellular processes as varied as proliferation, migration, survival, the formation of neuronal processes (Defrances et al., 1992; Hamanoue et al., 1996a; Maina et al., 1997; Maina and Klein, 1999; Seeds et al., 1999; Caton et al., 2000; Powell et al., 2001b; Powell et al., 2003a; Gutierrez et al., 2004; Niimura et al., 2006; Martins et al., 2011).

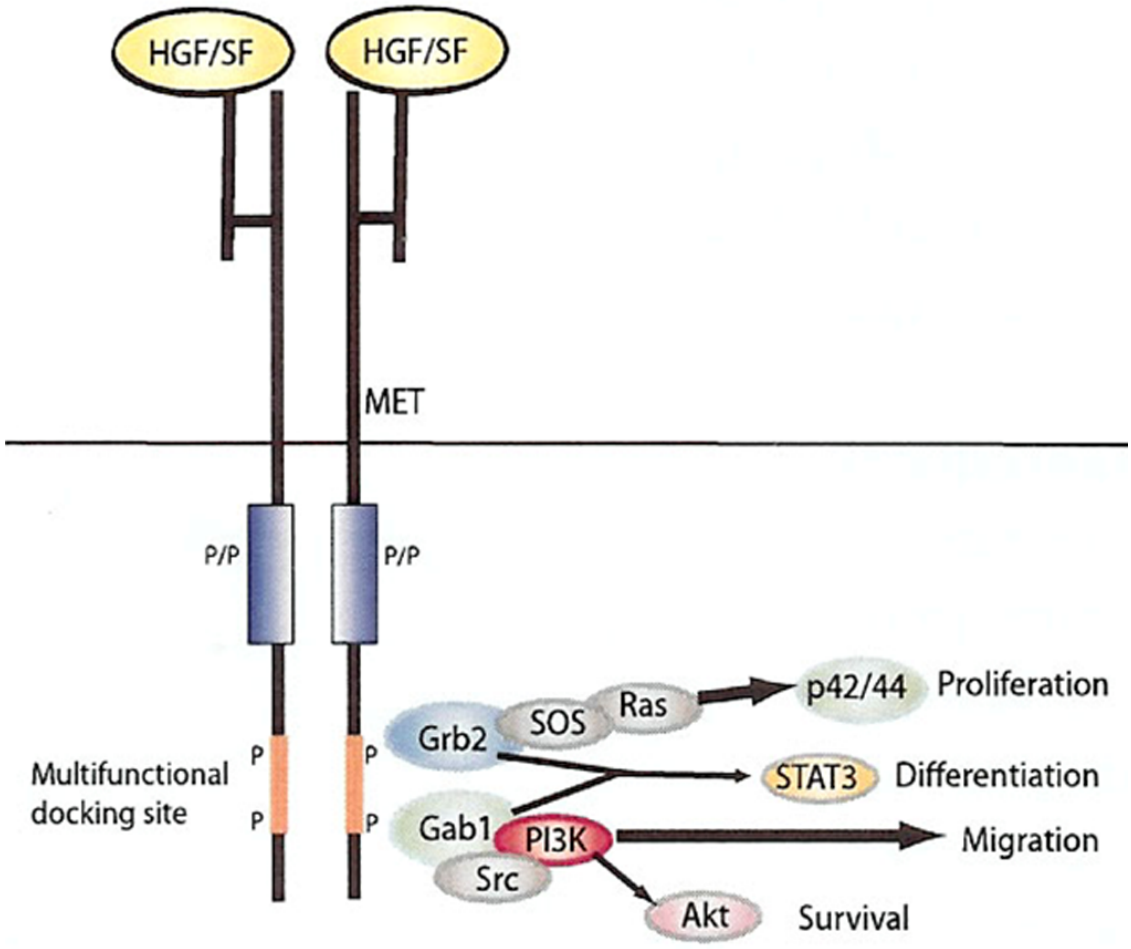

Figure 1.1. Schematic diagram showing Met protein and downstream targets.

The blue rectangles (P/P) represent the protein kinase domains, while the smaller pink shaded regions show the phosphorylated multifunctional docking site. In Met-Emx1 mice, exon 16, in the kinase domain, is flanked by loxP sites. Cre recombination removes exon 16, which contains an ATP binding site crucial for kinase function.

Both Met and HGF are expressed in the developing brain in rodents (Jung et al., 1994; Honda et al., 1995; Achim et al., 1997; Powell et al., 2001b; Martins et al., 2007; Judson et al., 2009a; Bae et al., 2010; Martins et al., 2011) as well as primates (Yamada et al., 1997; Judson et al., 2011). In mice, HGF and Met expression are detectable as early as E11.5. Expression of both HGF and Met is found in the cortical ventricular zone, and later in the cortical plate (Powell et al., 2001b). HGF is also expressed in the proliferative zone of the ganglionic eminence (Powell et al., 2001b). Met expression remains high from late embryonic through early postnatal development in the mouse (Powell et al., 2003c; Judson et al., 2009a; Bae et al., 2010) and at the corresponding ages in primate (Judson et al., 2011). At late embryonic and early postnatal stages, *Met* transcript is also found in the amygdala, septum, and hippocampus (Judson et al., 2009a). Expression of both HGF and Met persists in the adult brain, albeit at reduced levels (Iyer et al., 1990; Jung et al., 1994; Honda et al., 1995; Achim et al., 1997; Judson et al., 2009a; Martins et al., 2011). HGF-Met signaling may therefore participate in multiple phases of neurodevelopment. Furthermore, HGF and Met expression are found in multiple areas thought to be affected in autism spectrum disorders (ASD).

1.1 Genetic association of Autism with the Met signaling pathway

ASD is characterized by language and communication deficits as well as restricted interests and repetitive or stereotyped behaviors. Multiple neuroanatomical abnormalities have been observed in the brains of autistic patients (Bauman and Kemper, 1985;

Bauman, 1991; Sears et al., 1999b; Carper et al., 2002; Tsatsanis et al., 2003b; Schumann et al., 2004a; Amaral et al., 2008a). Genetics are thought to play a role in the etiology of ASDs, as they are highly heritable (Folstein and Rutter, 1977; Bailey et al., 1995; Comi et al., 1999; Folstein and Rosen-Sheidley, 2001b; Connors et al., 2005; Abrahams and Geschwind, 2008), although environmental influences could also play important roles (Connors et al., 2005; Croen et al., 2011). A number of genetic syndromes include autistic-like features or are associated with an increased risk of ASD, including Prader-Willi (Veltman et al., 2005; Hogart et al., 2010), Fragile X (Brown et al., 1982; Bailey et al., 1998), and Rett syndromes (Mount et al., 2003), as well as tuberous sclerosis (Lewis et al., 2012a). While multiple genomic regions have been linked with autism risk, a particularly strong candidate is a region on chromosome 7q (IMGSAC, 1998), which contains putative autism susceptibility genes such as *EN2*, *HOXA1*, *WNT2*, and *NrCAM* (Petit et al., 1995; Ingram et al., 2000; Wassink et al., 2001; Hutcheson et al., 2004; Benayed et al., 2005; Persico and Bourgeron, 2006). Chromosome 7q also contains the *MET* gene, located at 7q31 (Dean et al., 1985), as well as *HGF*, located at 7q21.1 (Fukuyama et al., 1991). Several *MET* variants have been shown to increase risk for ASDs (Campbell et al., 2006; Campbell et al., 2008; Campbell et al., 2009; Sousa et al., 2009b; Thanseem et al., 2010a; Zhou et al., 2011). One single nucleotide polymorphism (SNP) in particular, rs1858830, has been found to be associated with the co-occurrence of autism with gastrointestinal conditions (Campbell et al., 2009). Another gene involved in HGF signaling, *PLAUR* (which encodes uPAR, and is found on chromosome 19q13) (Borglum et al., 1992), has also been associated with autism. The T allele of the *PLAUR* promoter variant rs344781 is associated with a 1.93 relative risk for ASD (Campbell et

al., 2008). While some studies examining *MET* association with autism have failed to replicate the association of individual SNPs (Sousa et al., 2009b), evidence for the association of the gene as a whole is strong, especially when combined with the association of related genes.

In addition to genetic association, a number of *MET* variants have been shown to be functionally significant. The C allele of rs1858830 has been shown to reduce *MET* promoter activity (Campbell et al., 2006). MET protein levels are also reduced post-mortem in temporal cortex from patients with autism compared to typically developing patients (Campbell et al., 2007a). A few *MET* variants have even been shown to have functional consequences at the level of behavior. The C allele of rs1858830 is also associated with social and communication scores on the ADI-R, ADOS, and SRS tests (Campbell et al., 2010). A more recent functional study showed that individuals homozygous for the C allele of rs1858830 have increased activity in the default mode network (DMN) when viewing emotional face stimuli, compared with those homozygous for the non-risk G allele, as well as reduced connectivity between the posterior cingulate cortex (PCC) and medial prefrontal cortex (MPFC) (Rudie et al., 2012). Furthermore, the effect of the C allele was more pronounced in individuals with a diagnosis of autism spectrum disorder. In individuals with ASD, a single copy of the risk allele was sufficient to reduce activity in response to face stimuli, while in typically developing subjects only those with two copies of the C allele showed significantly reduced activity (Rudie et al., 2012). The C allele of rs2237717 and the G allele of rs42336 have also been associated with altered facial emotion perception (Lin et al., 2012), which is altered in ASD. Altered

Met signaling has also been shown to affect brain structure, particularly white matter. The rs1858830 C allele has been associated with decreased fractional anisotropy in white matter tracts of the temporal, parietal and occipital lobes, and has a greater effect in individuals with ASD (Rudie et al., 2012).

Given the repeated association of *MET* with autism, and the potential association of other genes in the pathway, it is highly likely that dysregulation of HGF-MET signaling could contribute to the pathology of ASD, in at least a subset of affected individuals. That some effects of reduced Met signaling appear stronger in individuals with ASD as compared to typically developing populations could be due to interactions of the Met pathway with other risk alleles, which would be more common in those with ASD. While such interactions could play important roles in the etiology of ASD, they could also cloud the role played by Met itself. To examine the role of the Met pathway in the absence of alterations in other risk genes, it is necessary to examine animal models, where Met and other related genes can be manipulated in an otherwise genetically homogenous population.

1.2 Mouse models with disruptions in the HGF-Met signaling pathway:

1.2.1 Anatomical consequences of altered Met signaling

While *MET* is well validated as a risk gene for autism (Campbell et al., 2006; Campbell et al., 2007b; Campbell et al., 2008; Sousa et al., 2009a; Lin et al., 2012), only a few

studies have examined the effects of loss of Met function in animals. This is likely due at least in part to the embryonic lethality of constitutive knockouts. Met function appears to be required for proper placental (Uehara et al., 1995) and liver development (Schmidt et al., 1995), and therefore global *Met* knockout mice die early during gestation. In order to avoid this, groups have used Cre-*loxP* recombination strategies to inactivate Met specifically in cells expressing Cre recombinase (Huh et al., 2004; Martins et al., 2007; Judson et al., 2009b; Martins and Powell, 2011). Mice in which exon 16 has been flanked by loxP sites allow the inactivation of Met in cells expressing Cre recombinase, as exon 16 contains a critical ATP binding site within the intracellular tyrosine kinase domain (Huh et al., 2004).

The *Dlx5/6-Cre* driver inactivates Met (*Met-Dlx5/6* mice) in post-mitotic GABAergic neurons originating in the ganglionic eminence (GE). GABAergic neurons from the GE become the inhibitory interneurons of the cerebral cortex, hippocampus, amygdala, and striatum, as well as the medium spiny neurons of the striatum (Marin and Rubenstein, 2003). The *Met-Dlx5/6* mice show increased numbers of parvalbumin (PV) and somatostatin (SST) positive interneurons in the striatum, as well as a reduction in PV interneuron numbers in the sensorimotor and orbitofrontal cortex, but not in visual cortex (Martins et al, 2011). Furthermore, at more caudal levels of the striatum, a greater percentage of the population of PV positive interneurons was found in medial (associative), and fewer in lateral (sensorimotor) regions of the striatum than in control mice. Loss of Met function in embryonic interneurons therefore seems to affect the

migration of GABAergic interneurons both within the striatum and between the embryonic striatum and cortex.

Hippocampal interneurons are also generated from the ganglionic eminence, and appear to be affected by loss of Met signaling. Fewer PV and calretinin (CR) positive interneurons were found in the CA3 region of the hippocampus in *Met-Dlx5/6* mice than in controls. Mice in which Met was inactivated in the proliferative zones of the ganglionic eminence using a *Six3-Cre* driver (*Met-Six3* mice) showed a similar loss of PV and CR cells in CA3, but further showed a loss of CR interneurons throughout the hippocampus, and an increase in PV interneurons in the dentate gyrus (Martins et al 2007). Alterations in the number of interneurons in the hippocampus of *Met-Dlx5/6* mice are likely due to a migration defect similar to that seen for cortical and striatal interneurons in these animals. Deficits in the *Met-Six3* mice could also be due to changes in the specification of different subtypes of interneuron. It is unlikely that the deficit in *Met-Six3* mice is due to decreased proliferation of interneurons, as a similar pattern of GABA staining found in the hippocampus (Martins et al., 2007).

In order to examine the functions of Met in the developing cortex, a similar system has been employed using Cre recombinase expressed under the control of the *Emx1* promoter to inactivate Met in excitatory neurons and glia of the cerebral cortex and hippocampus. Notably, this system does not directly ablate Met function in cortical GABAergic interneurons, which originate in the ganglionic eminence (Gorski et al., 2002a). Judson et

al. (Judson et al., 2009b) found that pyramidal neurons in layers II and III of the anterior cingulate cortex of *Met-Emx1* mice showed significant alterations in dendritic arbor. *Met-Emx1* neurons showed reduced apical dendritic arbor length distal to the cell body, and increased basal dendritic arbor length proximal to the cell body. These differences appear to be primarily due to changes in branching complexity. Since the distal apical dendritic arbor of pyramidal neurons receives distinct synaptic inputs from the basal and proximal apical arbor (Spruston, 2008), this could result in changes in synaptic connectivity. No difference was found in the number of dendritic spines between *Met-Emx1* and control mice, but an increase in the volume of spine heads was observed (Judson et al., 2010b). Interestingly, striatal medium spiny neurons (MSNs), were also found to show increases in both dendritic arbor length and spine head volume. Alterations in MSNs would suggest that loss of Met signaling in cortical pyramidal neurons may have effects on cells targeted by cortical efferents, as striatal MSNs are not targeted by the *Emx1-Cre* driver (Gorski et al., 2002a). As spine structure is closely related to function, and spines are the main target of glutamatergic synapses, alterations in spine head volume could produce changes in excitatory neurotransmission (Kasai et al., 2003). Indeed, alterations in excitatory neurotransmission have been shown in the cortex of *Met-Emx1* mice. In the anterior cingulate cortex of *Met-Emx1* mice, stimulation of layer II/III pyramidal neurons produced stronger excitatory post-synaptic potentials (EPSCs) in layer Vb corticostriatal projection neurons (Qiu et al., 2011a). While changes in EPSC amplitude in this population could be due to either presynaptic or postsynaptic alterations, no difference was found in paired pulse ratios between *Met-Emx1* mice and controls, suggesting that at least some presynaptic parameters (i.e. release probability) are unaltered by loss of Met

signaling. In contrast, no changes in EPSCs were found in corticopontine projection neurons after stimulation in layer II/III (Qiu et al., 2011a), further suggesting that the increased connection strength in corticostriatal neurons is likely due to post-synaptic mechanisms.

Alterations in cortical connectivity in *Met-Emx1* mice reflect some changes seen in ASD. Altered cortical connectivity is thought to play a role in the etiology of ASD (Courchesne and Pierce, 2005), including local hyperconnectivity (as demonstrated in *Met-Emx1* mice) as well as long-range hypoconnectivity. That hyperconnectivity in the *Met-Emx1* mice appears specific to corticostriatal projection neurons is significant, as both corticostriatal structural (Langen et al., 2012) and functional connectivity (Turner et al., 2006; Di Martino et al., 2011) have been shown to be altered in ASD. Furthermore, there is some evidence of an association between changes in striatal functional connectivity and repetitive behavior in children with ASD (Di Martino et al., 2011).

Unlike *Met*$^{-/-}$ or *Hgf*$^{-/-}$ mice which die before embryonic day 12 (Bladt et al., 1995; Schmidt et al., 1995), *Plaur*$^{-/-}$ mice live to adulthood (Dewerchin et al., 1996). These mice exhibit reduced HGF levels (Powell et al., 2001a; Bae et al., 2010), suggesting reduced HGF-Met signaling, and possible alterations to HGF mediated developmental processes. HGF has been reported to facilitate forebrain GABAergic interneuron migration (Powell et al., 2001a; Levitt et al., 2004). Several studies have found decreased numbers of GABAergic interneurons in the brains of *Plaur*$^{-/-}$ mice (Powell et al., 2003c;

Eagleson et al., 2005; Bae et al., 2010; Bissonette et al., 2010). Fewer GABA positive cells were found in the cingulate and parietal cortex of *Plaur*$^{-/-}$ mice than in WT mice (Powell et al., 2003). In a parallel study, Gad67^{+} cells were found to be decreased in the parietal cortex, as well as in the dentate gyrus and the CA1 region of the hippocampus (Eagleson et al., 2005). No change in either GABA or Gad67 staining was observed in occipital cortex (Powell et al., 2003c; Eagleson et al., 2005). Among GABAergic interneurons, PV expressing cells seem to be preferentially affected in *Plaur*$^{-/-}$ mice. Decreases in PV^{+} interneurons have been noted in the frontal areas, including the anterior cingulate (Powell et al., 2003c) and orbital frontal cortex (OFC) (Bissonette et al., 2010), and parietal cortex, in particular in somatosensory areas (Powell et al., 2003c; Eagleson et al., 2005; Bae et al., 2010), as well as in the striatum (Bissonette et al., 2010). In the hippocampus, however, the PV^{+} population is unaffected, and there is a reduction in somatostatin^{+} (SST^{+}) cells in the dentate gyrus and CA1(Eagleson et al., 2005). In the cases of the somatosensory and orbital frontal cortical regions and the striatum, overexpression of HGF in astrocytes restored the numbers of PV^{+} interneurons (Bae et al., 2010; Bissonette et al., 2010), suggesting that the decrease in HGF levels seen in *Plaur*$^{-/-}$ mice is responsible for the observed interneuron deficits.

1.2.2 Behavioral consequences of altered HGF - Met signaling

While cellular and physiological changes in mice with altered HGF-Met signaling are informative, they would not make for convincing animal models without accompanying behavioral alterations reflective of ASD symptoms. While not all of the mouse lines which have been examined have been extensively characterized, several show behavioral

phenotypes which suggest that altered HGF signaling could contribute to autistic-like behavior.

Plaur$^{-/-}$ mice show a number of behavioral alterations when compared to wild type (WT) littermates. Among these, *Plaur*$^{-/-}$ mice have been shown to display increased anxiety-like behaviors in the light-dark avoidance test and the elevated plus maze (Powell et al., 2003c; Bae et al., 2010). In addition to increased anxiety, *Plaur*$^{-/-}$ mice have impaired cognitive flexibility as measured by reversal learning a process which has been shown to be dependent on the OFC (Bissonette et al., 2008; Bissonette et al., 2010; Bissonette and Powell, 2012). *Plaur*$^{-/-}$ and WT animals both learn the rules similarly, but once the rules are reversed, the *Plaur*$^{-/-}$ mice require more trials to master the task (Bissonette et al., 2010). The *Plaur*$^{-/-}$ mice exhibit abnormal electroencephalogram (EEG) activity and have spontaneous seizures, as well as an increased sensitivity to chemically induced seizures (Powell et al., 2003c). HGF supplementation rescues the seizures and anxiety behaviors seen in *Plaur*$^{-/-}$ mice (Bae et al., 2010). Our recent findings indicate impaired social interactions and attentional processing in *Plaur*$^{-/-}$ mice (Bissonette et al., 2014) and current studies are focused on assessing communication responses in the WT and *Plaur*$^{-/-}$ groups.

Met-Dlx5/6 mice show no alterations in locomotor activity in the open field or in tests of anxiety-like behavior such as light-dark avoidance or the elevated plus maze (Martins and Powell, 2011). *Met-Dlx5/6* mice were also tested in the Morris water maze, which can be

used to test both spatial learning (mediated by the hippocampus) and procedural learning (mediated by the striatum) (Devan et al., 1996; Packard and Teather, 1997). In the water maze, *Met-Dlx5/6* mice performed similarly to controls during a probe test, as well as during a reversal probe test where the hidden platform was moved to the opposite quadrant from where it was during training. Both tests are used to measure hippocampal-dependent spatial learning (Devan et al., 1996; Vorhees and Williams, 2006). However, in a cued platform task, which is dependent on striatal function (Devan et al., 1996; Vorhees and Williams, 2006), *Met-Dlx5/6* mice were slower to reach the platform than control mice. This suggests that despite abnormalities in the population of interneurons in both the hippocampus and striatum of *Met-Dlx5/6* mice, hippocampal function remains relatively normal, while striatal function, mainly habit learning, is disrupted.

Reversal learning was also affected in *Met-Dlx5/6* mice (Martins and Powell, 2011), similarly to *Plaur*$^{-/-}$ mice. *Met-Dlx5/6* mice performed similarly to controls in learning the initial discrimination task, but required significantly longer to reach criterion during the reversal portion (Martins et al, 2011). That the mice acquire the initial discrimination normally suggests that they have no problem learning the task or discriminating between the cues, while their deficit in the reversal portion of the task suggests a lack of behavioral flexibility or a problem inhibiting the previously rewarded response. A similar loss of behavioral flexibility may be involved in the restricted or repetitive behavior which is frequently observed in autistic children (Turner, 1999).

1.3 Summary

Mice with altered HGF-Met signaling show alterations in the interneuron populations of the frontal cortex, striatum, and hippocampus. While spatial learning (dependent on the hippocampus) appears normal in *Met-Dlx5/6* and *Plaur*$^{-/-}$ *mice*, *Met-Dlx5/6* mice show deficits in procedural learning, and both strains are impaired on a reversal learning task. In *Plaur*$^{-/-}$ mice, restoration of normal HGF levels via genetic intervention restores both interneuron numbers and normal behavior. Repetitive behaviors are frequently observed in ASD (Turner, 1999), and have been associated with diminished inhibitory control of prior responses (Mosconi et al., 2009), which depends on frontal-striatal circuits (Kelly et al., 2004; Rubia et al., 2007). Inhibition of previously-rewarded responses is a critical component of reversal learning, and this may be inhibited in *Met-Dlx5/6* and *Plaur*$^{-/-}$ mice (Bissonette et al., 2010; Martins et al., 2011).

It would therefore appear as though the loss of GABAergic (and in particular PV^{+}) interneurons in the frontal cortex and striatum could contribute to the behavioral alterations observed in *Plaur*$^{-/-}$ mice, and possibly in *Met-Dlx5/6* mice as well. For example, the OFC has been shown to be required for normal reversal learning (Bissonette et al, 2008), and both *Plaur*$^{-/-}$ and *Met-Dlx5/6* mice show both reduced numbers of PV^{+} interneurons in the OFC and impaired reversal learning. Furthermore, supplementation of HGF levels in *Plaur*$^{-/-}$ mice restores both PV cell number and reversal learning to normal

(Bissonette et al., 2010). While other causes cannot be ruled out, it would appear that the changes in interneuron numbers in the striatum and frontal cortex could lead to the behavioral changes seen in *Plaur*$^{-/-}$ and *Met-Dlx5/6* mice by altering cortical and striatal signaling. While cortico-striatal signaling has been shown to be altered in *Met-Emx1 mice (Qiu et al., 2011b),* further studies are needed to elucidate the effects of loss of Met signaling in excitatory neurons on behavior.

Chapter 2: Age dependent forebrain structural changes in mice deficient in the autism associated gene *Met* tyrosine kinase

2.1 Introduction

Autism spectrum disorder (ASD) is characterized by communication and social interaction impairments, as well as repetitive behaviors and narrow interests (APA, 2000). Autisms are highly heritable (Folstein and Rosen-Sheidley, 2001a). Many single gene mutations, such as those underlying Fragile X (*FMR1*), Rett (*MECP2*) and tuberous sclerosis (*TSC1* and *TSC2*), lead to autistic behaviors in a significant fraction of patients (Smalley et al., 1992; Bailey et al., 2001; Gutknecht, 2001; Percy, 2011; Lewis et al., 2012b). While no single gene has been identified for idiopathic autism, multiple susceptibility factors are being identified (Anney et al., 2012; Griswold et al., 2012). ASDs show considerable variability in both symptoms and pathology, and it is possible that different genetic or environmental insults may underlie some of this variation (Abrahams and Geschwind, 2010; Stoltenberg et al., 2010; Hallmayer et al., 2011; Tassone et al., 2011; Williams and Casanova, 2011).

Studies have shown alterations in brain size in ASD (Redcay and Courchesne, 2005; Amaral et al., 2008b; Stigler et al., 2011). Regions such as the frontal and temporal cortex (Carper et al., 2002; Hazlett et al., 2006a), hippocampus (Schumann et al., 2004b), and caudate (Sears et al., 1999a; Hollander et al., 2005) have been shown to be expanded in autism, while the thalamus is reduced (Tsatsanis et al., 2003a). Several studies have also

found increases in white matter volume in autistic patients, particularly in radiate white matter (Herbert et al., 2003; Herbert et al., 2004; Freitag et al., 2009). Notably, the alterations in brain size in ASD appear to be age-dependent, with increases in brain size being reported more consistently in very young patients, leveling off during childhood and adolescence, and possible increased volume in some brain structures into adulthood (Piven et al., 1995a; Aylward et al., 2002; Carper et al., 2002; Redcay and Courchesne, 2005; Amaral et al., 2008b; Courchesne et al., 2011; Hazlett et al., 2011a; Duerden et al., 2012).

Met (also known as c-Met) is a receptor tyrosine kinase which binds the high-affinity ligand hepatocyte growth factor (HGF) (Naldini et al., 1991). Recently, decreased Met function has been found to increase the risk of developing autism spectrum disorders (Campbell et al., 2006; Sousa et al., 2009a; Thanseem et al., 2010b). Met is crucial during normal development (Birchmeier and Gherardi, 1998), and mediates cell survival, migration, proliferation, and the formation of neuronal processes (Maina et al., 1997; Powell et al., 2001a; Powell et al., 2003a; Gutierrez et al., 2004). Importantly, both Met and its ligand, HGF, are expressed in the brain during development (Honda et al., 1995; Achim et al., 1997; Powell et al., 2001a; Martins et al., 2007; Judson et al., 2009b; Bae et al., 2010; Martins and Powell, 2011). *Met* transcript expression is prominent in the cerebral cortex, hippocampus, and amygdala, while Met protein can also be detected in white matter tracts such as the corpus callosum (Judson et al., 2009b). Changes in Met signaling during development could therefore affect neuronal number as well as the complexity of the neuropil (Powell et al., 2003a; Martins et al., 2007; Bae et al., 2010;

Martins and Powell, 2011). Indeed, inactivation of Met in the cerebral cortex has been shown to alter the strength of local excitatory connections between layers II/III and V (Qiu et al., 2011a). Changes in Met function during development may therefore alter the structure or connectivity of cortical and subcortical structures, and ultimately impact their function.

Despite progress in the understanding of the neurobiology of autism, and the role Met plays in neurodevelopment, it remains unclear how disruption of HGF-Met signaling could contribute to defects like those seen in ASD. Anatomical studies in humans likely reflect the effects of multiple different changes at the genetic level, as reflected in the considerable heterogeneity observed between studies. Furthermore, human studies have generally not attempted to correlate changes in brain structure to specific genetic variations. To this end, I have utilized a mouse line in which Met is inactivated specifically in the cerebral cortex and hippocampus using a Cre-*loxP* recombination strategy. This allows us to examine the effects of loss of Met function on a constant genetic background. Unlike global *Met* null mutants (Bladt et al., 1995), *Met-Emx1* mice live to adulthood (Judson et al., 2009b), allowing us to examine brain structure during the postnatal and adult periods. Here I report long-term specific structural changes after altering Met signaling in the embryonic mouse dorsal telencephalon.

2.2 Material and Methods

2.2.1 Animals

Animal care procedures are discussed in Appendix 1: Common methods

2.2.2 MRI Imaging

At postnatal day 30 (P30) or after P90 (adult), mice were transcardially perfused with 0.9% saline followed by 4% buffered paraformaldehyde. The fixed brains were subsequently scanned via magnetic resonance imaging (MRI). All experiments were performed on a Bruker Biospec 7.0 Tesla 30 cm horizontal bore scanner equipped with a 12 cm inner diameter gradient and a gradient strength of 400 mT/m using Paravision 5.0 software. A Bruker ^{1}H surface coil array was used as the receiver and a Bruker 72 mm linear-volume coil as the transmitter. Three-dimensional (3D) T2-weighted images were acquired using a rapid acquisition with relaxation enhancement (RARE) sequence (TEeff/TR = 60/1500 ms, rare factor 16 , number of averages 3) with a field of view of 25.6 x 25.6 x 18 mm^3 for a 100 μm^3 spatial resolution. The total acquisition time for each sample was approximately 3 hours and 36 minutes.

2.2.3 Area and volume estimation

Post-imaging analysis for volume and area was performed using NIH ImageJ software (version 1.43u). Fig. 2.1 shows the boundaries of the regions of interest that were

measured in the coronal plane (Fig. 2.1 A-C), as well as in the mid-sagittal plane (Fig. 1D). Measurements of the whole brain included all structures from the rostral extent of the cerebral cortex (bregma ~4.0 mm, (Paxinos and Franklin, 2001)) to the caudal brainstem-spinal cord juncture (bregma ~ 8.5mm). The area of the cerebral cortex was measured from pia to white matter, with boundaries defined rostrally by the emergence of the olfactory bulb, caudally by the plane in which the deep white matter (dorsal hippocampal commissure) was no longer visible, and ventrally by the rhinal sulcus, end of the CC, or level of the anterior commissure (from caudal to rostral). Measurements of the hippocampus include both the upper and lower leaves. The hippocampus is bordered dorsally and laterally by the corpus callosum (CC), lateral ventricles, or fimbria, and ventrally and medially by the thalamus, third ventricle, alveus hippocampus, brachium superior colliculus, or optic tract.

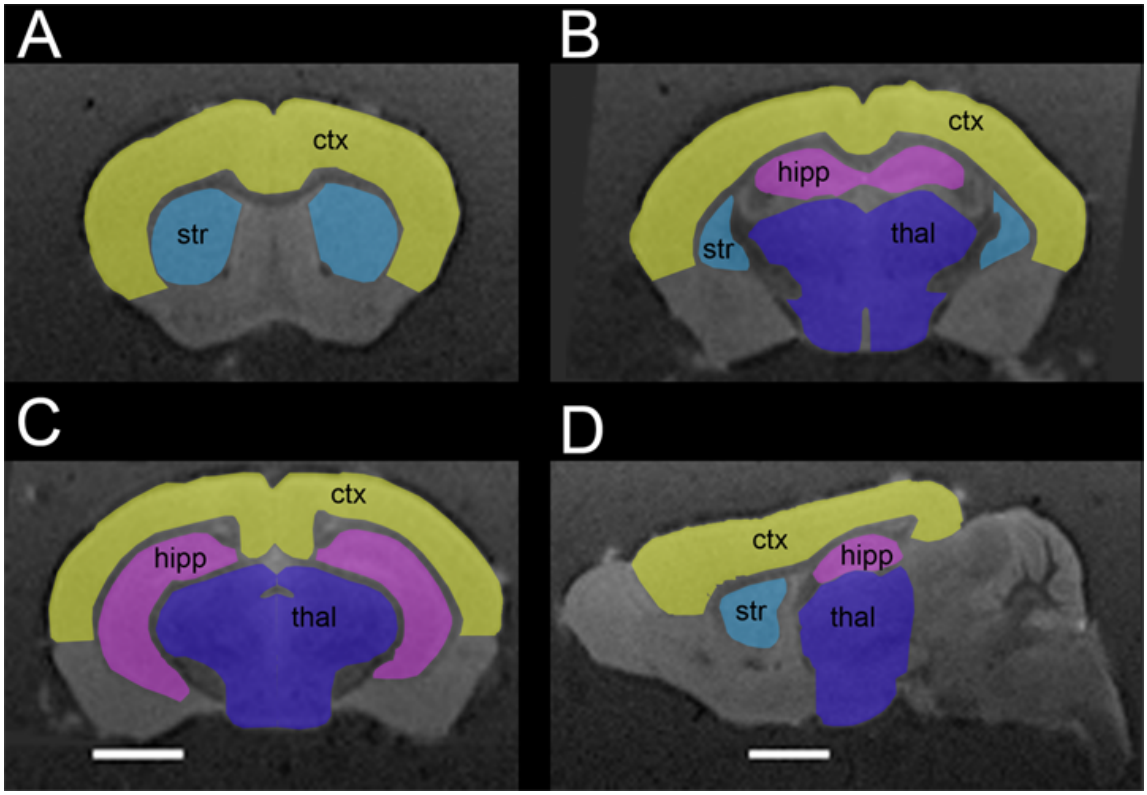

Figure 2.1 Schematics representing the areas included in measurements. The shaded areas show the areas which were measured for the cerebral cortex, hippocampus, striatum, thalamus and corpus callosum in coronal sections at bregma = +0.94mm (A) bregma = -1.36 mm (B) and bregma = -2.56 mm (C) and in a parasagittal section (D). Bar = 2 mm (A-C) and 2 mm (D).

Measurements of the striatum include the caudate and putamen. The boundaries of the striatum were defined medially by the lateral ventricles and internal capsule, laterally and dorsally by the external capsule, and ventrally by the anterior commissure. Measurements of the thalamus include both thalamic and hypothalamic nuclei. The boundaries of this region were defined laterally by the internal capsule and cerebral peduncle, dorsally by the hippocampus, and ventrally by the ventral surface of the brain. Measurements of the thalamus did not include the third ventricle or posterior commissure.

2.2.4 Black-gold staining:

Tissue sections were cut at 50µm on a Microm HM430 freezing slide microtome (Thermo scientific, Waltham, MA) and mounted on slides and allowed to dry overnight. Sections were then re-hydrated in distilled water for 2 minutes before being transferred to 0.3% Black-Gold II solution in 0.9% saline at 65°C. After 12 minutes, slides were briefly removed every 2 minutes to check the progress of labeling until the desired degree of myelin staining was observed (typically ~18 minutes). After staining, slides were rinsed for 2 minutes in distilled water, then transfered to a 1% sodium thiosulfate solution for 3 minutes. Slides were then rinsed three times for five minutes, dehydrated through graded ethanol, cleared in xylenes and cover-slipped with DPX mounting media.

2.2.5 Data analysis

Four brains were imaged for each of the P30 control, P30 *Met-Emx1*, adult control, and adult *Met-Emx1* groups. The images analyzed represent 100 μm thick sections, with a voxel size of 0.1 x 0.1 x 0.1 mm. With the exception of measurements of the whole brain, area measurements were taken separately for each hemisphere.

The distributions of cross-sectional areas across different rostrocaudal levels were compared between control and *Met-Emx1* mice at each age with Kolmogorov-Smirnov (K-S). For volume comparisons, measurements were made for the left and right hemispheres for each structure. The overall volume of each structure was compared using a two-way ANOVA in SigmaPlot12 (Systat Software, San Jose, CA) followed by a Bonferroni *t*-test as appropriate. Cortical thickness and surface area were compared between adult control and *Met-Emx1* mice using a Student's *t* test.

2.3 Results

2.3.1 Alterations in gray-matter structures in adult, but not juvenile, Met-Emx1 mice

Met was inactivated in the cerebral cortex and hippocampus by the selective removal of the intracellular signaling domain (encoded by exon 16) (Huh et al., 2004), using a Cre-*loxP* recombination strategy with the *Emx1-cre* mouse driver (Gorski et al., 2002b). The *Met-Emx1* mice were viable in agreement with previous reports (Judson et al., 2009b;

Judson et al., 2010a; Qiu et al., 2011a). Initial histological examination suggested altered cortical thickness (see Chapter 3) and prompted an MRI structural study of uncut fixed brains.

2.3.2 Whole brain

Total brain weight was measured for all groups (P30 control = 0.444 ± 0.01 g, P30 *Met-Emx1* = 0.421 ± 0.02 g, adult control = 0.411 ± 0.07, adult *Met-Emx1* = 0.514 ± 0.06 g). Two-way ANOVA found no overall effect of genotype ($F(1,15) = 2.548$, $p = 0.136$) or age ($F(1,15) = 1.395$, $p = 0.260$). A genotype x age interaction was found ($F(1,15) = 6.082$, $p = 0.030$), with a significant difference between P30 and adult *Met-Emx1* brains ($p = 0.024$) and between adult control and adult *Met-Emx1* brains ($p = 0.014$). These data suggest that while neither the *Met* allele nor age individually alter total brain weight, the combination contributes to an overall increased brain weight.

The cross-sectional area of the entire brain was estimated. Cross sectional area of the whole brain was similar for control and *Met-Emx1*mice at P30 (Fig. 2.2 A, $D = 0.0527$, $p = 0.514$, K-S test). The cross-sectional area was increased in adult *Met-Emx1* animals compared to control (Fig. 2.2 B, $D = 0.2345$, $p < 0.001$, K-S test). No significant effects of either genotype ($F(1,15) = 3.031$, $p = 0.107$) or age ($F(1,15) = 2.395$, $p = 0.148$, two-way ANOVA) were found on total brain volume, although the interaction of genotype x age approached significance ($F(1,15) = 4.418$, $p = 0.057$). In control mice, whole brain volume did not change from P30 to adult, from 406.1 ± 13.4 mm^3 to 391.5 ± 19.3 mm^3 (*p*

= 0.702, Bonferroni *t* test). By contrast, a significant increase in volume was observed in the *Met-Emx1* mice, from 396.6 ± 15.3 mm^3 at P30 to 492.7 ± 44.6 mm^3 in adults (p = 0.024, Bonferroni *t* test). Similar to the total brain weight, the combination of the *Met* allele and age lead to increased brain volume in the adult *Met-Emx1* mice.

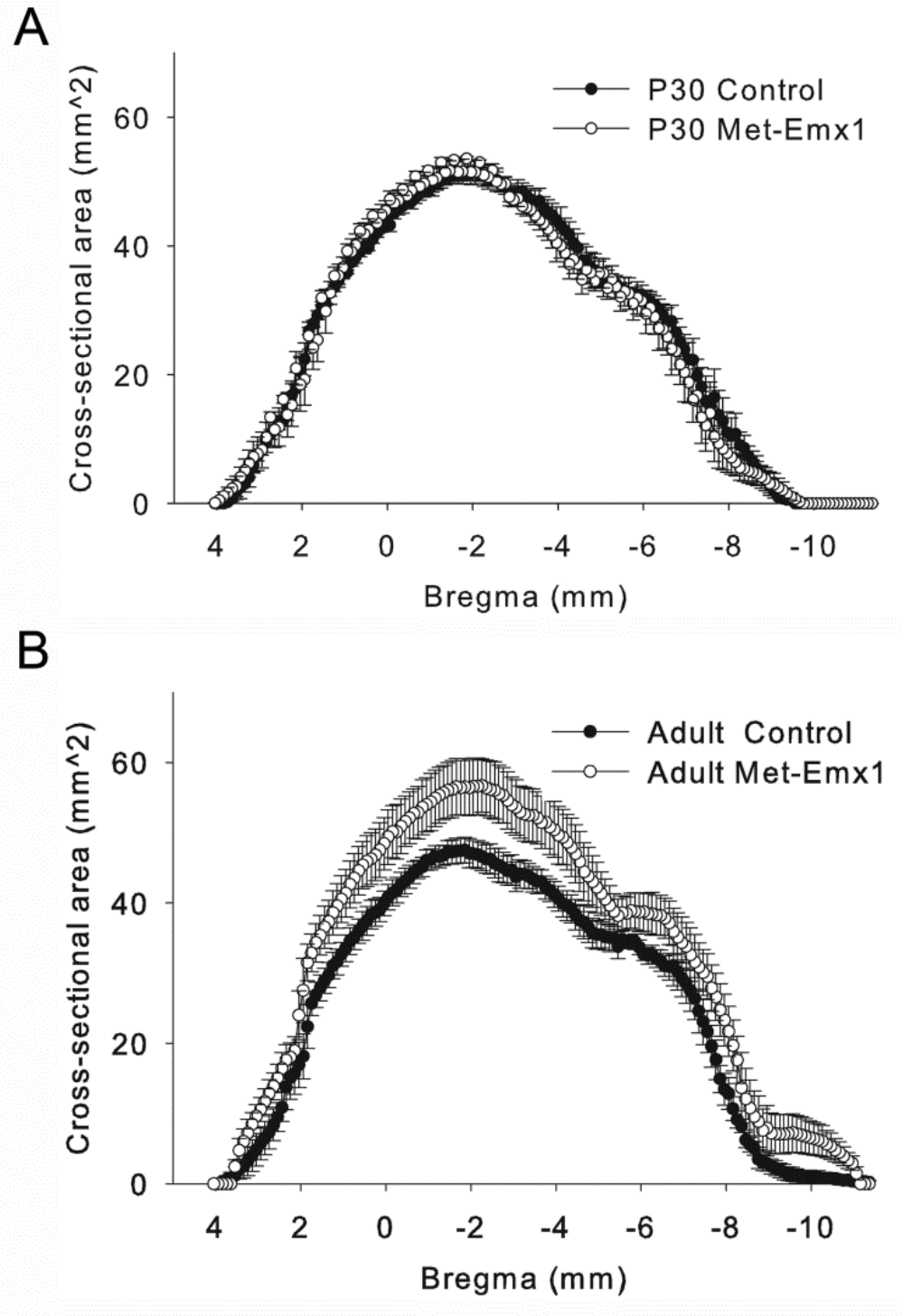

Figure 2.2. Loss of Met function alters whole-brain cross-sectional area. The average cross sectional area of the brain is plotted versus estimated bregma level for P30 (A) and adult (B) animals. Data represent n = 4 brains per genotype and age, points represent the mean areas with the error bars signifying the SEM.

2.3.3 Cerebral cortex

I initially focused on the cerebral cortex and hippocampus, the areas which were targeted by *Emx1-Cre* expression (Gorski et al., 2003). The brains from juvenile (P30) mice looked similar to *Met-Emx1* mice when compared to control, whereas the cerebral cortex in the adult *Met-Emx1* mouse appeared slightly larger overall (Fig. 2.3A-H). The distributions of areas were not significantly different for the juvenile control and *Met-Emx1* mice (Fig. 2.3I, $D = 0.1076$, $p = 0.067$, K-S test). Although in frontal regions (bregma levels > 2.5 mm), the areas in the *Met-Emx1* mice were larger on average than in control mice. In the adult mice, the distributions of cerebral cortical areas were significantly different between control and *Met-Emx1* mice (Fig 2.3J, $D = 0.220$, $p < 0.001$, K-S test).

Total cortical volume was estimated for control (96.98 ± 2.59 mm^3) and *Met-Emx1* mice (97.30 ± 3.48 mm^3) at P30. In the adult mice, the total cortical volumes were 89.69 ± 4.01 mm^3 (control) and 98.06 ± 3.47 mm^3 (*Met-Emx1)*. There was a significant main effect of genotype ($F(1,31) = 9.290$, $p = 0.006$), but not of age ($F(1,31) = 0.720$, $p = 0.404$), or hemisphere ($F(1,31) = 0.133$, $p = 0.719$, three-way ANOVA) on cortical volume. There was also a significant genotype x age interaction ($F(1,31) = 9.671$, $p = 0.005$). The cortical volume data were in agreement with the cross-sectional area distributions.

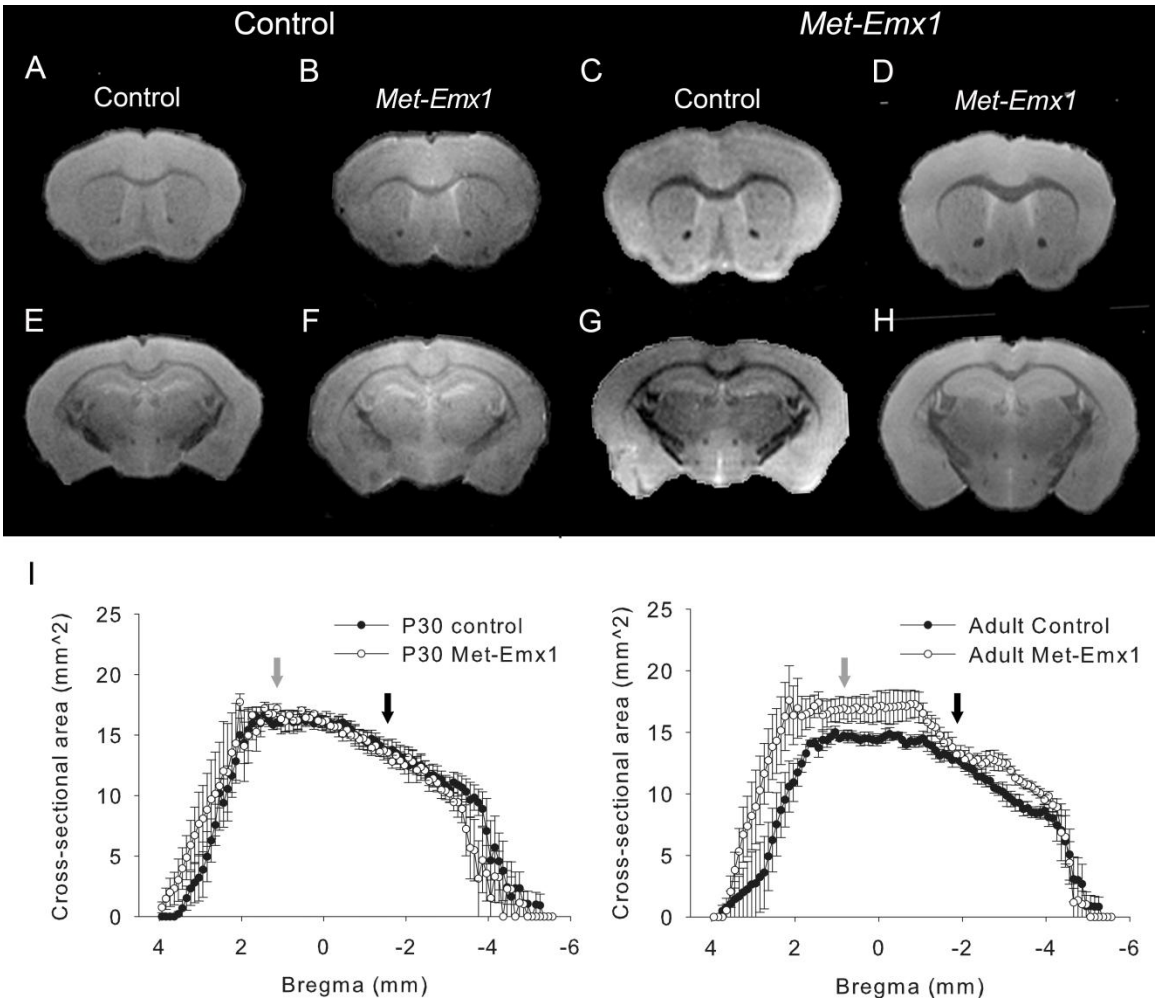

Figure 2.3. Structural differences in the cerebral cortex of *Met-Emx1* mice are age specific. (A-H) Representative MRI images at rostral (A-D, bregma = +1.04 mm) and caudal (*E-H*, bregma = -1.66 mm) levels. (I and J) The cross-sectional area of the cerebral cortex is plotted versus estimated bregma level for P30 (I) and adult (J) animals. The overall distributions of area are the same for control and *Met-Emx1* mice at P30 (D = 0.1029, p = 0.202, K-S test). Yet, the distributions are significantly different in control and *Met-Emx1* mice at adulthood (D = 0.3251, p < 0.001, K-S test). Arrows denote the levels for which the rostral (gray arrows) or caudal (black arrows) images are shown. Data represent n = 4 brains per genotype and age, points represent the mean areas with the error bars signifying the SEM.

The comparison of the cross-sectional areas showed an in increase in the *Met-Emx1* mice in the frontal and parietal cortical regions. The frontal cortical areas are associated with executive functions and emotional processing, which are altered in ASD. Therefore, I divided the dataset into rostral and caudal regions (at bregma = -1 mm), to specifically examine frontal areas. At P30, rostral and caudal volumes were similar between genotypes (control, rostral: 57.89 ± 2.42 $mm^3$and caudal: 39.10 ± 4.40 mm^3; *Met-Emx1*, rostral: 62.88 ± 4.77 mm^3 and caudal: 34.43 ± 4.33 mm^3). In adult *Met-Emx1* mice, the rostral half of cerebral cortex appeared larger than in control mice (control: 50.41 ± 4.03 mm^3, *Met-Emx1*: 63.06 ± 4.77 mm^3), while the caudal half remains similar (control: 39.28 ± 2.44 mm^3, *Met-Emx1*: 34.99 ± 4.06 mm^3). At rostral levels, there was no main effect of genotype ($F(1,31) = 1.219$, $p = 0.281$) or age ($F(1,31) = 1.365$, $p = 0.254$), but there was a significant genotype x age interaction effect ($F(1,31) = 5.691$, $p = 0.025$), again implying a combination of genotype and age leads to increased size. At caudal levels, I found no main effects of genotype ($F(1,31) = 1.476$, $p = 0.236$), age ($F(1,31) = 0.310$, $p = 0.580$) or genotype x age interaction ($F(1,31) = 0.01$, $p = 0.972$).

I next sought to determine which dimensions were expanded in the adult *Met-Emx1* cortex to account for the increase in volume. I first measured the thickness of the cortex from pia to white matter at the level of the barrel fields (bregma 0.34 mm to -1.96 mm) (Paxinos and Franklin, 2001). I found no significant difference in the thickness of the cortex at these levels in either the right (control: 1.15 ± 0.03 mm, *Met-Emx1*: 1.26 ± 0.06 mm, $p = 0.17$, Student's *t* test) or left hemispheres (control: 1.17 ± 0.03 mm, *Met-Emx1*: 1.24 ± 0.05 mm, $p = 0.28$, Student's *t* test). Next I measured the tangential length of the

cortical surface in each image, to determine the surface area of the cortex. The total surface area of the cortex is larger in *Met-Emx1* mice (115.63 ± 5.52 mm^2) than in controls (97.18 ± 3.47 mm^2, $p = 0.049$, Student's *t* test). Lastly, I compared the rostrocaudal distance spanned by the cerebral cortex. This appeared to be slightly longer in adult *Met-Emx1* mice (8.12 ± 0.13 mm) compared to adult control (7.70 ± 0.15 mm) , although this difference did not reach significnace ($p = 0.09$, Student's *t* test). No difference in rostrocaudal length was observed in P30 mice (control: 7.80 ± 0.10 mm; *Met-Emx1*: 7.53± 0.21 mm; $p = 0.32$, Student's *t* test). In summary, the cerebral cortex was larger in the adult *Met-Emx1* mouse. This difference appears to be due to a tangential, but not radial, expansion of the cortex. There may also be a rostrocaudal expansion of the cortex in the *Met-Emx1* mouse.

To confirm our findings, I examined the brains of adult *Met-Emx1* and control mice using basic histology. Indeed, an enlargement of the brain in *Met-Emx1* mice was also evident in cresyl violet stained tissue. Like in our MRI images, this enlargement appeared most pronounced in frontal sections, particularly between bregma +1.7 and bregma +2.4 (Fig. 2.4).

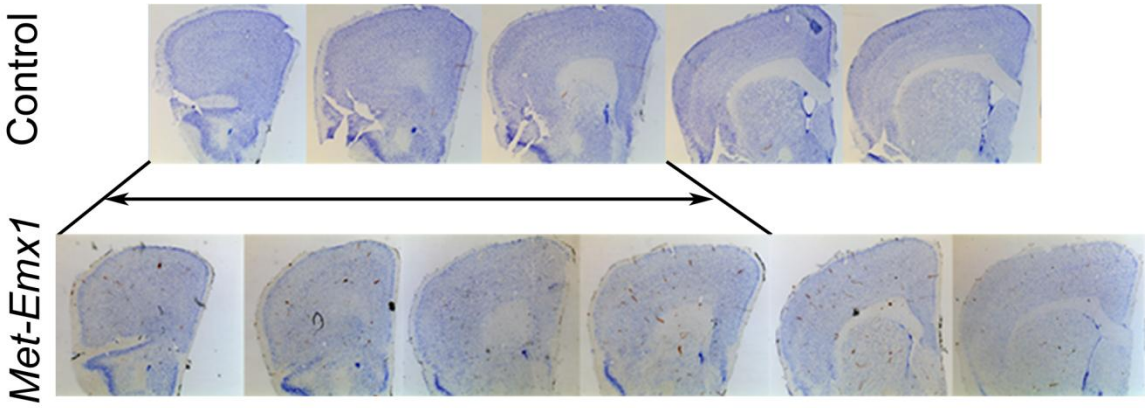

Figure 2.4. Expansion of the brain in *Met-Emx1* mice. Representative images of cresyl violet stained coronal sections from adult Met-Emx1 or control mice. Sections are shown for adult control (top row) and *Met-Emx1* (bottom row) mice between levels which in control mice correspond to bregma +2.34 (left) to bregma +0.74 (right) (Paxinos and Franklin, 2001). Note that an extra section is obtained in this anatomical range in *Met-Emx1* mice, suggesting a rostro-caudal expansion of the brain across this region.

2.3.4 Hippocampus

I measured the hippocampus, which also expresses *Emx1-cre* and may be affected by loss of Met signaling (Guo et al., 2000a; Gorski et al., 2002a). Lamination and subfields were grossly similar in all mice (Fig. 2.5A-H). Estimates of cross-sectional area showed no difference at P30 (Fig. 2.6AI, $D = 0.1113$, $p = 0.426$, K-S test), but a significant difference was found in the distribution of areas between adult control and *Met-Emx1* animals (Fig. 2.6B, $D = 0.2560$, $p = 0.001$, K-S test). This difference in the adult also translated to a difference in the total volume of the hippocampus (control: 13.67 ± 0.44 mm^3, *Met-Emx1*: 20.02 ± 2.94 mm^3, $p = 0.013$, Bonferroni *t* test). I found no main effect of either genotype ($F(1,31) = 2.950$, $p = 0.099$), or age ($F1,31) = 0.898$, $p = 0.353$), but there was a significant age x genotype interaction effect ($F(1,31) = 5.335$, $p = 0.030$, ANOVA). Like the total brain and cerebral cortex analyses, the overall increase in hippocampal volume is due to the combination of small effects of genotype and age.

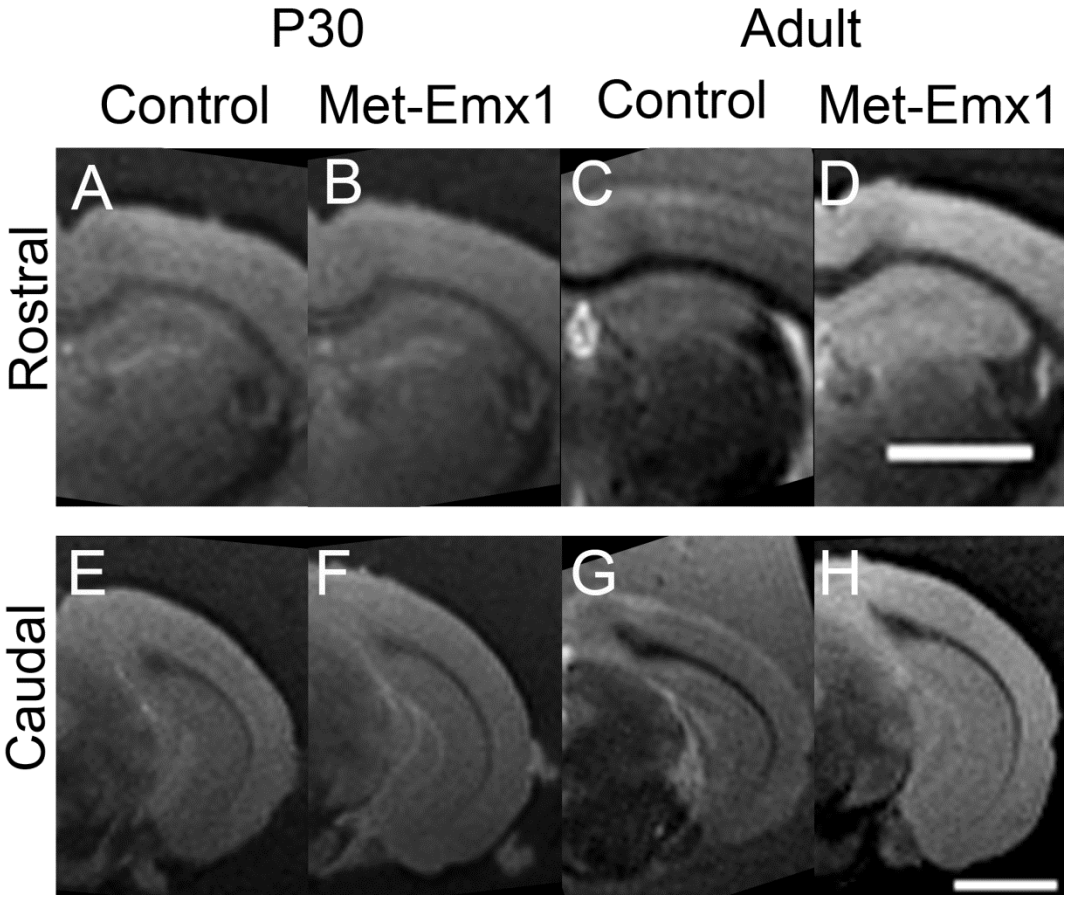

Figure 2.5. Loss of Met function alters hippocampal area in adult mice. *Met-Emx1* and control mice have similar hippocampal cross-sectional areas at P30 (D = 0.1399, p = 0.321, K-S test). The distributions of areas are significantly different between adult *Met-Emx1* and control mice (D = 0.2594, p = 0.001, K-S test). Representative images at rostral (A-D, approximate bregma = -1.66) and caudal (E-H, approximate bregma = -3.56) levels. Scale bar = 2 mm.

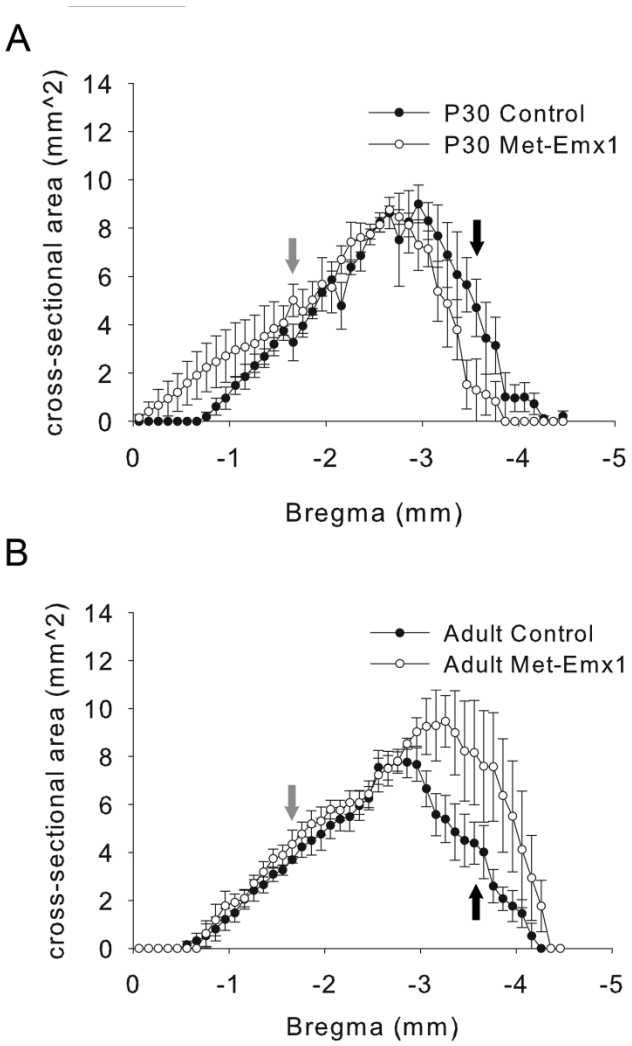

Figure 2.6. Loss of Met signaling alters hippocampal area in adult mice.

The average cross-sectional area of the hippocampus (upper and lower leaves) is plotted versus estimated bregma level for P30 (A) and adult (B) animals. Arrows denote the levels for which the rostral (gray arrows) or caudal (black arrows) images are shown. Data represent n = 4 brains per genotype and age, points represent the mean areas with the error bars signifying the SEM.

Frontal cortical regions project to the caudal portion of the hippocampus. When only the caudal portion (caudal to bregma < -2.50 mm) is considered, there was no main effect of genotype ($F(1,31) = 0.561$, $p = 0.461$) or age ($F(1,31) = 4.208$, $p = 0.056$), but there was a significant interaction between age and genotype ($F(1,31) = 12.880$, $p = 0.001$). In control mice, the caudal portion of the hippocampus had similar volumes at both P30 () and in adulthood (P30, 10.04 ± 1.46 mm^3; Adult, 7.65 ± 1.04 mm^3, $p = 0.38$, Bonferroni *t* test). But in the *Met-Emx1* mice the caudal portion of the hippocampus was significantly larger in adult, as compared to P30 mice (P30, 6.62 ± 1.17 mm^3; Adult, 12.93 ± 2.29 mm^3; $p = 0.029$, Bonferroni *t*-test). For the rostral portion (bregma > -2.50) of the hippocampus, no significant effect of genotype ($F(1,31) = 2.321$, $p = 0.141$), age ($F(1,31) = 0.758$, $p = 0.393$), or any genotype x age interaction ($F(1,31) = 0.523$, $p = 0.476$) was found (P30 control, 6.67 ± 0.33 mm^3; Adult control, 6.01 ± 0.65 mm^3; P30 *Met-Emx1*, 9.06 ± 2.7 mm^3; Adult *Met-Emx1*, 7.08 ± 0.77 mm^3). The increase in hippocampal volume therefore appears to be restricted to the caudal hippocampus.

2.3.5 Striatum -

The cross-sectional area of striatum of *Met-Emx1* animals was found to be similar to control at P30 (Fig 2.7A, $D = 0.0572$, $p = 0.984$, K-S test). However, the distributions between genotypes were different in the adult (Fig. 2.7B, $D = 0.2157$, $p = 0.002$, K-S test). The total striatal volume was calculated, and at P30 control mice had a volume of 16.60 ± 0.87 mm^3 and *Met-Emx1* mice had a volume of 16.44 ± 0.95 mm^3. For adult mice, the volumes were 16.96 ± 0.57 mm^3 for control mice and 21.95 ± 2.02 mm^3 for *Met-Emx1* mice. I found main effects of genotype ($F(1,31) = 7.559$, $p = 0.011$) and age

($F(1,31) = 11.172$, $p = 0.003$), and a significant genotype x age interaction ($F(1,31) = 8.570$, $p = 0.011$). Striatal volume was increased in adult *Met-Emx1* mice relative to adult control mice ($p = 0.002$, Bonferroni *t* test) and P30 *Met-Emx1* mice ($p = 0.003$, Bonferroni *t* test).

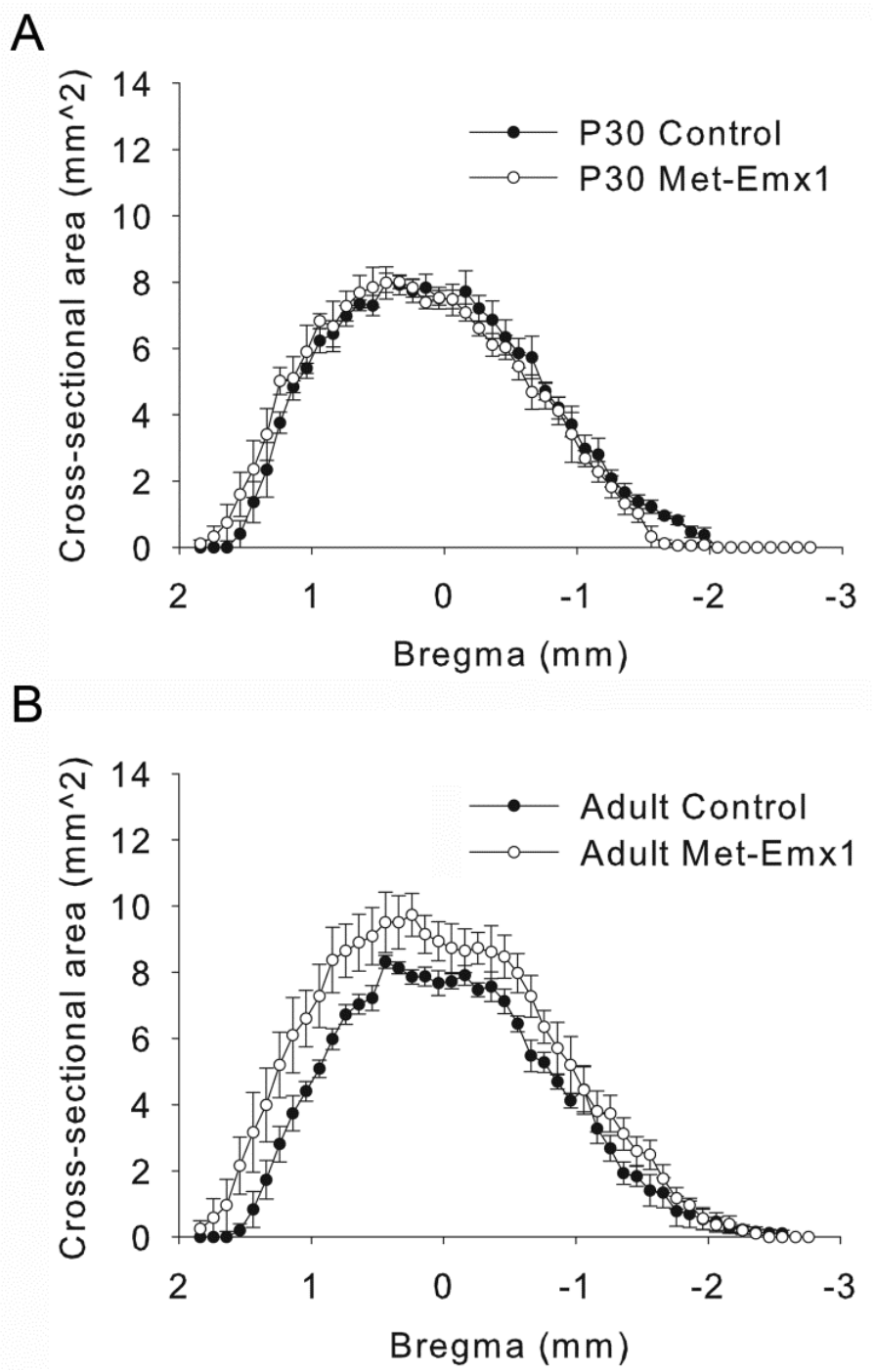

Figure 2.7. The striatum of adult *Met-Emx1* mice is larger than the striatum of control mice.

Average cross-sectional area of the striatum is plotted versus estimated bregma level for P30 (A) and adult (B) animals. Overall the distribution of area is significantly different in adult control and *Met-Emx1* mice, but not between P30 control and *Met-Emx1* mice. Data represent n = 4 brains per genotype and age, points represent the mean areas with the error bars signifying the SEM.

2.3.6 Thalamus

I next measured the area of the thalamus, which followed a similar pattern to the other structures. No difference was observed at P30 between control and *Met-Emx1* mice (Fig. 2.8A, $D = 0.2002$, $p = 0.056$, K-S test), but a significant increase was found in the thalamus of adult *Met-Emx1* compared to adult control mice (Fig.2.8B, $D = 0.3960$, $p < 0.001$, K-S test). I also calculated the volume of the thalamus. At P30, thalamic volume is 26.04 ± 1.79 mm^3 in control mice and 24.86 ± 1.48 mm^3 in *Met-Emx1* mice. In the adult, the volume of the thalamus is 20.87 ± 3.34 mm^3 in control mice and 29.41 ± 2.09 mm^3 in *Met-Emx1* mice. I found no main effect of genotype ($F(1,31) = 3.256$, $p = 0.084$) or age ($F(1,31) = 0.025$, $p = 0.875$). Yet, the genotype x age interaction ($F(1,31) = 9.504$, $p = 0.005$) indicated a difference among the dataset. Post hoc analysis revealed that the thalamic volume of the adult *Met-Emx1* mice was significantly different from adult control mice ($p = 0.04$, Bonferroni *t* test).

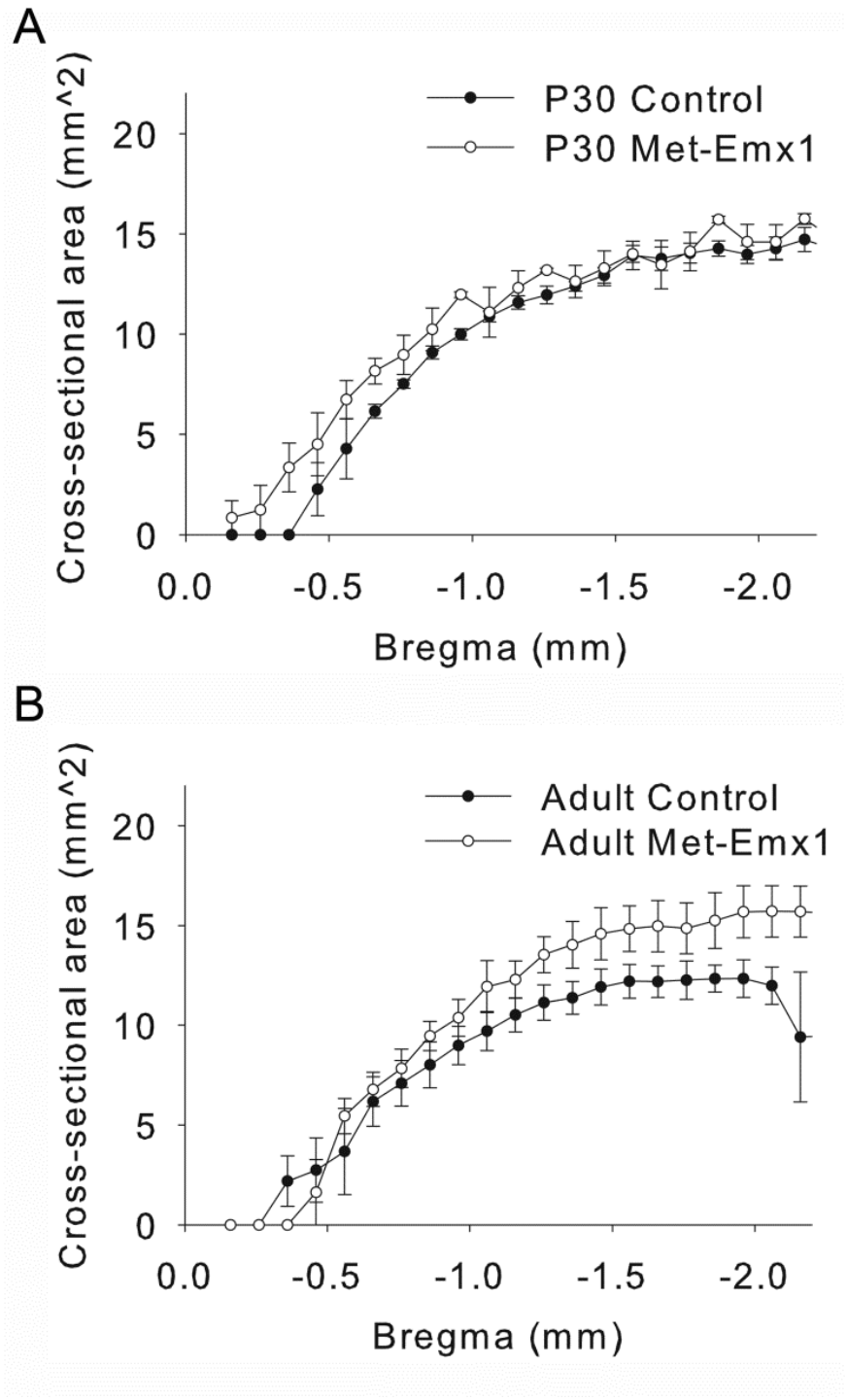

Figure 2.8. Loss of Met function alters thalamic area in adult mice. Average cross-sectional area of the thalamus is plotted versus estimated bregma level for P30 (A) and adult (B) animals. Overall the distribution of area is significantly different in control and *Met-Emx1* mice in adulthood ($D = 0.3960$, $p < 0.001$, K-S test), but not at P30 ($D = 0.2002$, $p = 0.056$, K-S test). Data represent n = 4 brains per genotype and age, points represent the mean areas with the error bars signifying the SEM.

2.3.7 Altered white matter morphology in adult, but not juvenile, Met-Emx1 mice

Met has previously been implicated in neurite extension, as well as axonal outgrowth and survival (Hamanoue et al., 1996b; Maina et al., 1997; Powell et al., 2003a) Therefore, I measured the thickness of the CC at the midline across the rostrocaudal extent, (bregma = +1.14 mm to -2.96 mm, Fig. 2.9 A-D). I found no difference between *Met-Emx1* and control mice at P30 (Fig. 2.10A, $D = 0.0723$, $p = 0.893$, K-S test). However, adult *Met-Emx1* mice have a significantly thicker CC than control mice (Fig. 2.10B, $D = 0.2239$, $p = 0.001$, K-S test). The difference appears greatest towards the rostral end (bregma levels +0.1 to 1.0 mm) of the CC (Fig. 2.8B). For example, at bregma +0.74 mm, the thickness of the CC is 0.32 ± 0.03 mm in control mice and 0.54 mm ± 0.08 mm in *Met-Emx1* mice, and, at bregma -1.06, the CC was and 0.20 ± 0.02 mm in control mice and 0.24 ± 0.04 mm in *Met-Emx1* mice.

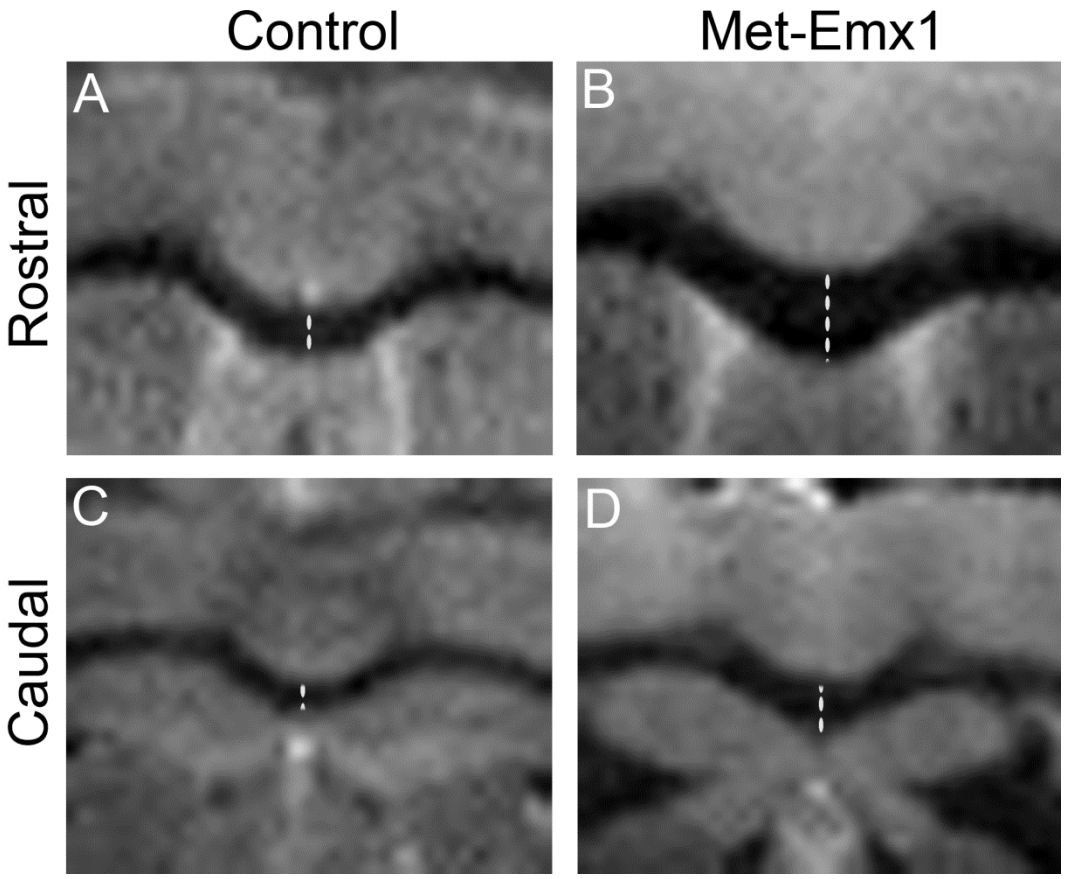

Figure 2.9. The corpus callosum is expanded at rostral levels in adult *Met-Emx1* mice.

(A-D) Representative MRI images at approximate bregma = +0.94 mm (A, B) and -1.16 mm (C, D) levels. Dotted line demonstrates the location of the thickness measurement.

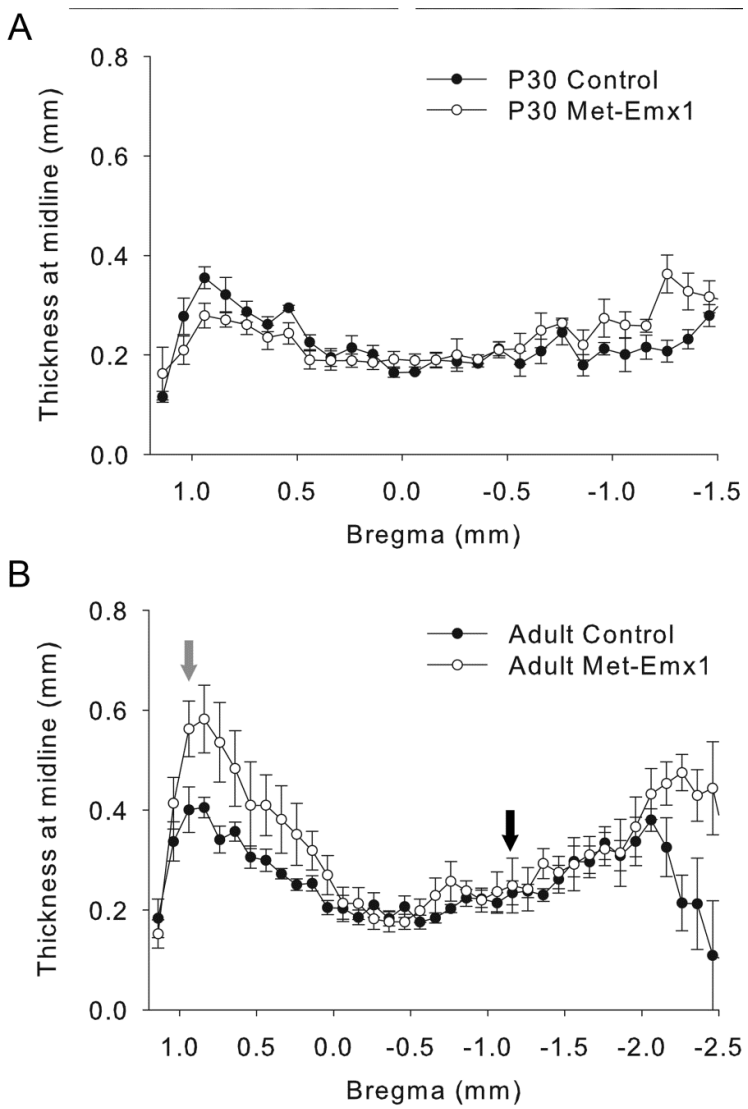

Figure 2.10. The corpus callosum is expanded at rostral levels in adult Met-Emx1 mice.

The average thickness of the corpus callosum at the midline is plotted versus estimated bregma level for P30 (A) animals and adult (B) mice. Arrows denote the level at which images are shown for rostral (gray) and caudal (black) levels. The distribution of thickness is significantly different in control and *Met-Emx1* mice in adulthood (D = 0.2239, p = 0.001, K-S test), but not at P30 (D = 0.0723, p = 0.893, K-S test). Data represent n = 4 brains per genotype, points represent the mean areas with the error bars signifying the SEM.

I also examined white matter in the striatum, specifically the cortico-striatal fascicles, in adult mice. I found some indication that the size of these bundles is altered in *Met-Emx1* mice. The distribution of fascicle areas is altered in *Met-Emx1* mice compared to controls (Figure 2.11, K-S test, $D = 0.0853$), with more large fascicles in *Met-Emx1* mice (Fig. 2.11C). I did not, however, find a difference in the number of cortico-striatal fascicles between control and *Met-Emx1* mice (control, 479.7 ± 83.3; *Met-Emx1*, 410.3 ± 22.7; Student's *t* test, $p = 0.505$).

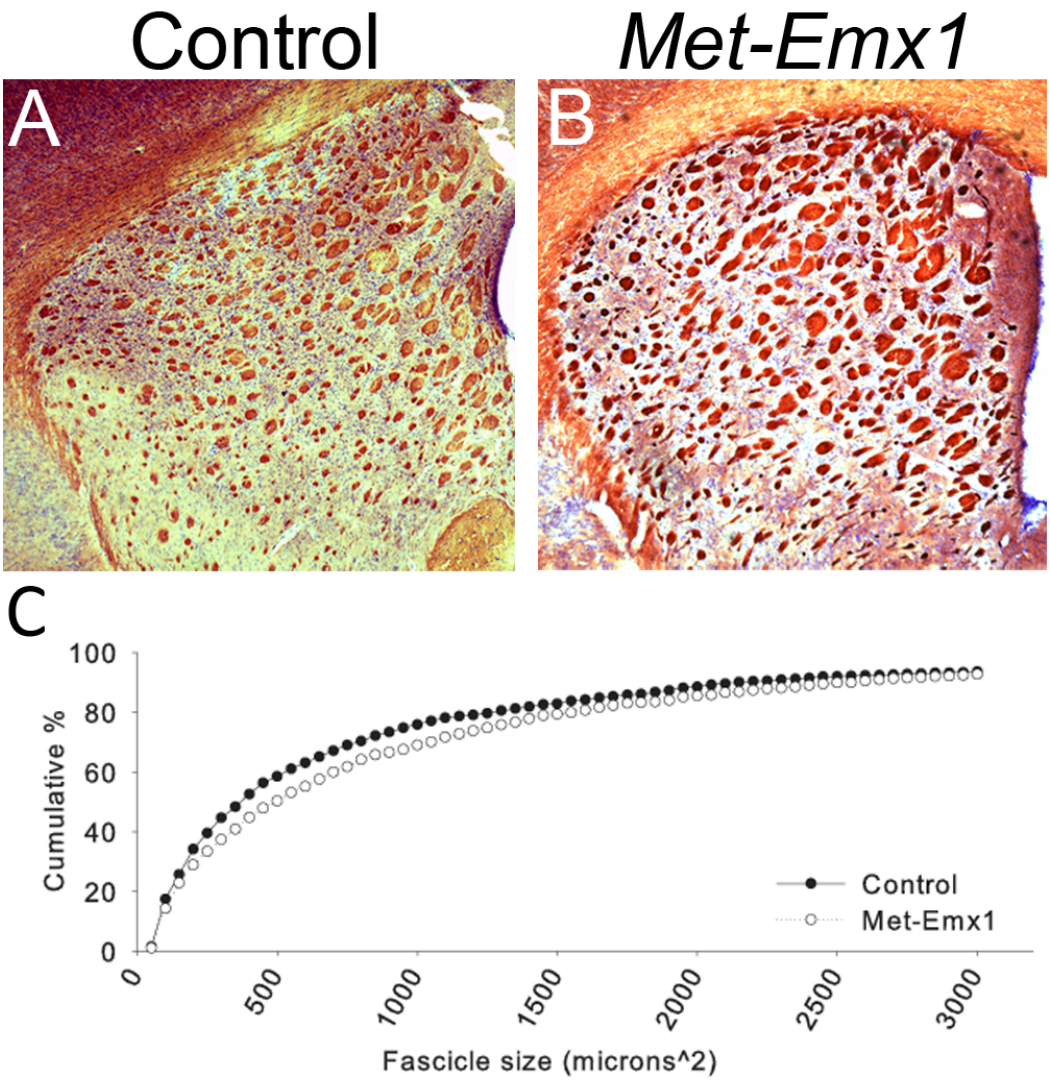

Figure 2.11. Loss of Met signaling alters corticostriatal fascicles.

Representative images show black-gold myelin staining (red) along with cresyl violet nuclear stain (purple) in the dorsal striatum of control (A) and *Met-Emx1* (B) mice. The distribution of fascicle sizes is shifted towards larger fascicles in *Met-Emx1* mice relative to controls (C).

2.4 Discussion

Our results demonstrate widespread alterations in forebrain structure in adult mice with impaired Met signaling. In the adult *Met-Emx1* mice, I observed an expansion in the rostral pole, in frontal cortical areas, and an enlargement in the caudal hippocampal areas that connect to the frontal regions. The striatum and thalamus are expanded as well, but more evenly across the rostrocaudal extent. None of the differences between adult *Met-Emx1* and control mice were detected in juvenile (P30) mice. The differences observed in the adult mice support the idea of a progressive defect.

The late postnatal nature of the enlargement of these brain areas could be due to continued growth in the *Met-Emx1* mice, or a lack of normal pruning. The cerebral cortex and hippocampus are directly targeted by the *Emx1-Cre* driver (Gorski et al., 2002a), so alterations in those structures could be due to either increased cell numbers or size of neurons or glia (Groszer et al., 2001; Geisert et al., 2002), or increases in the size or number of axonal or dendritic processes. The expression pattern of the *Emx1-Cre* driver is largely uniform with regards to the rostrocaudal extent of the cerebral cortex (Gorski et al., 2003), excluding the possibility that the differential effects are due to driver expression. However, Met expression has been reported to be in a low rostral – high caudal pattern during the first postnatal month (Judson et al., 2009b). In another mutant mouse, the urokinase plasminogen activator receptor (*Plaur*) null, Met levels were reported to be selectively decreased in embryonic frontal and parietal cortical areas

leading to seizures and impaired cognition (Powell et al., 2003c; Bae et al., 2010; Bissonette et al., 2010), providing support that loss of Met has greatest consequences in frontal regions. Frontal and limbic structures continue to develop through adolescence. The larger frontal structures in the *Met-Emx1* mice may represent the compensatory changes due to abnormal ontogeny of the frontal pole.

Changes in the subcortical structures, the striatum and thalamus, are perhaps best explained by an increase in white matter volume, as reflected in the increased thickness of the CC, as well as by changes in the cortico-striatal bundles observed in our Black-Gold staining. The CC is composed primarily of contralaterally projecting axons from cortical pyramidal neurons, both cortico-cortical and sub-cortical projections. An increase in the thickness of the CC could be caused by an increase in the number, size, or branching of axonal processes originating from affected cells, by increased myelination, or some combination of these factors. Both the striatum and thalamus exchange reciprocal connections with the cortex, including the frontal cortical areas which I found to be expanded in *Met-Emx1* mice. Notably, the ventral hippocampus also has reciprocal connections with the frontal cortex (Fanselow and Dong, 2010). The ventral division of the hippocampus is found in more caudal sections where the hippocampus appears to be expanded in adult *Met-Emx1* mice, raising the possibility that the change in hippocampal size may be due to altered cortical afferents rather than direct effects of loss of Met signaling in the hippocampus.

Changes in both white and gray matter volume have been detected in autistic humans. The brain is slightly smaller in individuals with ASD at birth and undergoes a period of early over-growth, leading to increased brain volume and head circumference within the first few years of life (Redcay and Courchesne, 2005; Courchesne et al., 2011). A study of autistic patients and controls from ages 18 months to 5 years found increased cortical volume, gray matter volume, and white matter volume in autistic patients, with no change in cortical thickness (Hazlett et al., 2011a). The authors therefore attributed the increase in cortical volume to increased surface area (volume ÷ thickness). After the initial period of overgrowth, the discrepancy in growth rate diminishes, and consequently brain volume and head circumference values approach those of typically developing children (Redcay and Courchesne, 2005). For example, an MRI study using individuals with a mean age near 10 years found no difference in total brain volume, nor in gray or white matter volume in autistic patients, although they did find an increase in cortical thickness at this age (Hardan et al., 2006). While most studies focus on childhood, some studies that included older children and adults report overall increases in brain size (Piven et al., 1995a; Aylward et al., 1999), raising the possibility that such increases could persist into adulthood in some cases. The earliest time I examined in the mice was P30 which represents the juvenile, closer to the 10 year old children, and this presents a limitation that I do not have earlier structural data.

Studies focusing on white matter structures using diffusion tensor imaging also found different changes in autistic patients depending on age. While one study on children between 1.8 and 3.3 years found increased fractional anisotropy in the genu and splenium

of the CC, as well as in portions of the internal and external capsules and the forceps minor (Ben Bashat et al., 2007), others in a slightly older population have found reduced fractional anisotropy values in the CC and frontal white matter tracts (Barnea-Goraly et al., 2004; Alexander et al., 2007). While some reports have shown decreases in CC size (Piven et al., 1997; Freitag et al., 2009), or no change in autistic subjects (Piven et al., 1997; Herbert et al., 2004), others have found increased white matter volume in autistic individuals (Herbert et al., 2003; Herbert et al., 2004; Freitag et al., 2009). None of these studies were correlated with genetic information, and they likely represent a spectrum of diverse genetic and environmental factors leading to the ASD diagnosis. A more recent study found that individuals with the rs1858830 C allele, which is associated with increased risk for autism, have decreased fractional anisotropy values in several tracts in temporal, parietal, and occipital regions (Rudie et al., 2012).

The structural changes I observed in the brains of adult *Met-Emx1* mice may resemble some of those reported in patients with autism (Amaral et al., 2008b). While the cause in each case remains uncertain, alterations in white matter structures seem to make a contribution in both cases. Despite this similarity, the time course of the alterations is divergent between the two species. In addition to simple species differences, a few factors may contribute to this divergence. Most notably, the *Met-Emx1* mice undergo what I believe to be a complete loss of the kinase activity of Met in the cells affected by the *Emx1-cre* driver, namely neurons and glia in the cerebral cortex and hippocampus. Changes in the striatum and thalamus are likely due to the cortical and hippocampal afferents to these regions. By contrast, the Met polymorphism associated with autism in

humans leads to decreased transcription of *MET* (Campbell et al., 2006), presumably affecting all brain areas which normally express *MET*. Since Met function is not completely ablated in the brains of humans with the polymorphism, there is the possibility that changes in the regulation of the pathway could eventually compensate for reduced transcription, as is found with MET in the cancer environment (Straussman et al., 2012). Similarly, the complete loss of Met in our mouse model may lead to compensatory changes in HGF levels, or other related pathways, that do not occur after the partial reduction in Met signaling seen in humans. Finally, our dataset relies on separate animals for each time point, and it was not a longitudinal study, and so conclusions regarding developmental trajectory are limited by group data. By pairing the imaging study with a single mutation and a defined phenotype, I was able to view the contribution of a single gene. The human situation is far more complex, yet multiple allelic variants may contribute to different stages of the ASD phenotype over the lifespan of the individual. Future studies will focus on the cellular and molecular underpinnings of the anatomical changes seen in these mice.

Chapter 3: Altered cortical lamination in mice deficient in Met tyrosine kinase

3.1 Introduction

The fifth edition of The Diagnostic and Statistical Manual of Mental Disorders (DSM V, American Psychiatric Association, 2013) lists two main categories of symptoms for ASD - deficits in social communication or interaction, and restricted or repetitive patterns of behavior. The previous edition, DSM IV, also included language deficits among the core symptoms (American Psychiatric Association, 2000). Autisms are highly heritable (Folstein and Rosen-Sheidley, 2001a). However, no single gene has been identified for idiopathic autism, and environmental factors are believed to play a role (Abrahams and Geschwind, 2010; Williams and Casanova, 2011). ASDs show considerable variability in both symptoms and pathology, and it is possible that different genetic or environmental insults may underlie some of this variation (Stoltenberg et al., 2010; Hallmayer et al., 2011; Tassone et al., 2011).

Numerous studies have examined anatomical alterations in the brains of patients with autism, focusing largely on areas thought to be involved in the functions most impacted by ASD, including the frontal lobe, superior temporal cortex, parietal cortex, orbitofrontal cortex, and amygdala (Carper et al., 2002; Hazlett et al., 2006b; Rojas et al., 2006; Girgis et al., 2007; Amaral et al., 2008a). Changes in the structure of such areas would be expected to impact their function, and indeed studies have shown correlations

between the size of various cortical regions and social deficits (Rojas et al., 2006; Girgis et al., 2007) or repetitive behaviors (Rojas et al., 2006), which are core features of ASD. Other studies have found correlations between changes in white matter structure and ASD symptoms (Cheung et al., 2009; Gibbard et al., 2013). Taken together, these studies show that alterations in cortical structures can have profound behavioral effects, and are likely to contribute to ASD pathology.

Met, the receptor for hepatocyte growth factor (HGF) has been linked with ASD by a number of genetic association studies (Campbell et al., 2006; Campbell et al., 2008; Campbell et al., 2009; Sousa et al., 2009a; Thanseem et al., 2010b). A number of *MET* polymorphisms have been associated with autism, or with autistic-like features in healthy subjects including rs1858830, rs38845, rs2237717, and rs42336 (Campbell et al., 2006; Sousa et al., 2009b; Thanseem et al., 2010a; Zhou et al., 2011; Lin et al., 2012). Of these variants, only a few have been characterized beyond their association with ASD. The rs2237717 and rs42336 single nucleotide polymorphisms (SNPs) are associated with altered facial emotion perception (Lin et al., 2012). The best characterized, however, is the SNP rs1858830. The rs1858830 allele is a common variant (0.523 allele frequency) located in the promoter region of *MET*, and the risk allele at this locus substantially reduces *MET* transcription (Campbell et al., 2006; Jackson et al., 2009). Furthermore, a recent study found that those with this risk allele show reduced deactivation of the default mode network (DMN) in response to emotional face stimuli, in addition to reduced connectivity between posterior cingulate cortex (PCC) and medial prefrontal cortex (mPFC), and reduced fractional anisotropy (FA) in the corpus callosum (Rudie et al.,

2012). Despite this progress in understanding the role of MET in ASD risk, the high degree of heterogeneity among ASDs remains a complication to studies of patients with autism. For example, a single copy of the rs185883 *C* allele has different effects on typically developing individuals than on patients with autism, suggesting that other genes present in the ASD population modify the effect of the *MET* risk allele (Rudie et al., 2012). I therefore sought to examine the effect of loss of Met signaling in an inbred mouse line, where genetic heterogeneity is more limited.

Met is expressed throughout the cerebral cortex from early in development (Jung et al., 1994; Powell et al., 2001b; Sun et al., 2002; Judson et al., 2009a). In *Met-Emx1* mice, Met is inactivated in cells derived from the *Emx1* lineage. *Emx1* is expressed in the cerebral cortex from approximately E9.5 (Gorski et al., 2002a) and Cre recombination is observable from roughly E10.5 (Guo et al., 2000b). Excitatory neurons and glia, but not inhibitory neurons, are derived from the *Emx1* lineage (Gorski et al., 2002a), and Met is therefore inactivated in these cells in *Met-Emx1* mice. Previous work from our lab (Smith et al., 2012) has shown that adult mice in which Met has been rendered kinase-dead in the developing cerebral cortex and hippocampus (*Met-Emx1* mice), have larger brains than control mice. Increased volume in the *Met-Emx1* mice is particularly prominent in frontal cortical regions, which are involved in behaviors thought to be disrupted in ASDs (Mundy, 2003; Courchesne and Pierce, 2005). I also found that the corpus callosum (CC) was thicker at rostral levels in *Met-Emx1* mice. In order to determine more specifically how the brain is expanded in *Met-Emx1* mice, I examined cortical structure at the cellular level using histology and immunohistochemical staining.

3.2 Material and Methods

3.2.1 Animals

Animal care procedures are discussed in Appendix 1: Common Methods

3.2.2 Immunohistochemistry and histology

Brains from adult control or *Met-Emx1* mice were processed for immunohistochemistry according to standard laboratory techniques, as described in appendix 1. The primary antibodies used were rabbit anti-Cux1 (1:100, Santa Cruz Biotechnology, Inc, Santa Cruz, CA), rat anti-Ctip2 (1:500, abcam), or mouse anti-Satb2 (1:500, abcam, Cambridge, MA), followed by appropriate secondary antibodies. DAPI staining was performed by incubating floating sections for 5 minutes in DAPI diluted 1:1000 in TBS, followed by two five minute washes in TBS prior to mounting.

3.2.3 Cell counts and analysis

For analysis of the distributions of Cux1-immunoreactive ($Cux1^+$), $Satb2^+$, or $Ctip2^+$ cells, the cerebral wall was divided into 100 µm bins. A 200 µm wide radial strip of somatosensory cortex was analyzed for each of 3 control brains and 3 *Met-Emx1* brains. For total cell counts in the cerebral cortex, 3 control brains and 3 *Met-Emx1* brains were analyzed using the Neurolucida system (MicroBrightField, Inc., Williston, VT, USA). Unbiased stereological cell counts were obtained from at least three sections spaced 400

μm apart from somatosensory cortex (from bregma level 1.10 mm extending caudally to −1.94 mm), prelimbic cortex (PL), or orbitofrontal cortex (OFC) (Paxinos and Franklin, 2001) using the optical fractionator method. Volume was estimated using the Cavalieri method (Regeur and Pakkenberg, 1989). Statistical significance was determined for total counts from each region and for each antigenic marker using a Student's *t*-test analysis with a significance level of $p < 0.05$ in Microsoft Excel or SigmaPlot. Differences between distributions of cells were determined using the Kolmogorov-Smirnov test.

3.3 Results

3.3.1 Abnormal lamination in Met mutants

I first sought to determine if lamination was affected by loss of Met function in the cerebral cortex by measuring the thicknesses of individual layers, using tissue stained with DAPI to visualize cell nuclei. I found that the cerebral cortex was significantly thinner in *Met-Emx1* mice as compared to controls at the level of the somatosensory barrel field (Fig. 3.1A, B, control: 1226 ± 22 μm, *Met-Emx1*: 1118 ± 52 μm, $p = 0.029$, Student's *t* test). This difference seemed to be accounted for primarily by a reduction of the thickness of layers II/III in *Met-Emx1* mice (Fig. 3.1C. Student's *t* test, $p = 0.024$), while other layers were not significantly altered. The relative sparing of deep layers suggests that superficial layers were preferentially affected in *Met-Emx1* mice.

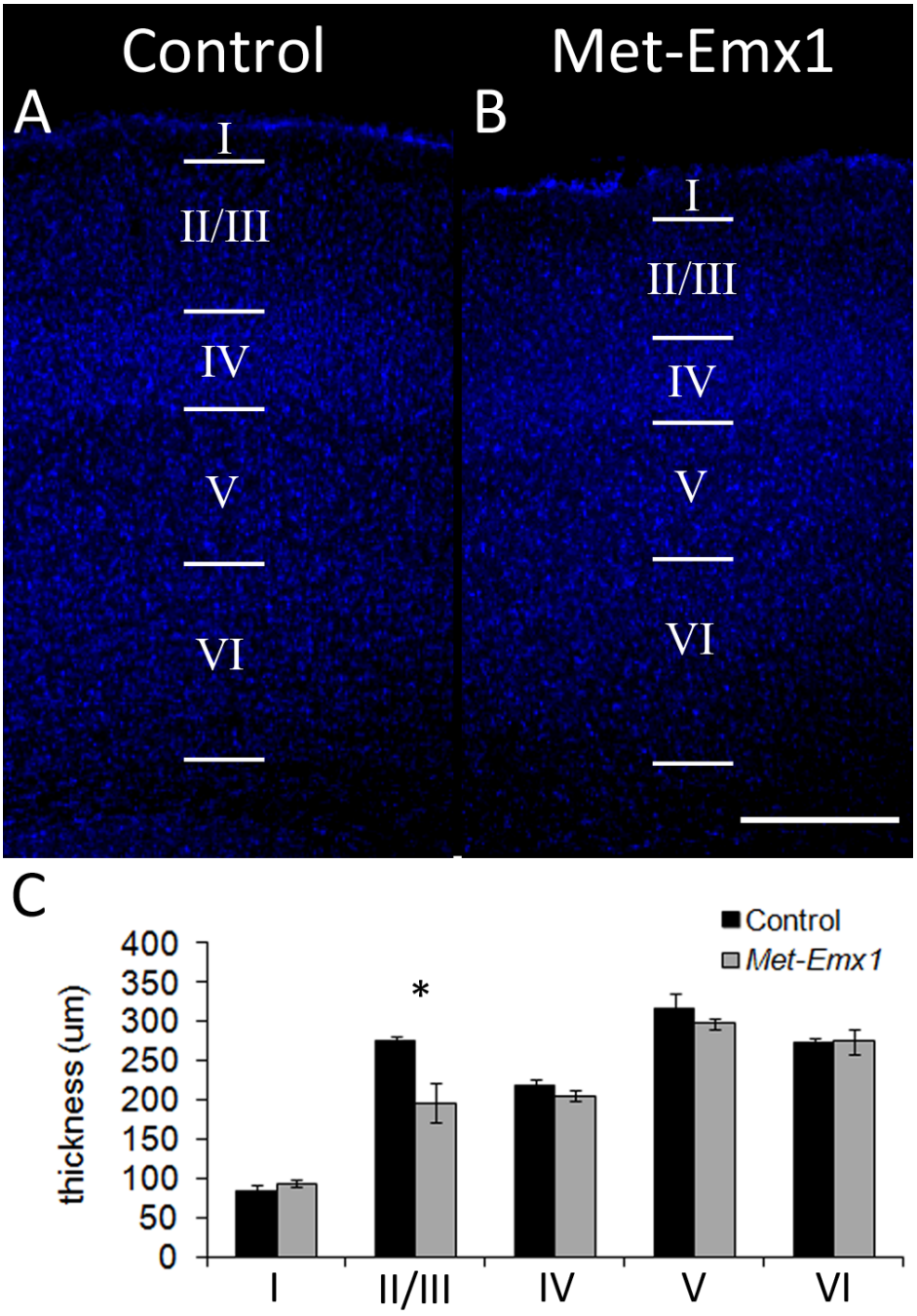

Figure 3.1. Reduced cortical thickness in *Met-Emx1* mice.

DAPI staining in control (A) and *Met-Emx1* (B) mice was used to allow measurement of the thickness of each cortical layer (C). Layer II/III is thinner relative to total cortical thickness in *Met-Emx1* mice compared to controls, while other layers are unaltered. Scale bar represents 200 µm.

Next I sought to determine if cell area was altered in *Met-Emx1* mice. To do this, I measured cell body area in pyramidal neurons of layers III and V of the somatosensory cortex. I found no significant difference in the average area of pyramidal neurons in either layer III (Fig. 3.2 A,B; control, 106.8 ± 8.8 μm^2; *Met-Emx1*, 123.2 ± 11.3 μm^2; Student's t test, $p = 0.317$) or layer V (Fig. 3.2C,D; control, 141.6 ± 10.2 μm^2; *Met-Emx1*, 148.5 ± 3.8 μm^2; Student's t test, $p = 0.560$).

In addition to cell body area, I also measured the length of the apical dendritic arbor in layer 5 pyramidal neurons of the somatosensory and motor cortex. I used Scholl analysis to compare the distribution of the dendritic arbor by distance from the cell body. There was no overall difference in the total length of the dendritic arbor between *Met-Emx1* and control mice (control, 383 ± 45 µm; *Met-Emx1*, 430 ± 65 µm; Student's *t* test, $p = 0.547$). There was, however, a change in the distribution of the dendritic arbor. A greater proportion of the total apical dendritic length is found close to the cell body in *Met-Emx1* mice, while more is found distal to the cell body in controls (Fig 3.3D; two-way ANOVA, genotype x radius interaction, $F = 2.240$, $p = 0.002$). I also found a slight, but significant increase in tortuosity in the apical dendrites of *Met-Emx1* mice (Figure 3.3C; control 1.08 ± 0.01; *Met-Emx1*, 1.11 ± 0.01, Mann-Whitney rank sum test, $p = 0.032$)

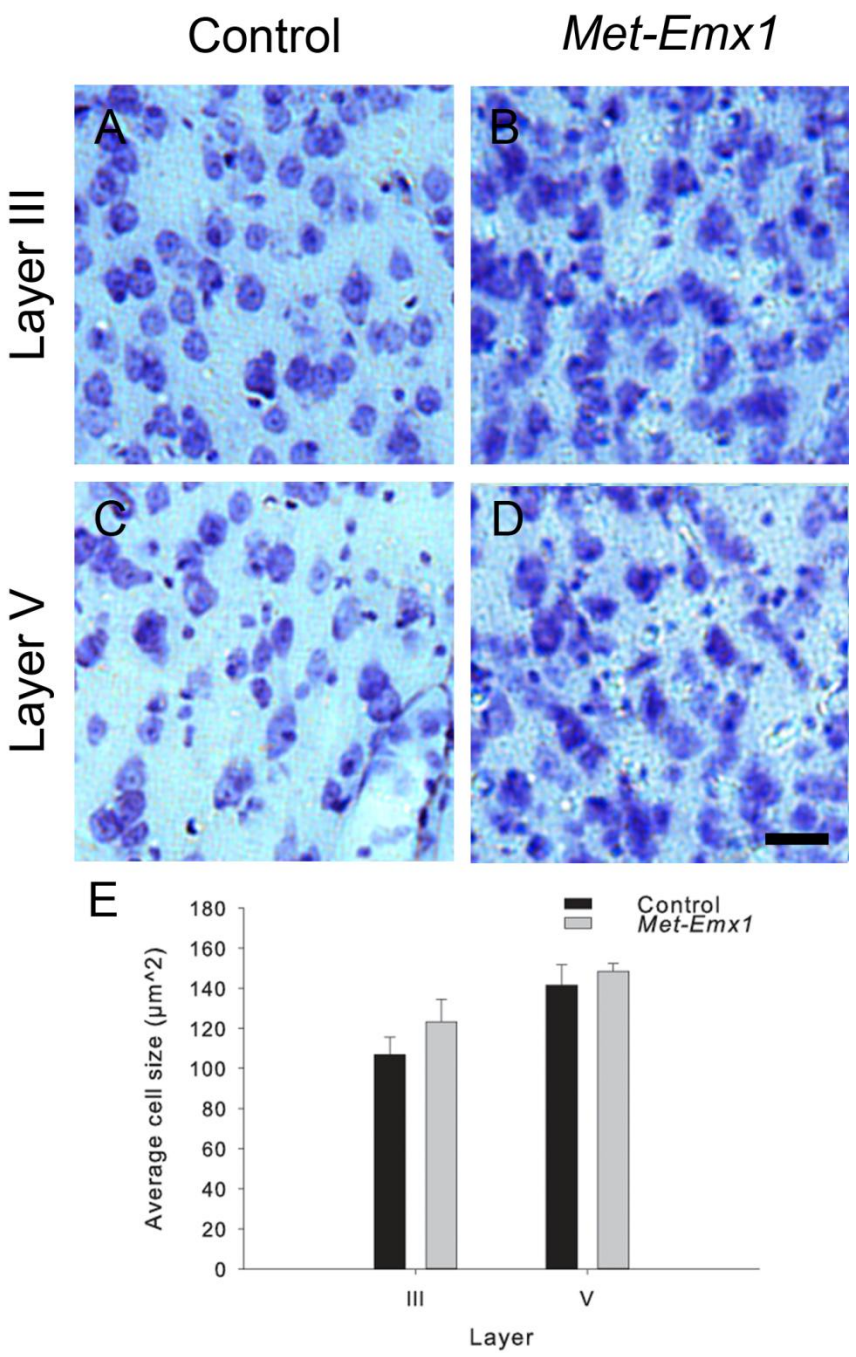

Figure 3.2 Cell size is unaltered in *Met-Emx1* mice.

Representative images of cresyl violet stained sections from adult control and *Met-Emx1* mice are shown in layer III (A, B) or V (C, D) of somatosensory cortex. (E) shows a quantification of average cell size in control and *Met-Emx1* mice for each layer. Scale bar in D represents 25µm

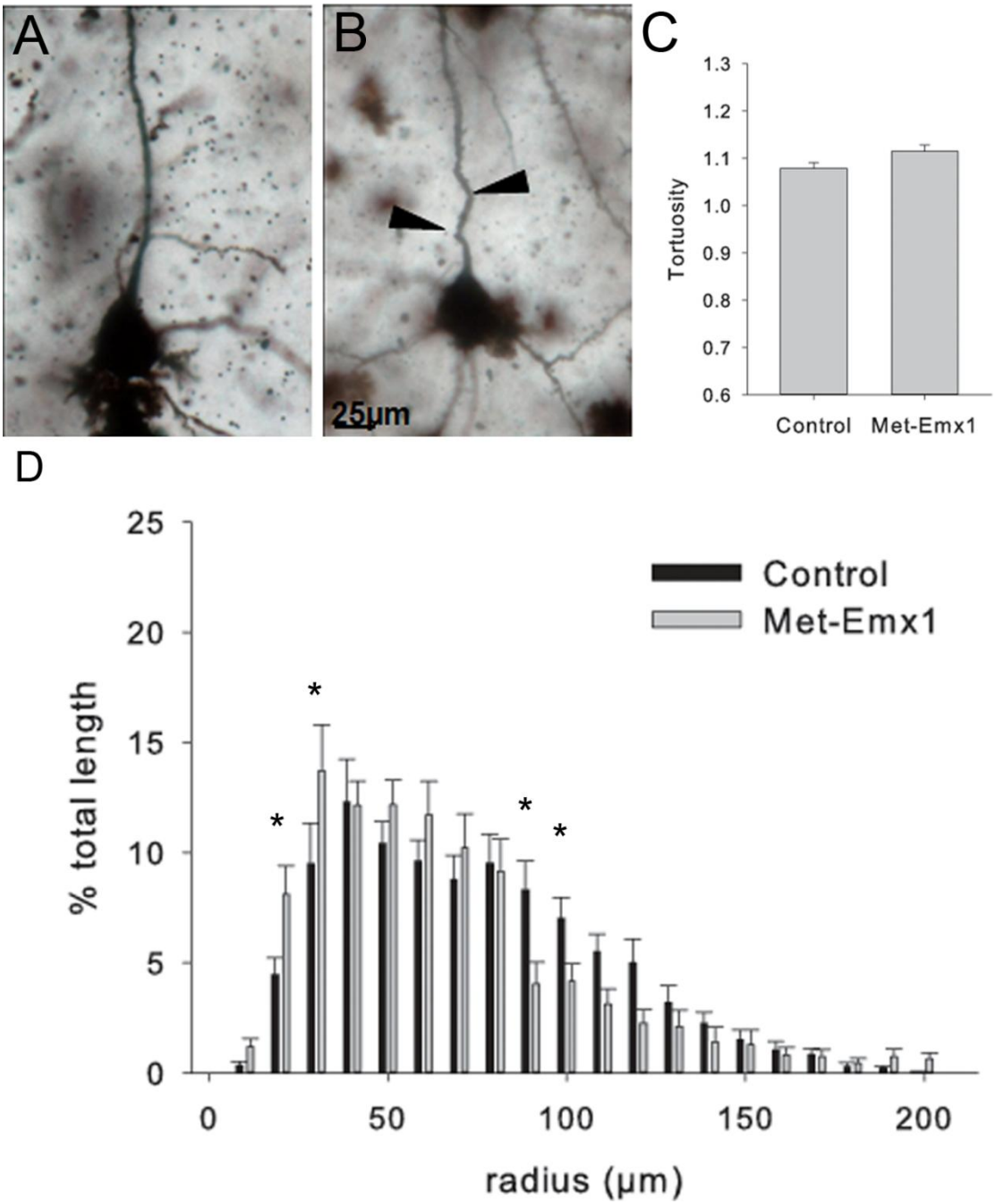

Figure 3.3 Altered dendritic morphology in *Met-Emx1* mice.

(A, B) show representative images of Golgi-stained pyramidal neurons from control (A) and *Met-Emx1* (B) mice. Arrowheads in B indicate stereotypical kinks in the apical dendrite. (C) shows a quantification of tortuosity in control and *Met-Emx1* cells. (D) shows the percentage of total dendritic arbor present in 10 µm radial bins centered on the cell body for control and *Met-Emx1* cells. * indicates $p < 0.05$, Holm-Sidak post-hoc test.

Next I sought to confirm the alterations in laminar morphology by examining biochemical markers whose expression profiles are restricted to distinct cortical layers in adult mice. I examined Cut-like homeobox 1 (Cux1), a transcription factor expressed in layers II-IV (Nieto et al., 2004) as well as COUP-TF interacting protein 2 (Ctip2), which is expressed in layer V projection neurons (Arlotta et al., 2005) and Forkhead box P2 (Foxp2), which marks layer VI (Ferland et al., 2003). These proteins were chosen to mark superficial (Cux1) and deep (Ctip2 and Foxp2) layer neurons, and to allow us to determine if these cells were distributed to the appropriate layers. Figure 3.4 shows a schematic representation of where each marker is expressed.

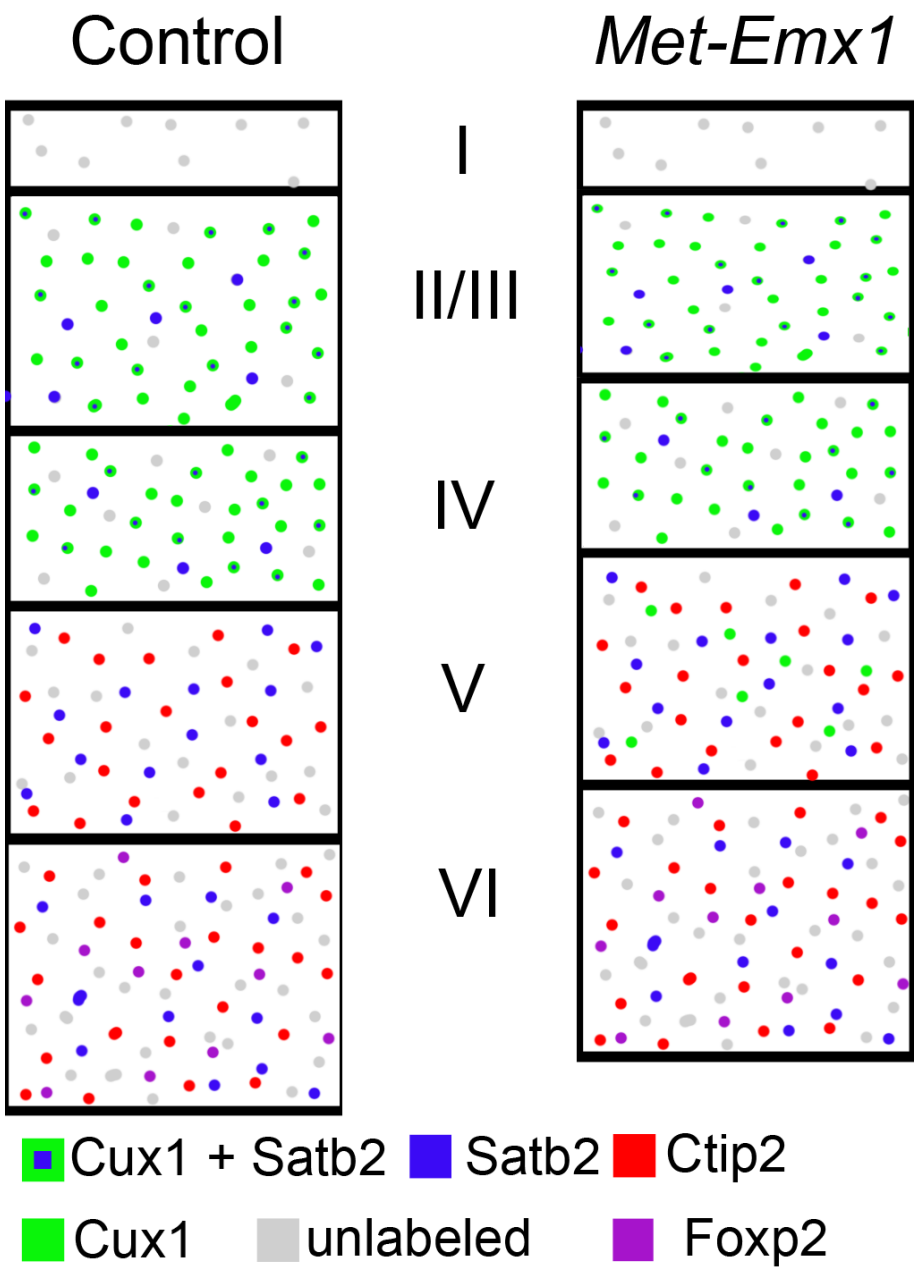

Figure 3.4 Schematic of layer marker staining in control and *Met-Emx1* mice.

Colored dots indicate neurons stained for each of the various markers used in this study, as indicated by the color code at the bottom. At left, the normal pattern of staining in S1 is indicated through each cortical layer (marked in the center). Notably, Satb2 staining overlaps with Cux1 staining in superficial layers, while Satb2 and Ctip2 do not overlap. At right, the staining pattern observed in *Met-Emx1* mice is shown. Notable changes include the reduction in thickness of layer II/III, and the presence of Cux1^{+} cells (green) in deep layers.

I found that the thickness of the Cux1$^+$ layers (II-IV) in S1 was 295 ±16 μm in control and 264 ±12 μm in *Met-Emx1* mice. As total thickness varied significantly between control and *Met-Emx1* mice, I normalized layer II/III thickness to total cortical thickness. Layer II/III composed a significantly smaller percentage of the total cortical wall in *Met-Emx1* animals as compared to control (Fig. 3.4A,B, control: 37 ± 1%, *Met-Emx1*: 32.4 ± 1% of cortical thickness, $p = 0.029$). I found that the thickness of the Ctip2$^+$ layer (V) was 227 ± 24 μm in control and 208 ±19 μm in *Met-Emx1* mice. After normalizing for total cortical thickness, I found no change in the relative thickness of layer V (Fig. 3.4 E, F, control: 18 ± 1%, *Met-Emx1*: 19 ± 1% of cortical thickness, $p = 0.379$). I found that the thickness of the Foxp2$^+$ layer (VI) was 291 ± 38 μm in control and 290 ± 37 μm in *Met-Emx1* mice. After normalizing for total cortical thickness, I found no change in the relative thickness of layer VI, as assessed by staining for Foxp2 (control: 32 ± 4%, *Met-Emx1*: 30 ± 4% of cortical thickness, $p = 0.77$).

While examining Cux1 immunoreactivity, I noticed an increase in the number of Cux1$^+$ cells in deep layers in *Met-Emx1* mice (Fig. 3.5B, arrows). I therefore assessed the distribution of Cux1$^+$ cells across the thickness of the cortex. I found that the distribution of Cux1$^+$ cells differed between *Met-Emx1* and control mice, with more Cux1$^+$ cells in deep layers of S1 in *Met-Emx1* animals (Fig. 3.5D, K-S test, $D = 0.1478$, $p < 0.01$). I again saw some indication of a change in the distribution of Cux1$^+$ cells across the thickness of the cortex in OFC, although this change did not reach significance (Fig. 3.6,

K-S test, $D = 0.0914$, $p = 0.099$). I found no such change in the distribution of Ctip2^{+} cells in either the somatosensory (Fig. 3.5, K-S test, $D = 0.0695$, $p = 0.310$) or prelimbic cortex (Fig. 3.7, K-S test, $D = 0.0566$, $p = 0.539$).

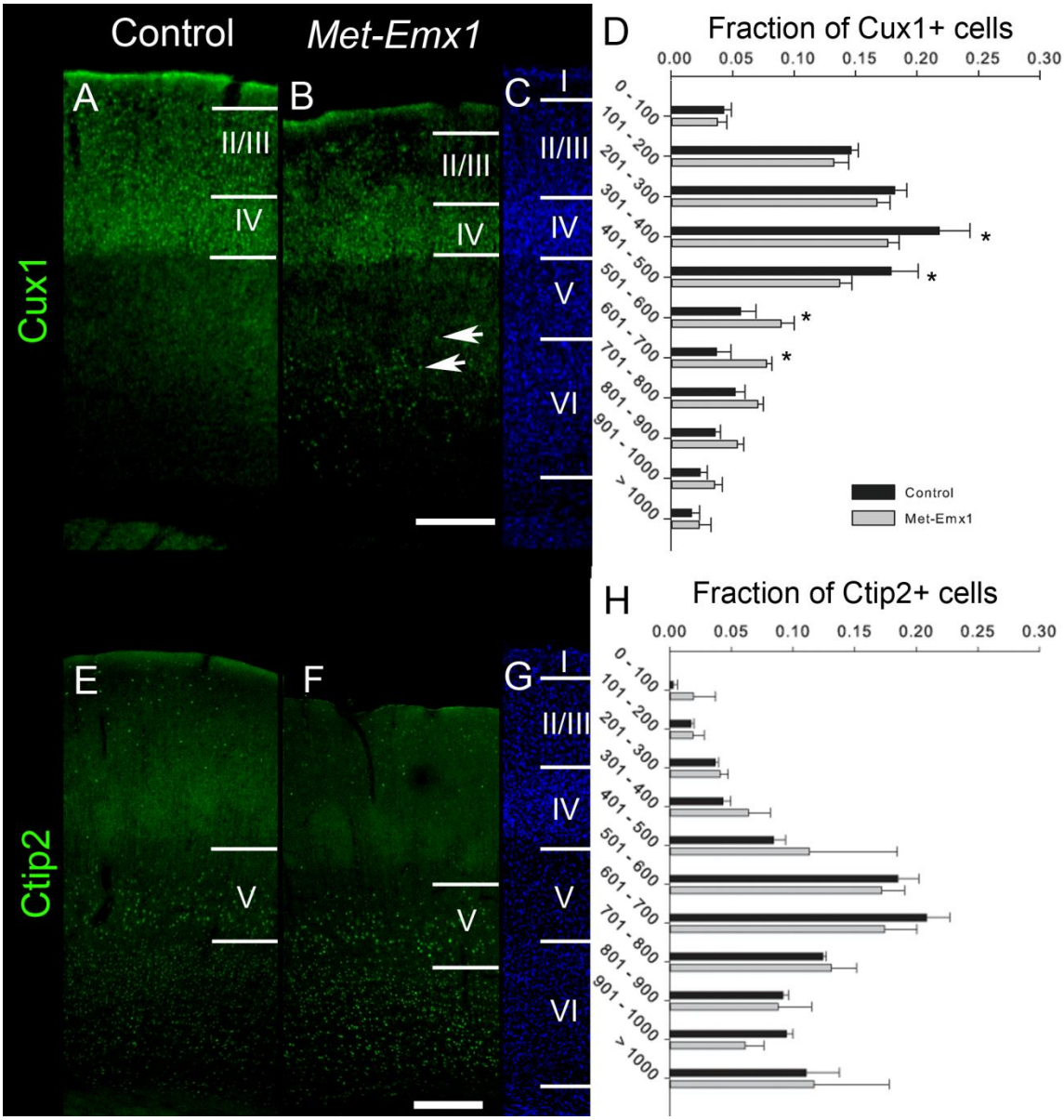

Figure 3.5. Superficial layer neurons distribute abnormally in *Met-Emx1* mice.

Representative images from adult control (A, E) and *Met-Emx1* (B, F) mice are shown for Cux1 (A-C) and Ctip2 (E-G) stained tissue. Arrows in (B) indicate ectopic $Cux1^+$ cells in deep layers. (C, G) show DAPI staining in control tissue for comparison. The distribution of $Cux1^+$ (D) or $Ctip2^+$ (H) cells by distance from pia is shown at right. Asterisks indicate $p < 0.05$. Scale bars in B and F represent 200 µm.

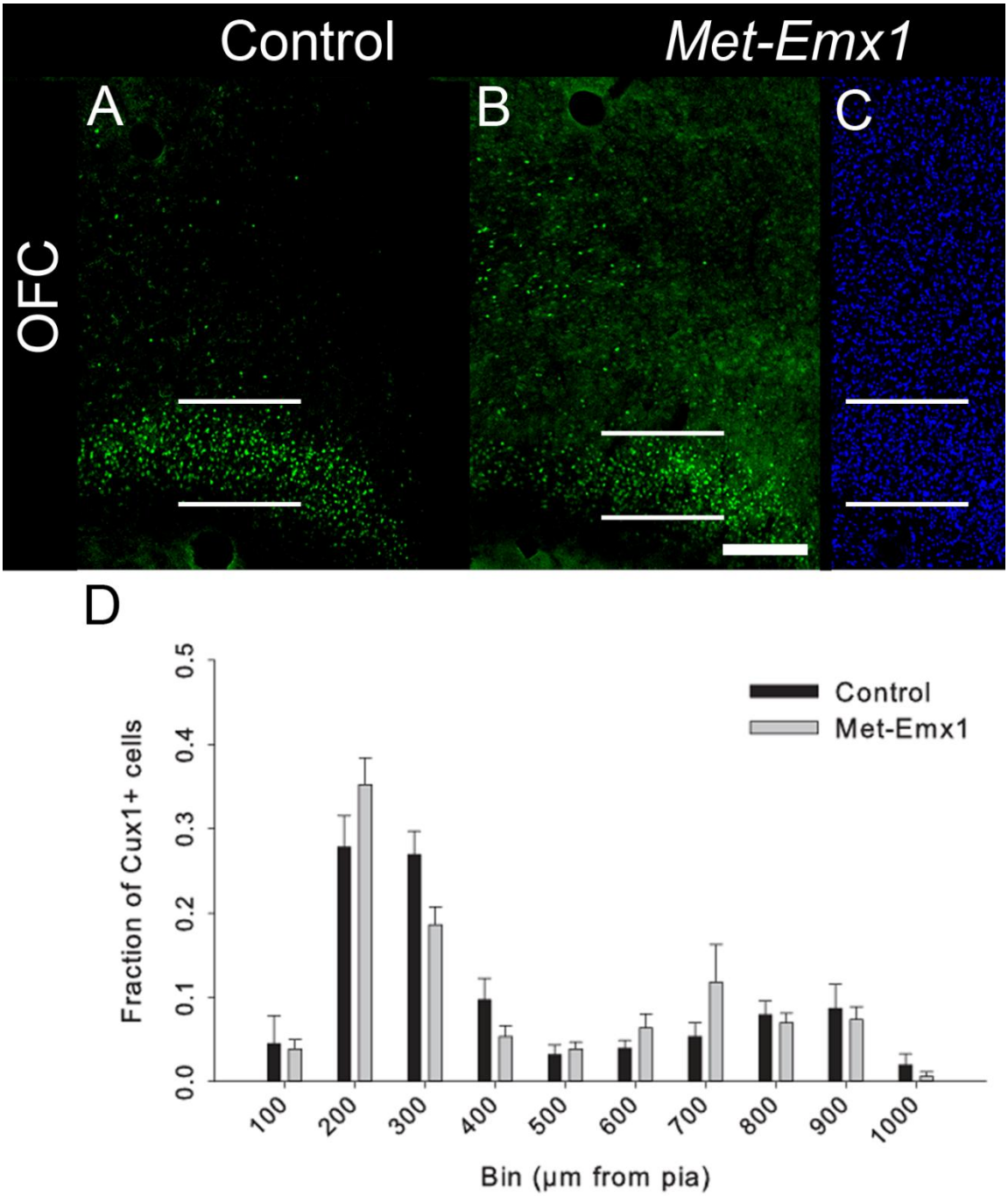

Figure 3.6. Loss of Met signaling does not alter the distribution of Cux1^{+} cells in OFC.

Representative images showing Cux1 immunoreactivity in the OFC are shown for adult control (A) and *Met-Emx1* (B) mice, along with nuclear staining (DAPI, C) in from a control mouse for reference. (D) shows a quantification of the number of Cux1^{+} cells by distance from pia in 100 µm bins. Scale bar in B represents 200 µm.

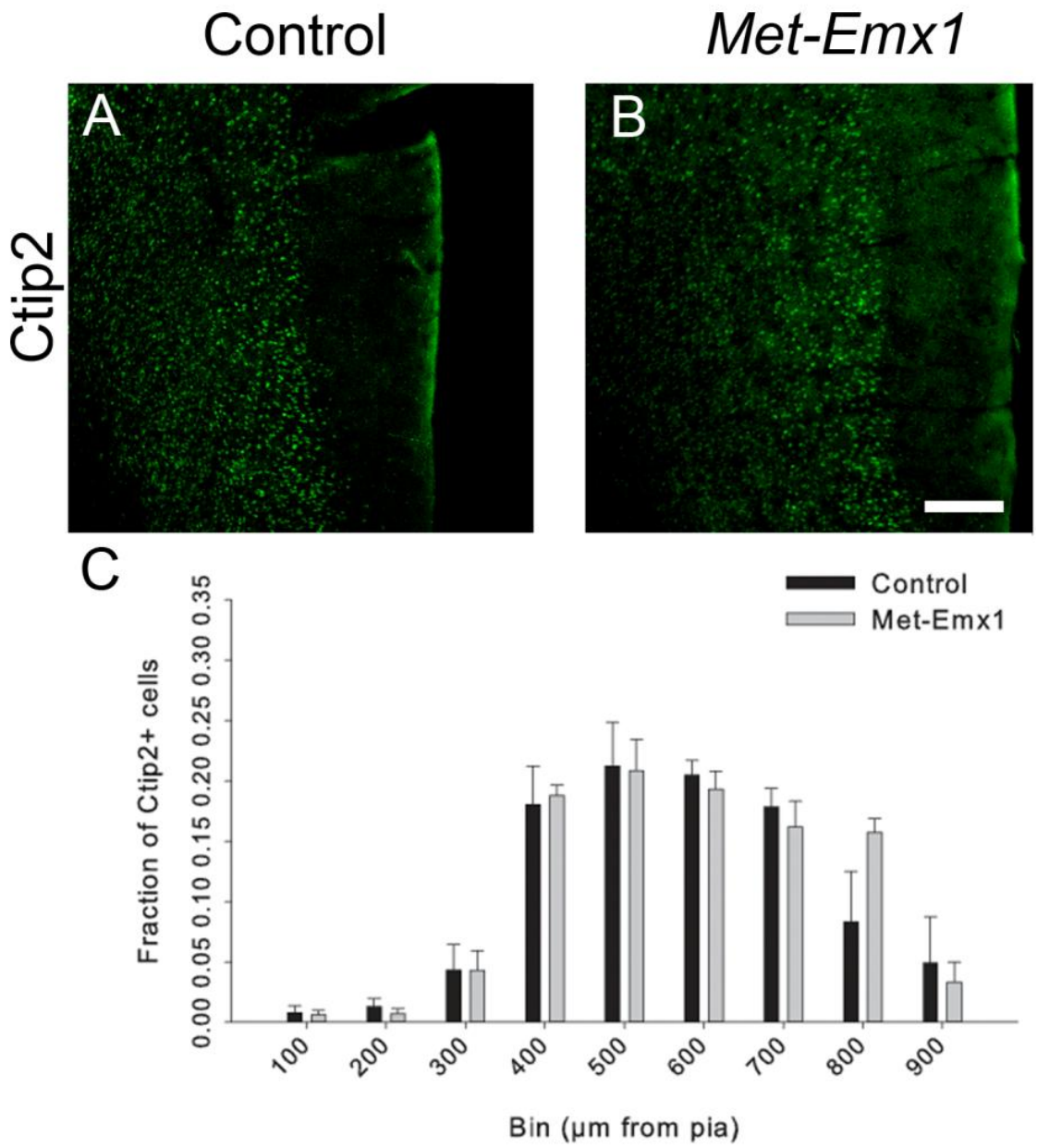

Figure 3.7. Loss of Met signaling does not impact deep layers in frontal cortex.

Representative images from Ctip2 staining of prelimbic (PL) cortex are shown for adult control (A) and *Met-Emx1* (B) mice. The bar graph in (C) shows the distribution of Ctip2^{+} cells through the cortex, in 100 µm bins by distance from pia.

Next I determined if the total numbers of cells expressing superficial or deep layer markers were altered in *Met-Emx1* mice. I performed stereological cell counts of $Cux1^+$ or $Ctip2^+$ cells in the barrel field of the somatosensory cortex using the optical fractionator method. I found no difference in the total number of either $Cux1^+$ (control: $1.3 \times 10^5 \pm 8.7 \times 10^3$, *Met-Emx1*: $1.6 \times 10^5 \pm 1.5 \times 10^4$, $p = 0.16$) or $Ctip2^+$ (control: $3.4 \times 10^4 \pm 3.9 \times 10^3$, *Met-Emx1*: $2.8 \times 10^4 \pm 1.8 \times 10^3$, $p = 0.25$) cells between control and *Met-Emx1* mice. As my previous findings indicated that the differences in brain size were greatest at rostral levels, I also performed stereological cell counts in frontal cortex (prelimbic for Ctip2 and Satb2, and orbitofrontal for Cux1, as Cux1 is not expressed in prelimbic cortex). I found no difference in the total number of $Cux1^+$ cells in the OFC (control, $6.3 \times 10^4 \pm 8.4 \times 10^3$; *Met-Emx1*, $6.3 \times 10^4 \pm 8.0 \times 10^3$; Student's *t*-test, $p = 0.979$). Neither did I find any difference in the number of $Ctip2^+$ cells in prelimbic cortex (control, $3.5 \times 10^4 \pm 3.5 \times 10^3$; *Met-Emx1*, $3.8 \times 10^4 \pm 2.8 \times 10^3$; Student's *t*-test, $p = 0.565$). Together, these findings indicate that loss of Met signaling does not alter the number of superficial or deep layer neurons in adult mice.

I have previously shown an increase in the thickness of the corpus callosum in adult *Met-Emx1* mice (Smith et al., 2012). As the majority of callosal projection neurons reside in superficial layers (Alcamo et al., 2008; Fame et al., 2011), I examined the cells that are immunoreactive for Satb2, a transcription factor expressed in callosal projection neurons (CPN) (Alcamo et al., 2008). I found no significant difference in the total number of $Satb2^+$ cells in the somatosensory barrel field of adult *Met-Emx1* mice relative to controls

(control: $1.1 \times 10^5 \pm 1.2 \times 10^4$, *Met-Emx1*: $9.2 \times 10^4 \pm 8.4 \times 10^3$, Student's *t* test, $p = 0.25$), nor did I see any difference in prelimbic cortex (control, $9.6 \times 10^4 \pm 6.3 \times 10^3$; *Met-Emx1*, $9.6 \times 10^4 \pm 2.9 \times 10^3$; Student's *t*-test, $p = 0.716$). Satb2$^+$ CPN are normally distributed from layers 2 through 5, with approximately 80% in upper layers (Fame et al., 2011). To determine if Satb2$^+$ cells were distributed normally in the *Met-Emx1* mice, I measured the distance of each cell in a 200 μm radial bin from pia. I found no change in the distribution of Satb2$^+$ cells in either the somatosensory (K-S test, $D = 0.0732$, $p = 0.725$) or prelimbic cortex (K-S test, $D = 0.0210$, $p = 0.994$).

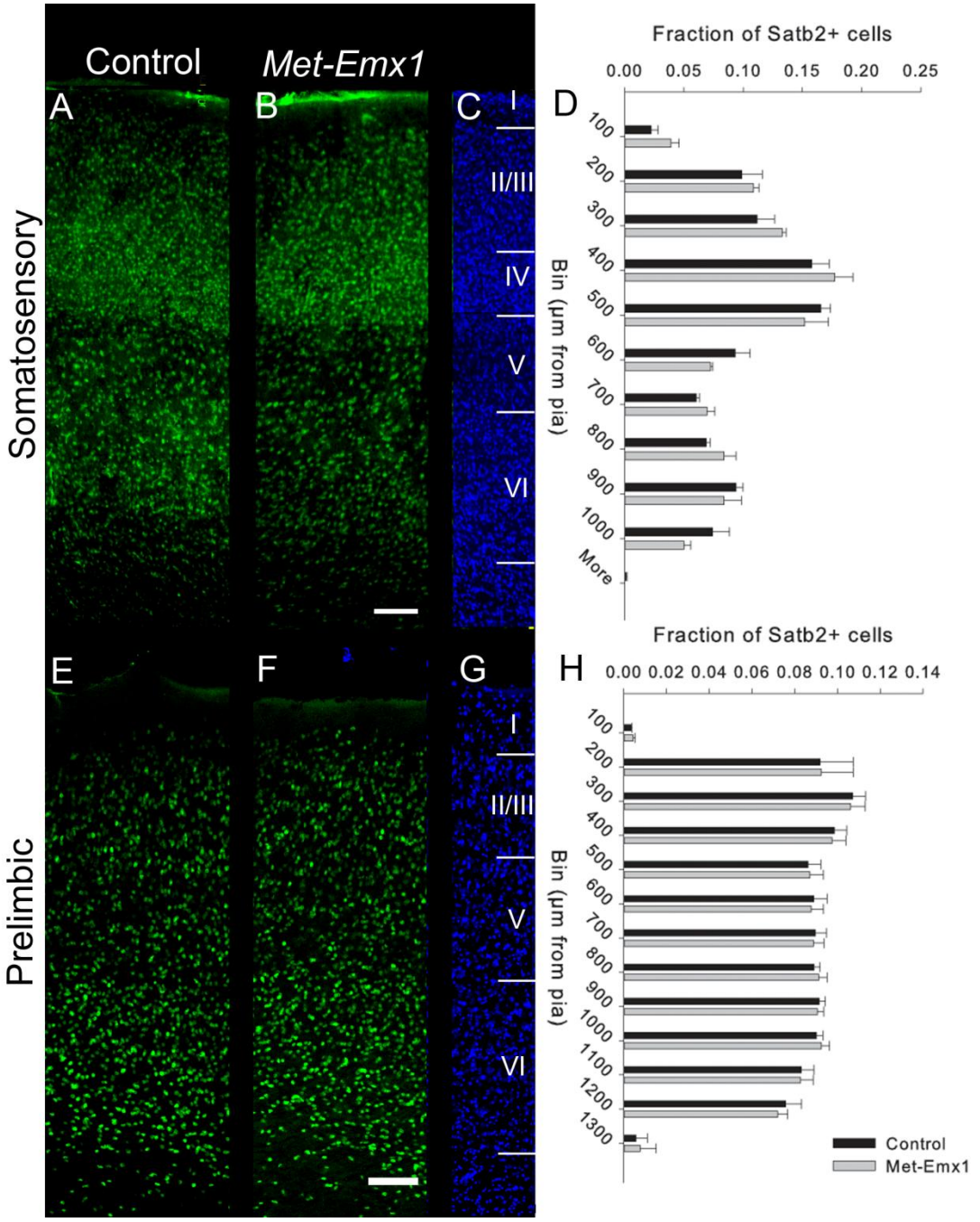

Figure 3.8. The distribution of callosal projection neurons is altered in *Met-Emx1* mice.

Representative images from control (A, C, E, G) and *Met-Emx1* (B, F) mice from somatosensory (A, B, C) and prelimbic (E, F, G) are shown. (C, G) show DAPI staining in control tissue for comparison. The distribution of Satb2^{+} cells by distance from pia is shown at right in (D) and (H). Scale bars in B and F represents 100 µm.

3.4 Discussion

Cortical neurogenesis has long been known to proceed in an inside-out fashion, with deep layer neurons being born first and more superficial layers being born later and migrating past earlier-born cells on their way to their final positions (Angevine and Sidman, 1961; Rakic, 1972; Takahashi et al., 1999). The generation of cortical cell types further progresses from neurogenesis early during development to gliogenesis in late embryonic and postnatal stages (Qian et al., 2000; Sauvageot and Stiles, 2002). While the progression of cortical progenitors through different phases of neurogenesis and gliogenesis is to some degree intrinsic to the progenitors themselves (Qian et al., 2000), it can also be influenced by extrinsic cues such as growth factors (Menard et al., 2002; Sauvageot and Stiles, 2002) and cytokines (Bonni et al., 1997; Rajan and McKay, 1998). For example, increased β-catenin signaling promotes deep-layer cell fate, while reduced signaling promotes superficial layer fate (Mutch et al., 2010).

Here, I have noted that *Met-Emx1* mice have a thinner cerebral cortex (in somatosensory areas) in adulthood, and that superficial layers II/III account for much of this difference while deep layers are relatively unaffected. That this deficit is specific to superficial layers would seem to indicate a defect during later neurogenesis, when superficial layers are formed. Oddly, despite the changes in cortical thickness, I observed no change in the number of superficial layer neurons marked by Cux1, nor did I see a significant change in the number of deep layer neurons as marked by Ctip2 staining. While the majority of superficial layer neurons are marked by Cux1, a subset of superficial layer neurons do not

express this marker, including parvalbumin positive interneurons (Nieto et al., 2004). It is possible that changes in the Cux1 negative population of layer II/III may account for the reduction in thickness.

I observed no significant changes in the size of pyramidal cell bodies, nor any change in the length of pyramidal cell dendritic arbor in *Met-Emx1* mice compared to controls. Previous work from another lab has also shown that *Met-Emx1* mice have a normal total dendritic arbor length, and reduced dendritic arbor distal to the cell body (Judson et al., 2010b), in agreement with our results. The lack of any significant changes in cell size or total dendritic arbor in *Met-Emx1* mice makes it unlikely that the changes I have observed in cortical volume or layer II/III thickness are due to changes in the size of individual pyramidal neurons.

After neurons are generated, they must migrate to their proper place in the cortical column. HGF-Met signaling has previously been shown to promote neuronal migration, particularly in interneurons (Powell et al., 2001b; Garzotto et al., 2008), but also in cultured cortical neurons (Sun et al., 2002; Segarra et al., 2006) and cortical explant culture (Sun et al., 2002; Giacobini et al., 2007). It is possible that loss of Met signaling alters cortical structure by impairing the migration of newborn neurons to their final positions. While I did not find any changes in total cell number for any of the layer markers examined, I did note that some $Cux1^{+}$ cells were located in abnormally deep

layers in *Met-Emx1* mice, suggesting that this mis-localization could contribute to the reduction in the size of layer II/III.

While not examined here, another possibility is that loss of Met signaling could alter laminar fate by influencing earlier fate choices between progenitor cell types. Specifically, transit amplifying cells known as intermediate progenitor cells (IPCs) are generated from radial glia and are thought to preferentially generate superficial layer neurons (Zimmer et al., 2004; Wu et al., 2005). Signaling molecules such as β-catenin have been shown to regulate INP population numbers (Mutch et al., 2010). Interestingly, HGF has been shown to induce β-catenin phosphorylation and nuclear localization in culture (Liou et al., 2002; Brembeck et al., 2004; David et al., 2008), and Met co-precipitates with β-catenin from hippocampal neurons (David et al., 2008). Future experiments will therefore address the effects of loss of Met signaling on the population of INPs in the developing cortex.

A further possibility which could explain the reduction in superficial layer thickness, as well as the ectopic $Cux1^+$ cells, is a change in neuronal proliferation in mice lacking functional Met in the cerebral cortex. In order to determine if cell proliferation could be altered by loss of Met signaling, I examined BrdU labeling in the cortex after a series of injections representing times at which deep or superficial layers are born. These data are presented in chapter 4.

Chapter 4: Loss of Met signaling alters cell proliferation in the embryonic cerebral cortex.

4.1 Introduction

The size of the cerebral cortex is largely determined by the regulation of proliferation in cortical progenitors (Caviness et al., 1995; Chenn and Walsh, 2002). Proliferation in the cortex is influenced by a number of factors, including growth factor signaling (Vaccarino et al., 1999; Raballo et al., 2000; Rash et al., 2011; Tiberi et al., 2012; Rash et al., 2013). In addition to influencing the overall size of the cerebral cortex, the timing of cell divisions, differentiation, and cell cycle exit during neural proliferation have profound effects on the laminar structure of the cortex (Caviness et al., 1995; Takahashi et al., 1999; Land and Monaghan, 2003; Roy et al., 2004; Mairet-Coello et al., 2012; Colasante et al., 2013).

I have previously shown that loss of Met signaling in *Met-Emx1* mice results in greater cerebral cortical volume in adult *Met-Emx1* mice (Smith et al., 2012), as well as changes in layer morphology (see Chapter 3). HGF-Met signaling has been shown to promote proliferation in cultured cortical stem cells (Kokuzawa et al., 2003), accelerate the differentiation of sympathetic neurons (Maina et al., 1998), and promote neuronal differentiation of embryonic stem (ES) derived cells (Kato et al., 2004). I therefore sought to examine if loss of Met signaling in the cerebral cortex influences cell proliferation during the neurogenic period. In order to do this, I performed a series of injections of bromodeoxyuridine (BrdU) at specific time points during cortical

neurogenesis. BrdU is a thymidine analog which incorporates into the DNA of cell in S phase (Nowakowski et al., 1989), and can be detected by immunohistochemical staining in order to locate cells which originated from those which were dividing around the time of a BrdU injection. I subsequently assessed BrdU labeling in the primary somatosensory (S1) or prelimbic (PL) cortex at postnatal day 0 (P0), in order to determine if loss of Met signaling altered the number of cells born at each embryonic age.

4. 2 Methods

4.2.1 Animals

Animal care procedures are described in Appendix 1: Common methods

4.2.2 BrdU injections

Met^{fx} dams were mated with *Met*^{fx}*/Emx1*^{Cre} sires, and checked daily for the appearance of a vaginal plug. The date of observation of a plug was counted as embryonic day 0.5 (E0.5). Dams were given a single intraperitoneal injection of 5-bromo-2'-deoxyuridine (BrdU, 50 mg/kg, Sigma Chemical Co, St. Louis, MO) on either E12.5, 14.5, or 16.5. For some experiments, pups were killed on postnatal day 0 (P0, the day of birth) and the brains were collected and submerged in 4% buffered paraformaldehyde and subsequently processed for immunohistochemistry. For co-localization experiments, P30 animals were transcardially perfused with 0.9% sterile saline and 4% buffered paraformaldehyde prior to collection of the brain.

4.2.3 Immunohistochemistry and histology

Brains were processed for immunohistochemistry according to standard laboratory techniques, as described in Appendix 1. The primary antibodies used were rabbit anti-Cux1 (1:100, Santa Cruz Biotechnology, Inc, Santa Cruz, CA), rabbit anti-Ctip2 (1:500, abcam), or rat anti-BrdU (1:1000, abcam), followed by appropriate secondary antibodies.

4.2.4 Cell counts and analysis

BrdU immunopositive cells found in a 200 µm wide radial strip of somatosensory or prelimbic cortex were counted, and their position relative to pia recorded, using the analyze particles tool in NIH ImageJ version 1.43. To compare counts at various levels of the cortex, $BrdU^+$ cells were assigned to radial bins by their distance from pia, normalized to total cortical thickness for each sample. At least 3 control brains and 3 *Met-Emx1* brains were measured for each injection time.

I counted three adjacent, non-overlapping strips within S1 (with the white matter side of the center sample window just lateral from the hippocampus or lateral ventricle) from three coronal sections spaced 400 µm apart, with the middle section corresponding to plate 6 of Jacobowitz and Abbott's *Chemoarchitectonic Atlas of the Developing Mouse Brain* (Jacobowitz and Abbott, 1998), containing the rostral end of the hippocampus. For PL, only one strip was counted, in order to avoid sampling from adjacent cortical areas such as anterior cingulate cortex. Measurements for PL were taken from two sections

spaced 400 µm apart corresponding to plates 3 and 4 (Jacobowitz and Abbott, 1998), rostral to the crossing of the corpus callosum and caudal to the level where the genu of the corpus callosum is no longer present in the sections.

Statistical significance was determined for total counts across all bins using a Student's *t*-test analysis in Microsoft Excel or SigmaPlot, or for individual bins using a Holm-Sidak multiple comparisons test. Differences between the distributions of $BrdU^+$ cells across the cortex (by distance from pia) were determined using the Kolmogorov-Smirnov test.

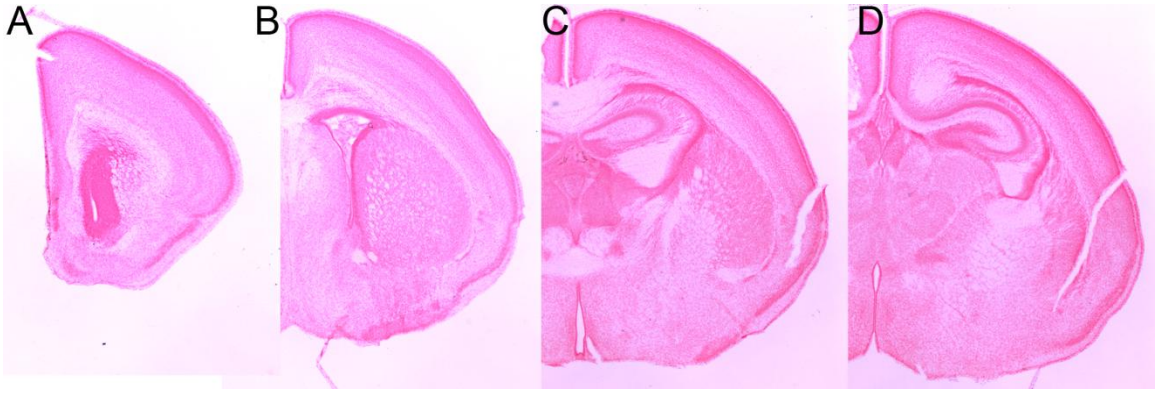

Figure 4.1. Sampling levels for BrdU counts

Representative images show nuclear fast red stained coronal sections from a P0 control brain at the levels from which measurements were taken of PL (A) and S1 (B-D), and correspond roughly to plates 4 (A), 5 (B), 6, (C) and 7 (D) of Jacobowitz and Abbott's *Chemoarchitectonic Atlas of the Developing Mouse Brain* (Jacobowitz and Abbott, 1998).

4.3 Results

To determine if changes in layer morphology could be due to altered neuroprogenitor proliferation, I sought to determine if loss of Met signaling in the cerebral wall altered the number of cells born at various points during corticogenesis. During development, cortical layers are generated in an inside-out fashion, with early born cells populating deep layers, and later born cells forming progressively more superficial layers (Angevine and Sidman, 1961). I therefore examined BrdU staining in P0 *Met-Emx1* and control mice after BrdU injections at E12.5, E14.5, and E16.5. The majority of cells born around E12.5 in mice populate layer VI, with some cells moving into layer V (Takahashi et al., 1999). By E14.5, most of the deep layer cells have been generated and newborn cells begin to populate more superficial layers, beginning with layer IV. The gestational age E16.5 is nearing the tail end of the neurogenic period, and most cells born around this time will populate layers II and III (Takahashi et al., 1999). To determine if loss of Met function alters when cells are generated in the cortex, I counted the number of $BrdU^+$ cells in 200 µm wide strips of either S1 (plates 5-7 (Jacobowitz and Abbott, 1998)) or PL (plates 3-4 (Jacobowitz and Abbott, 1998)) cortex in P0 *Met-Emx1* and control mice after injections at E12.5, E14.5, or E16.5.

4.3.1 BrdU incorporation: Somatosensory cortex

After injections at E12.5, I first sought to determine if $BrdU^+$ cell density differed among sampling locations within S1. I found that there was no effect of medio-lateral sampling area on $BrdU^+$ cell density at P0 in either control (one-way ANOVA, $F(2,23) = 0.132$, $p = 0.876$) or *Met-Emx1* mice (one-way ANOVA, $F(2,32) = 1.21$, $p = 0.313$). I did, however, find a significant effect of rostro-caudal sampling location on BrdU cell density in both control (one-way ANOVA, $F(2, 23) = 3.70$, $p = 0.042$) and *Met-Emx1* mice (one-way ANOVA, $F(2, 32) = 5.034$, $p = 0.013$), with higher densities at caudal levels (Holm-Sidak test, $p = 0.024$), so here I consider each level separately.

I found no significant difference in $BrdU^+$ cell density at the level of plate 5, either across the overall thickness of the cortex (Fig. 4.1, control, $6.0 \times 10^4 \pm 9.7 \times 10^3$ cells/mm^3 *Met-Emx1*, $6.6 \times 10^4 \pm 7.5 \times 10^3$ cells/mm^3; Student's t test, $p = 0.607$), or in individual bins (Holm-Sidak test, $p > 0.05$ for all bins).At the level of plate 6, however, I found a significant increase in $BrdU^+$ cell density in *Met-Emx1* mice compared to controls across the overall thickness of the cerebral cortex (Fig. 4.2., control, $3.6 \times 10^4 \pm 5.9 \times 10^3$ cells/mm^3; *Met-Emx1*, $6.6 \times 10^4 \pm 6.5 \times 10^3$ cells/mm^3; Student's *t* test, $p = 0.004$). I also found increases in $BrdU^+$ cell density in numerous bins across the thickness of the cortical wall at this level, from 30-35% to 80-85% of the thickness of the cortex (Holm-Sidak test, $p < 0.05$). At the level of plate 7, I again found a significant increase in $BrdU^+$ cell density in S1 after injections at E12.5 (Fig 4.3., control, $6.2 \times 10^4 \pm 4.7 \times 10^3$ cells/mm^3; *Met-Emx1*, $9.9 \times 10^4 \pm 1.1 \times 10^4$ cells/mm^3; Holm-Sidak test, $p = 0.019$). I also

found increases in $BrdU^+$ cell density in several more superficial bins, ranging from 20-25% of cortical thickness to 45-50% (Holm-Sidak test, $p < 0.05$), although the increase was not as pronounced as at the level of plate 6.

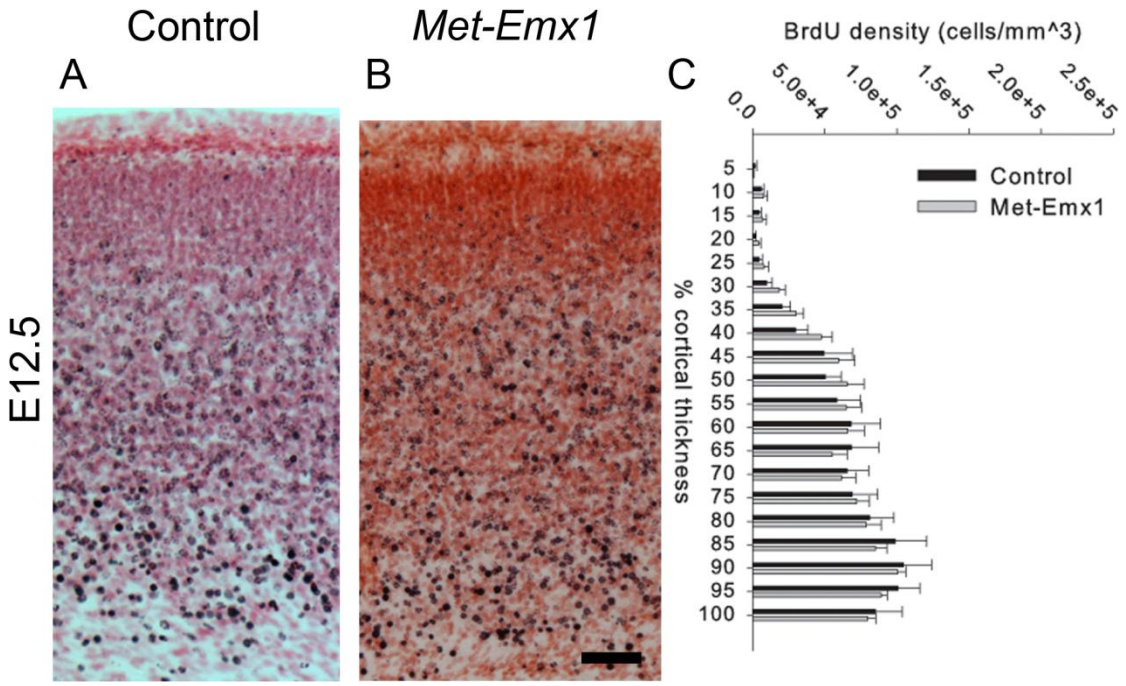

Figure 4.2. Unaltered BrdU labeling at the level of plate 5 in somatosensory cortex of *Met-Emx1* mice after BrdU injections at E12.5.

Representative images of P0 somatosensory cortex are shown for control (A) and *Met-Emx1* (B) mice after BrdU injections at E12.5. Quantifications of the density of BrdU labeled cells in radial bins each comprising 5% of the total cortical thickness are shown at right (C). * indicates $p < 0.05$ (Holm-Sidak test).Scale bar in B represents 50 µm.

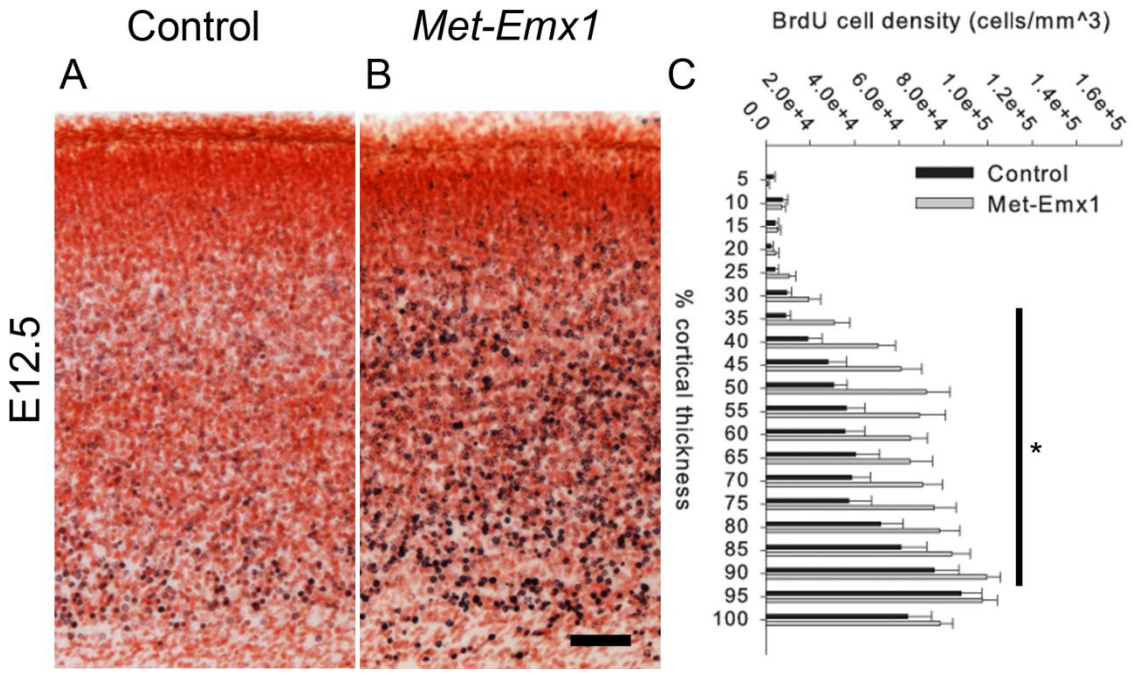

Figure 4.3. Increased BrdU cell density at the level of plate 6 in somatosensory cortex of *Met-Emx1* mice after injections at E12.5.

Representative images of P0 somatosensory cortex are shown for control (A) and *Met-Emx1* (B) mice after BrdU injections at E12.5. Quantifications of the density of BrdU labeled cells in radial bins each comprising 5% of the total cortical thickness are shown at right (C). * indicates $p < 0.05$ (Holm-Sidak test).Scale bar in B represents 50 µm.

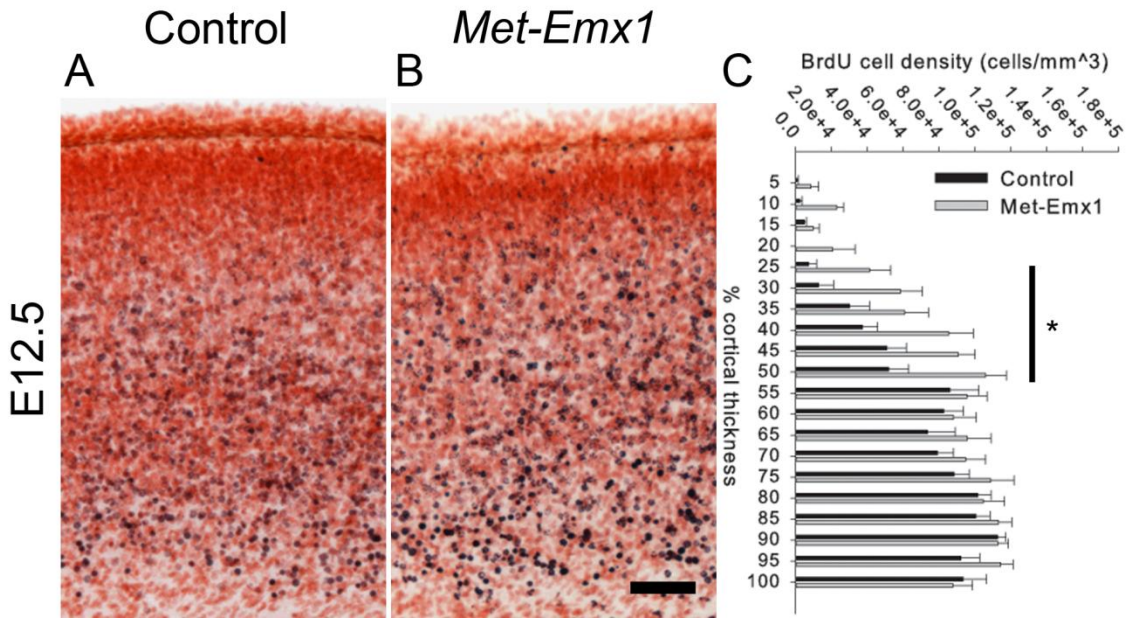

Figure 4.4. Increased BrdU cell density at the level of plate 7 in the somatosensory cortex of *Met-Emx1* mice after injections at E12.5

Representative images of P0 somatosensory cortex are shown for control (A) and *Met-Emx1* (B) mice after BrdU injections at E12.5. Quantifications of the density of BrdU labeled cells in radial bins each comprising 5% of the total cortical thickness are shown at right (C). * indicates $p < 0.05$ (Holm-Sidak test).Scale bar in B represents 50 µm.

When I examined BrdU labeling in S1 after injections at E14.5, I saw no difference in BrdU labeling between different medio-lateral sampling locations within S1 within either control (one-way ANOVA, F (2, 38) = 0.042, p = 0.959) or *Met-Emx1* (one-way ANOVA, F (2, 31) = 0.078, p = 0.925) mice. I therefore collapsed these measurements within each rostral-caudal level. While there were no significant differences between BrdU cell densities at different rostro-caudal levels in *Met-Emx1* mice (one-way ANOVA, F (2, 31) = 2.169, p = 0.132), the difference in BrdU cell densities between levels in control animals approached significance (one-way ANOVA, F (2, 38) = 3.19, p = 0.053), so here I consider each level separately.

No overall change in BrdU cell density was observed in *Met-Emx1* mice at the level of plate 5 after injections at E14.5, (Fig. 4.4. control, 6.3 x 10^4± 4.3 x 10^4 cells/mm^3; *Met-Emx1*, 7.3 x 10^4± 2.9 x 10^3 cells/mm^3; Student's t test, p = 0.074). I did, however, see a reduction in BrdU$^+$ cell density in a few of the most superficial bins (0-5%, control 4.2 x 10^4 ± 6.1 x 10^3 cells/mm^3; *Met-Emx1*, 1.4 x 10^4 ± 4.4 x 10^3 cells/mm^3; Holm-Sidak test, p = 0.012; 5-10%, control, 8.4 x 10^4 ± 6.8 x 10^3 cells/mm^3; *Met-Emx1*, 4.7 x 10^4 ± 8.1 x 10^3 cells/mm^3; Holm-Sidak test, p < 0.001; 10-15%, control, 1.3 x10^5 ± 3.4 x 10^3 cells/mm^3; *Met-Emx1*, 9.5 x0 10^4 ± 1.0 x 10^4 cells/mm^3; Holm-Sidak test, p = 0.003).

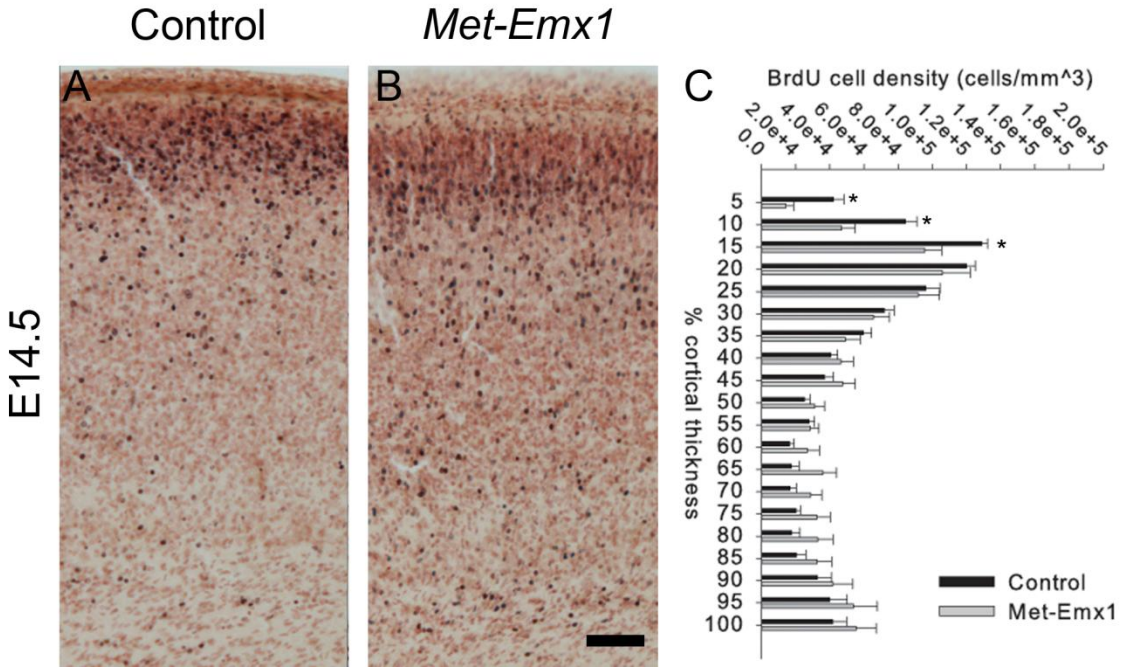

Figure 4.5. Altered BrdU labeling at the level of plate 5 in the somatosensory cortex of *Met-Emx1* mice after BrdU injections at E14.5.

Representative images of P0 somatosensory cortex are shown for control (A) and *Met-Emx1* (B) mice after BrdU injections at E14.5. Quantifications of the density of BrdU labeled cells in radial bins each comprising 5% of the total cortical thickness are shown at right (C). * indicates $p < 0.05$ (Holm-Sidak test).Scale bar in B represents 50 µm.

At the level of plate 6, I found a significant decrease in overall BrdU cell density in *Met-Emx1* mice after injections at E14.5 (Fig. 4.5. control, 7.7 x 10^4± 5.1 x 10^4 cells/mm^3; *Met-Emx1*, 5.8 x 10^4± 4.3 x 10^5 cells/mm^3; Student's *t* test, $p = 0.013$). Decreases in $BrdU^+$ cell density were found in the 5-10% (control, 7.7 x 10^4 ± 1.0 x 10^4 cells/mm^3; *Met-Emx1*, 3.0 x 10^4 ± 4.8 x 10^5 cells/mm^3; Holm-Sidak test, $p < 0.001$), 15-20% (control, 1.0 x 10^5 ± 8.6 x 10^3 cells/mm^3; *Met-Emx1*, 8.9 x 10^{-5} ± 1.0 x 10^4 cells/mm^3; Holm-Sidak test, $p = 0.040$), and 95-100% (control, 6.6 x 10^4 ± 1.0 x 10^4 cells/mm^3; *Met-Emx1*, 5.0 x 10^4 ± 8.9 x 10^5 cells/mm^3; Holm-Sidak test, $p = 0.003$) bins.

At the level of plate 7, the overall density of BrdU labeled cells was again lower in *Met-Emx1* mice, although this did not reach significance (Fig 4.6. control, 7.7 x 10^4 ± 3.2 x 10^4 cells/mm^3; *Met-Emx1*, 6.4 x 10^4± 6.3 x 10^5 cells/mm^3; Student's *t* test, $p = 0.071$). When I examined $BrdU^+$ cell density in individual bins, I found substantial decreases in *Met-Emx1* mice in the 10-15% (control, 1.4 x 10^5 ± 1.7 x 10^4 cells/mm^3; *Met-Emx1*, 9.7 x 10^4 ± 7.3 x 10^5 cells/mm^3; Holm-Sidak test, $p < 0.001$), 15-20% (control, 1.5 x 10^5 ± 1.5 x 10^4 cells/mm^3; *Met-Emx1*, 9.1 x 10^4 ± 1.4 x 10^4 cells/mm^3; Holm-Sidak test, $p < 0.001$), 20-25% (control, 1.4 x 10^5 ± 1.3 x 10^4 cells/mm^3; *Met-Emx1*, 7.7 x 10^4 ± 1.3 x 10^4 cells/mm^3; Holm-Sidak test, $p < 0.001$), and 25-30% (control, 9.3 x 10^4 ± 7.8 x 10^3 cells/mm^3; *Met-Emx1*, 6.6 x 10^4 ± 1.1 x 10^4 cells/mm^3; Holm-Sidak test, $p = 0.003$) bins.

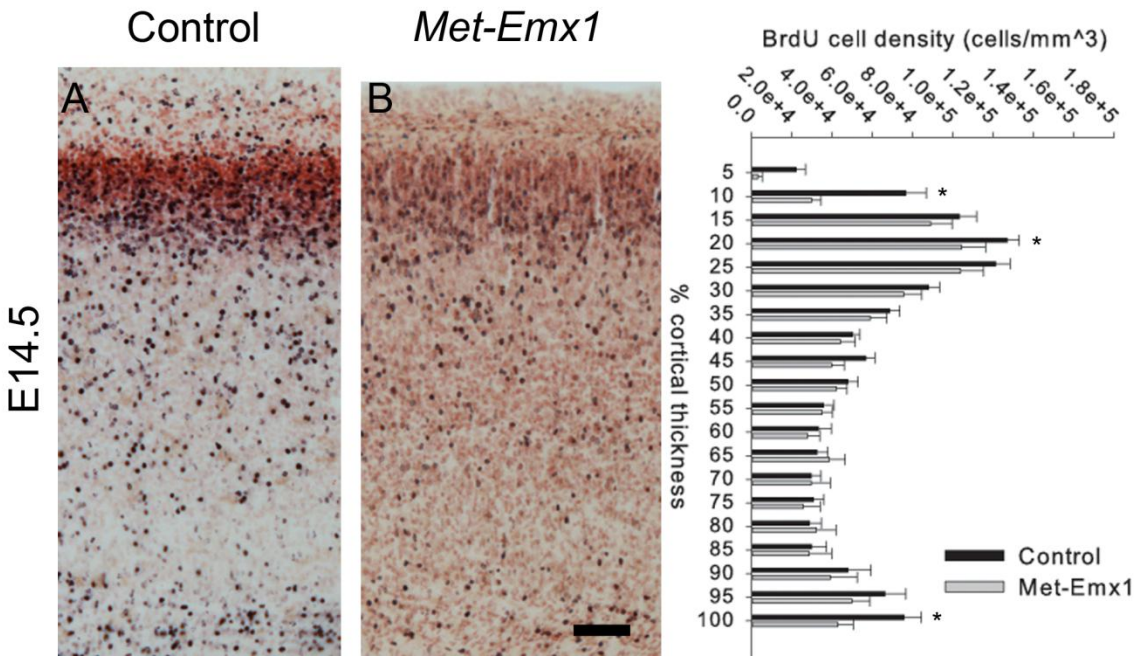

Figure 4.6. Reduced BrdU cell density at the level of plate 6 in the somatosensory cortex of *Met-Emx1* mice after BrdU injections at E14.5.

Representative images of P0 somatosensory cortex are shown for control (A) and *Met-Emx1* (B) mice after BrdU injections at E14.5. Quantifications of the density of BrdU labeled cells in radial bins each comprising 5% of the total cortical thickness are shown at right (C). * indicates $p < 0.05$ (Holm-Sidak test).Scale bar in B represents 50 µm.

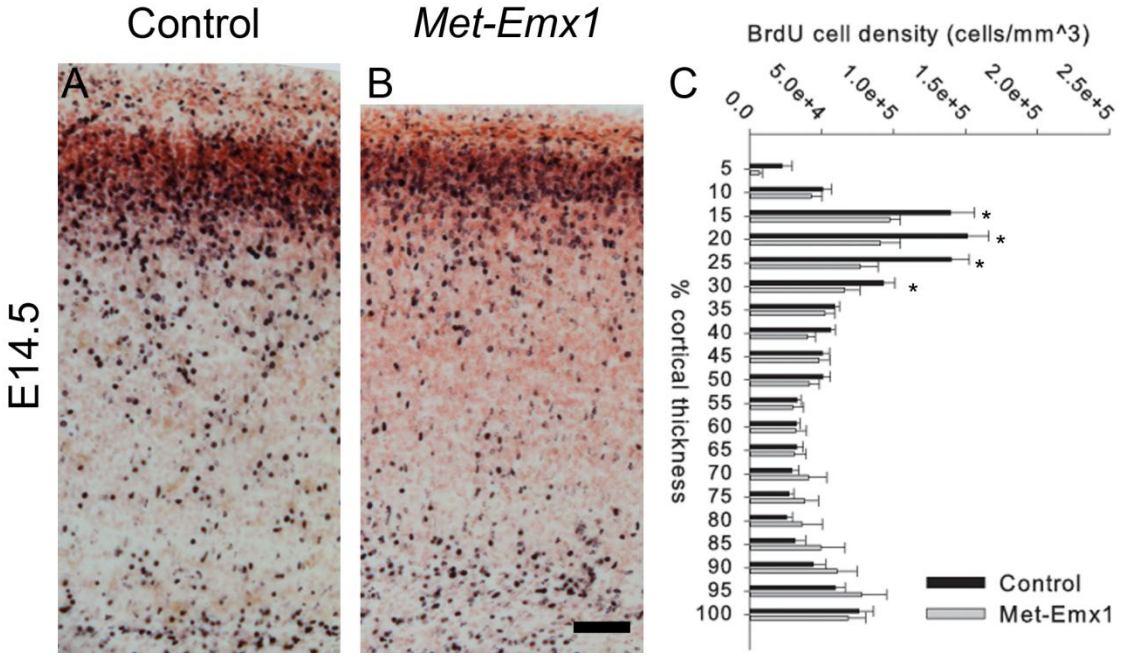

Figure 4.7. Reduced BrdU cell density at the level of plate 7 in the somatosensory cortex of *Met-Emx1* mice after BrdU injections at E14.5

Representative images of P0 somatosensory cortex are shown for control (A) and *Met-Emx1* (B) mice after BrdU injections at E14.5. Quantifications of the density of BrdU labeled cells in radial bins each comprising 5% of the total cortical thickness are shown at right (C). * indicates $p < 0.05$ (Holm-Sidak test).Scale bar in B represents 50 µm.

After injections at E16.5, I again saw no effect of medial-lateral level on BrdU density in either control (p = 0.438) or *Met-Emx1* (p = 0.196), and so I collapsed these measurements across each rostral-caudal level. I did see a difference in BrdU cell density across rostral-caudal levels in *Met-Emx1* mice after injections at E16.5 (one-way ANOVA, F (2, 22) = 5.18, p = 0.015), with higher densities at the level of plate 7 compared to plate 5 (Holm-Sidak, p = 0.013)

At the level of plate 5, I found a significant decrease in the overall density of BrdU cells in S1 in *Met-Emx1* mice relative to controls after injections at E16.5 (Fig. 4.7. Control, $8.8 \times 10^4 \pm 1.1 \times 10^4$ cells/mm^3; *Met-Emx1*, $4.8 \times 10^4 \pm 5.2 \times 10^3$ cells/mm^3; Student's t test, p = 0.006). Specifically, significant reductions were observed in deepest bins, at 90-95% (control, $1.4 \times 10^5 \pm 5.2 \times 10^4$ cells/mm^3; *Met-Emx1*, $4.3 \times 10^4 \pm 5.9 \times 10^3$ cells/mm^3; Holm-Sidak test, $p < 0.001$) and 95-100% (control, $2.0 \times 10^5 \pm 6.2 \times 10^4$ cells/mm^3; *Met-Emx1*, $7.0 \times 10^4 \pm 1.2 \times 10^3$ cells/mm^3; Holm-Sidak test, $p < 0.001$) of the thickness of the cortical wall.

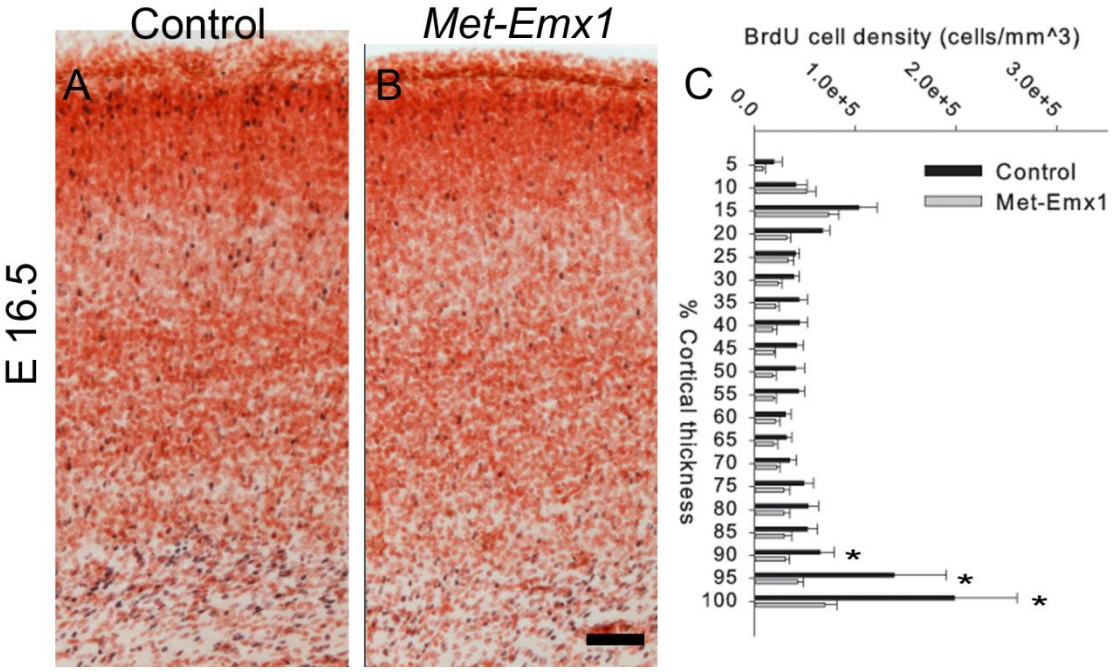

Figure 4.8. Reduced BrdU cell density at the level of plate 5 in the somatosensory cortex of *Met-Emx1* mice after BrdU injections at E16.5.

Representative images of P0 somatosensory cortex are shown for control (A) and *Met-Emx1* (B) mice after BrdU injections at E16.5. Quantifications of the density of BrdU labeled cells in radial bins each comprising 5% of the total cortical thickness are shown at right (C). * indicates $p < 0.05$ (Holm-Sidak test).Scale bar in B represents 50 µm.

At the level of plate 6, I again found a significant decrease in the overall density of BrdU cells in S1 in *Met-Emx1* mice relative to controls (Fig 4.8. control, $8.9 \times 10^4 \pm 1.1 \times 10^4$ cells/mm^3; *Met-Emx1*, $6.0 \times 10^4 \pm 5.8 \times 10^3$ cells/mm^3; Student's *t* test, $p = 0.039$). Reductions in BrdU cell density were found in both deep (90-95%; control, $1.2 \times 10^5 \pm 3.2 \times 10^4$ cells/mm^3; *Met-Emx1*, $5.8 \times 10^4 \pm 1.2 \times 10^4$ cells/mm^3; Holm-Sidak test, $p < 0.001$; and 95-100%; control, $1.4 \times 10^5 \pm 3.5 \times 10^4$ cells/mm^3; *Met-Emx1*, $1.0 \times 10^5 \pm 1.9 \times 10^4$ cells/mm^3; Holm-Sidak test, $p = 0.012$) and superficial bins (10-15%; control, $1.4 \times 10^5 \pm 2.0 \times 10^4$ cells/mm^3; *Met-Emx1*, $7.6 \times 10^4 \pm 2.0 \times 10^4$ cells/mm^3; Holm-Sidak test, $p < 0.001$; and 15-20%; control, $1.0 \times 10^5 \pm 1.5 \times 10^4$ cells/mm^3; *Met-Emx1*, $6.0 \times 10^4 \pm 9.0 \times 10^3$ cells/mm^3; Holm-Sidak test, $p = 0.018$).

The effect of loss of Met signaling on overall BrdU cell density was no longer significant at the level of plate 7 (Fig 4.9. Control, $8.3 \times 10^4 \pm 1.1 \times 10^4$ cells/mm^3; *Met-Emx1*, $7.5 \times 10^4 \pm 5.5 \times 10^3$ cells/mm^3; Student's *t* test, $p = 0.577$). At this level, I found a reduction in BrdU density in only one bin, between 90 and 95% of cortical thickness (control, $1.4 \times 10^5 \pm 5.6 \times 10^4$ cells/mm^3; *Met-Emx1*, $5.9 \times 10^4 \pm 6.3 \times 10^3$ cells/mm^3; Holm-Sidak test, $p = 0.006$).

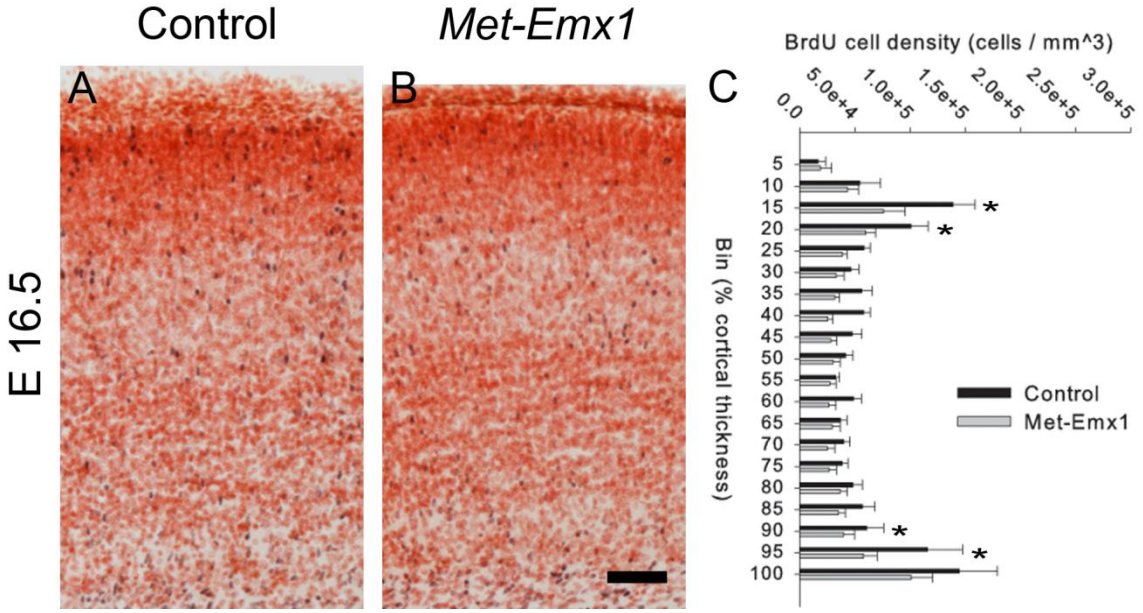

Figure 4.9. Reduced BrdU cell density at the level of plate 6 in the somatosensory cortex of *Met-Emx1* mice after BrdU injections at E16.5.

Representative images of P0 somatosensory cortex are shown for control (A) and *Met-Emx1* (B) mice after BrdU injections at E16.5. Quantifications of the density of BrdU labeled cells in radial bins each comprising 5% of the total cortical thickness are shown at right (C). * indicates $p < 0.05$ (Holm-Sidak test).Scale bar in B represents 50 µm.

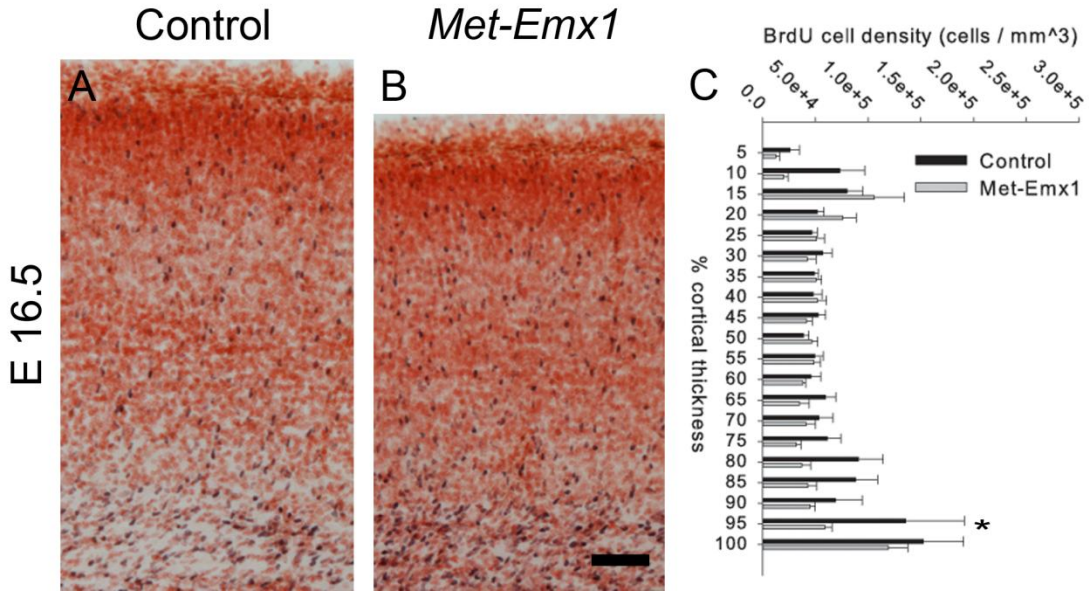

Figure 4.10. Reduced BrdU cell density at the level of plate 7 in the somatosensory cortex of *Met-Emx1* mice after BrdU injections at E16.5.

Representative images of P0 somatosensory cortex are shown for control (A) and *Met-Emx1* (B) mice after BrdU injections at E16.5. Quantifications of the density of BrdU labeled cells in radial bins each comprising 5% of the total cortical thickness are shown at right (C). * indicates $p < 0.05$ (Holm-Sidak test).Scale bar in B represents 50 µm.

4.3.2. BrdU incorporation: Prelimbic cortex

Counts in PL were taken from a single 200 µm radial strip for each section, located medial to the genu of the corpus callosum, at the level of coronal plates 3-4 (Jacobowitz and Abbott, 1998). I found no difference in BrdU labeling between rostral-caudal levels within PL for either control or *Met-Emx1* mice at any of the injection times examined (Student's *t* test, $p > 0.05$ in each case), so the two levels were combined for subsequent analysis.

After injections at E12.5, I found an increase in the overall $BrdU^+$ cell density in PL in *Met-Emx1* mice relative to controls (Fig 4.10., control, $3.4 \times 10^4 \pm 3.6 \times 10^3$ cells/mm^3; *Met-Emx1*, $5.1 \times 10^4 \pm 5.0 \times 10^3$ cells/mm^3; Student's *t* test, $p = 0.033$). There were also increases in BrdU cell density specifically within the 55-60% (control, $6.8 \times 10^4 \pm 1.0 \times 10^4$ cells/mm^3; *Met-Emx1*, $3.7 \times 10^4 \pm 7.7 \times 10^3$ cells/mm^3; Holm-Sidak test, $p = 0.039$), 60-65% (control, $7.2 \times 10^4 \pm 1.1 \times 10^4$ cells/mm^3; *Met-Emx1*, $3.6 \times 10^4 \pm 6.3 \times 10^3$ cells/mm^3; Holm-Sidak test, $p = 0.018$), 70-75% (control, $7.8 \times 10^4 \pm 1.0 \times 10^4$ cells/mm^3; *Met-Emx1*, $4.7 \times 10^4 \pm 6.7 \times 10^3$ cells/mm^3; Holm-Sidak test, $p = 0.040$), and 90-95% bins (control, $1.1 \times 10^5 \pm 2.4 \times 10^4$ cells/mm^3; *Met-Emx1*, $6.5 \times 10^4 \pm 6.8 \times 10^3$ cells/mm^3; Holm-Sidak test, $p = 0.001$).

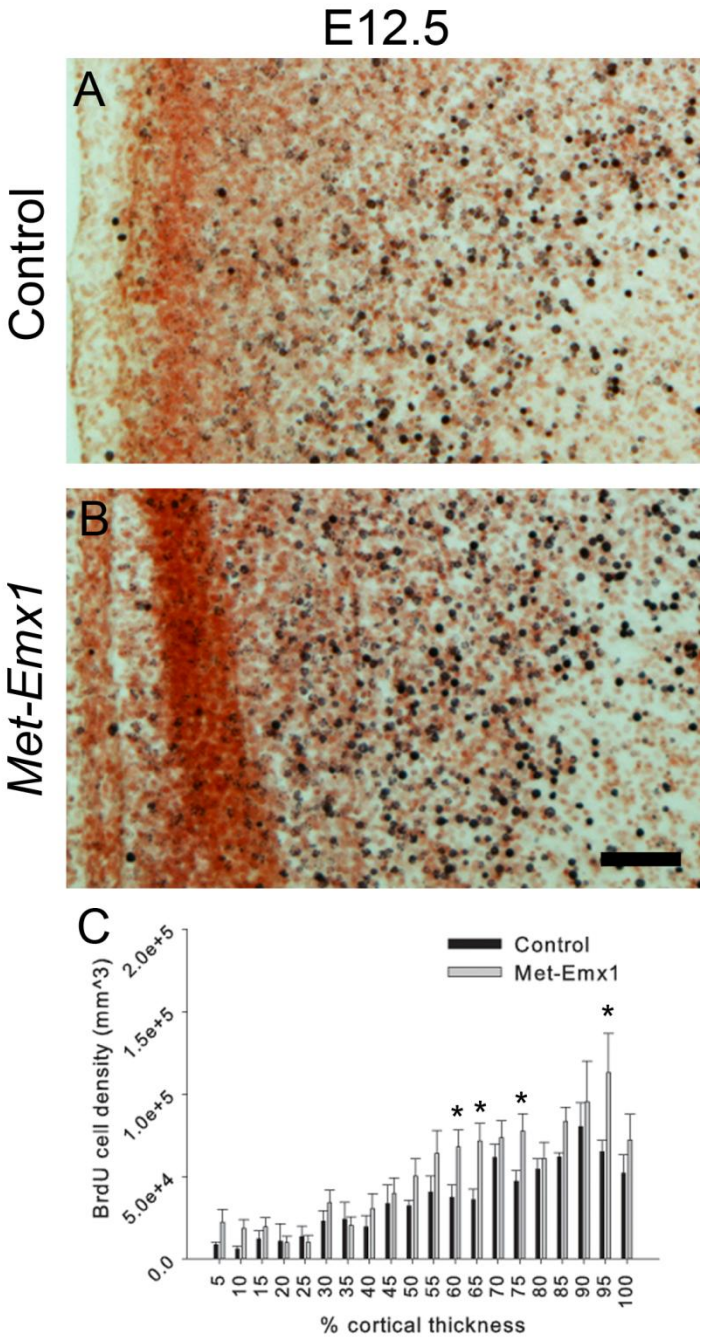

Figure 4.11. Altered BrdU labeling in prelimbic cortex of *Met-Emx1* mice after BrdU injections at E12.5.

Representative images of P0 prelimbic cortex are shown for control (A) and *Met-Emx1* (B) mice after BrdU injections at E12.5. Quantifications of the density of BrdU labeled cells in bins representing 5% of total cortical thickness are shown in (C). * indicates $p < 0.05$ (Holm-Sidak test). Medial is to the left. Scale bar in (B) represents 50 µm.

After injections at E14.5, there was a substantial reduction in the overall density of $BrdU^+$ cells across PL in *Met-Emx1* mice (Fig. 4.11., control, $9.7 \times 10^4 \pm 6.0 \times 10^3$ cells/mm^3; *Met-Emx1*, $5.4 \times 10^4 \pm 5.6 \times 10^3$ cells/mm^3; Student's *t* test, $p < 0.001$). This effect appeared most pronounced in superficial layers. I saw a significant decrease in $BrdU^+$ cell density in the 10-15% (control, $2.2 \times 10^5 \pm 4.7 \times 10^4$ cells/mm^3; *Met-Emx1*, $1.1 \times 10^5 \pm 2.6 \times 10^4$ cells/mm^3; Holm-Sidak test, $p < 0.001$) and 15-20% (control, $3.7 \times 10^5 \pm 9.0 \times 10^4$ cells/mm^3; *Met-Emx1*, $1.6 \times 10^5 \pm 2.8 \times 10^4$ cells/mm^3; Holm-Sidak test, $p < 0.001$) bins in *Met-Emx1* mice.

After injections at E16.5, I saw no change in the overall density of $BrdU^+$ cells in PL in *Met-Emx1* mice relative to controls (Fig 4.12., control, $3.6 \times 10^4 \pm 8.1 \times 10^3$; *Met-Emx1*, $2.5 \times 10^4 \pm 4.3 \times 10^3$, Student's *t* test, $p = 0.249$). I did, however, find significant decreases in $BrdU^+$ cell density in the 10-15% (control, $5.0 \times 10^4 \pm 1.4 \times 10^3$ cells/mm^3; *Met-Emx1*, $2.2 \times 10^4 \pm 7.7 \times 10^3$ cells/mm^3; Holm-Sidak test, $p = 0.031$) and 95-100% (control, $1.1 \times 10^5 \pm 2.5 \times 10^4$ cells/mm^3; *Met-Emx1*, $6.7 \times 10^4 \pm 1.5 \times 10^4$ cells/mm^3; Holm-Sidak test, $p = 0.003$) bins.

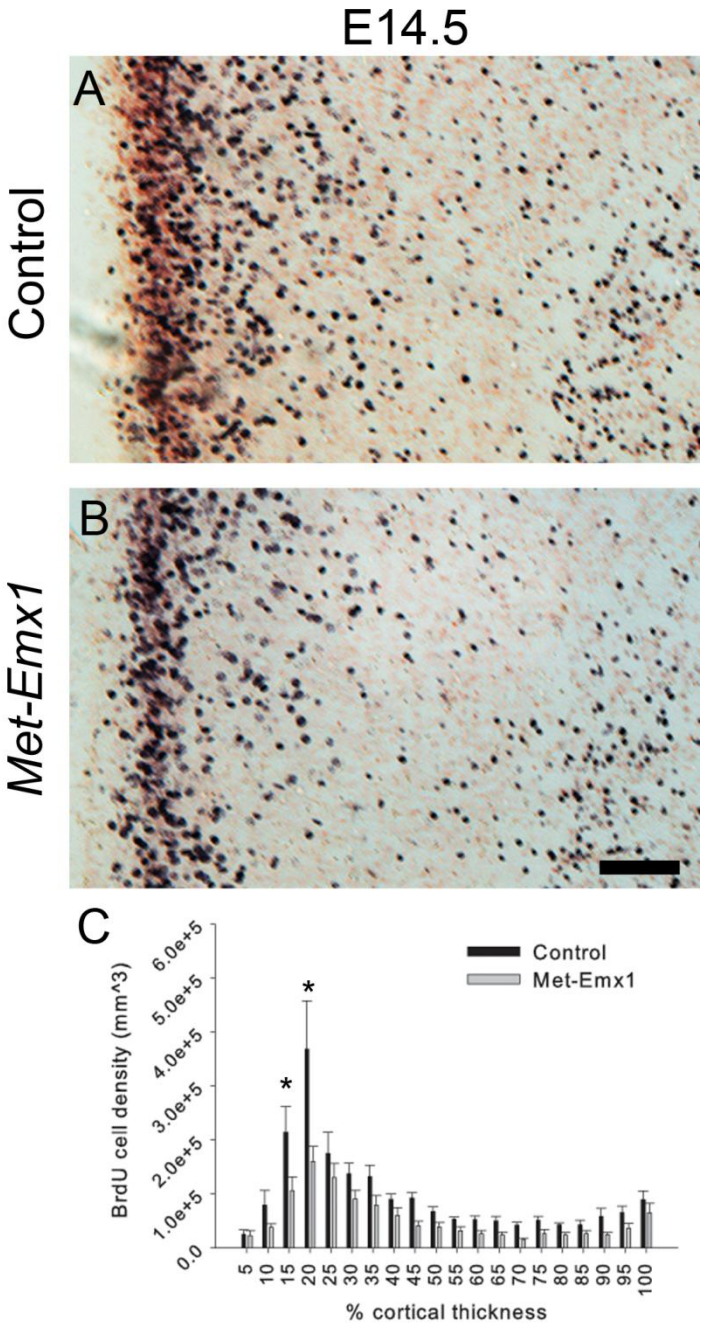

Figure 4.12. Altered BrdU labeling in prelimbic cortex of *Met-Emx1* mice after BrdU injections at E14.5.

Representative images of P0 prelimbic cortex are shown for control (A) and *Met-Emx1* (B) mice after BrdU injections at E12.5. Quantifications of the density of BrdU labeled cells in bins representing 5% of total cortical thickness are shown in (C). * indicates $p < 0.05$ (Holm-Sidak test). Medial is to the left. Scale bar in (B) represents 50 µm.

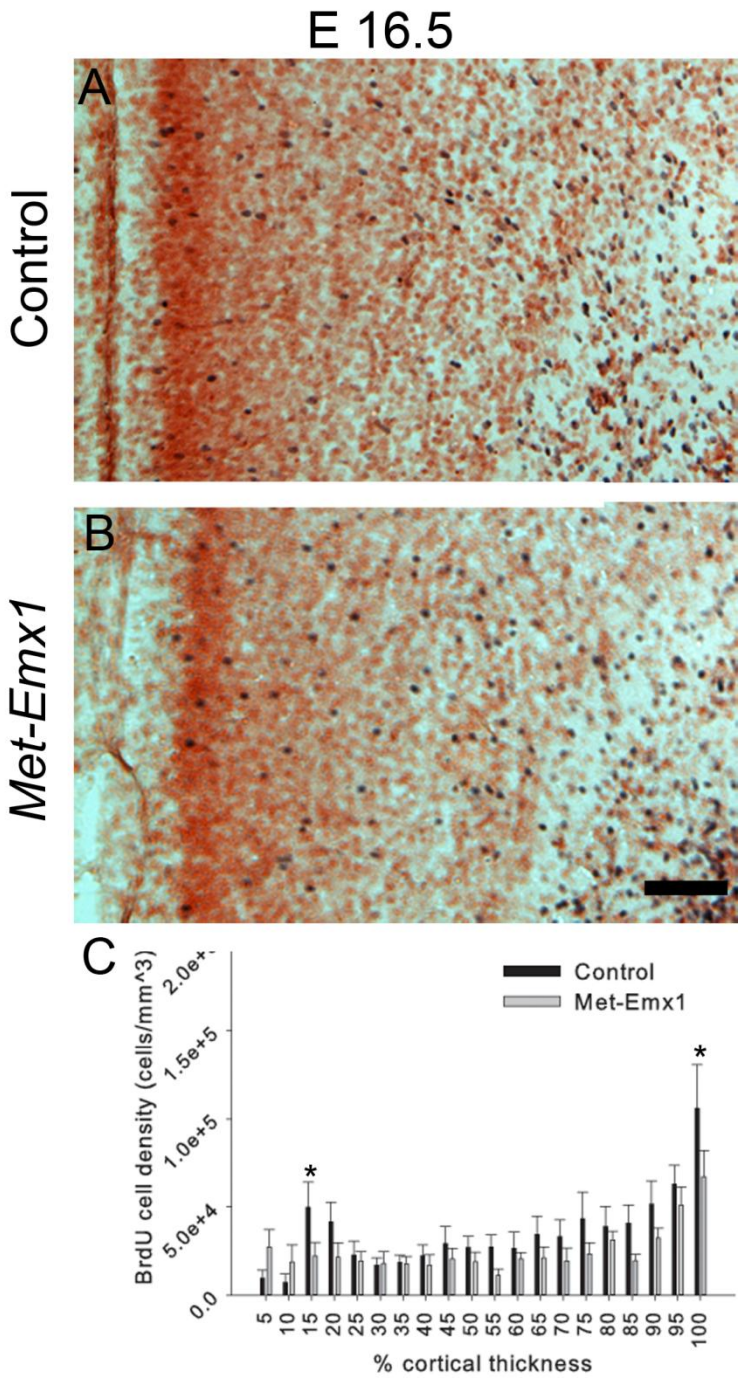

Figure 4.13. Altered BrdU labeling in prelimbic cortex of *Met-Emx1* mice after BrdU injections at E16.5.

Representative images of P0 prelimbic cortex are shown for control (A) and *Met-Emx1* (B) mice after BrdU injections at E12.5. Quantifications of the density of BrdU labeled cells in bins representing 5% of total cortical thickness are shown in (C). * indicates $p < 0.05$ (Holm-Sidak test). Medial is to the left. Scale bar in (B) represents 50 µm.

I also compared changes in the total number of $BrdU^+$ cells counted per radial strip for each rostro-caudal level and injection time. The pattern of changes is largely the same as for cell density, with the exceptions that changes in cell number in *Met-Emx1* mice do not reach significance at the level of plate 6 after injections at E14.5 (Fig. 4.13., control, 406.0 ± 23.6 cells; *Met-Emx1*, 339.6 ± 24.8 cells, Holm-Sidak test, $p = 0.061$) or E16.5 (Fig. 4.13., control, 292.2 ± 33.8 cells; *Met-Emx1*, 203.0 ± 32.9 cells, Holm-Sidak test, $p = 0.088$). Significant differences were still found in S1 after injections at E12.5 at the levels of plate 6 (Fig. 4.13., control, 159.7 ± 23.0 cells; *Met-Emx1*, 267.8 ± 30.4 cells, Holm-Sidak test, $p = 0.013$) and plate 7 (Fig. 4.13., control, 230.5 ± 15.9 cells; *Met-Emx1*, 338.9 ± 31.4 cells, Holm-Sidak test, $p = 0.035$), as well as at the level of plate 5 after injections at E16.5 (Fig. 4.13., control, 294.9 ± 52.3 cells; *Met-Emx1*, 162.9 ± 22.7 cells, Holm-Sidak test, $p = 0.013$). The same pattern of changes was also observed in PL, with significantly more $BrdU^+$ cells in PL after injections at E12.5 (Fig. 4.13., control 152.3 ± 12.1 cells; *Met-Emx1*, 229.0 ± 25.7 cells; Student's t test, $p = 0.042$) and fewer $BrdU^+$ cells after injections at E14.5 (Fig. 4.13., control 352.6 ± 26.9 cells; *Met-Emx1*, 216.40 ± 21.6 cells; Student's t test, $p < 0.001$). It does not appear that differences in the number or density of BrdU+ cells are due to differences in cortical thickness, as cortical thickness was not significantly different between control and Met-Emx1 mice at P0 at any of the levels examined (Fig. 4.15, two-way ANOVA, main effect of genotype $F(1,34) = 1.194$, $p = 0.284$; genotype x bregma, $F(3,34) = 0.181$, $p = 0.909$)

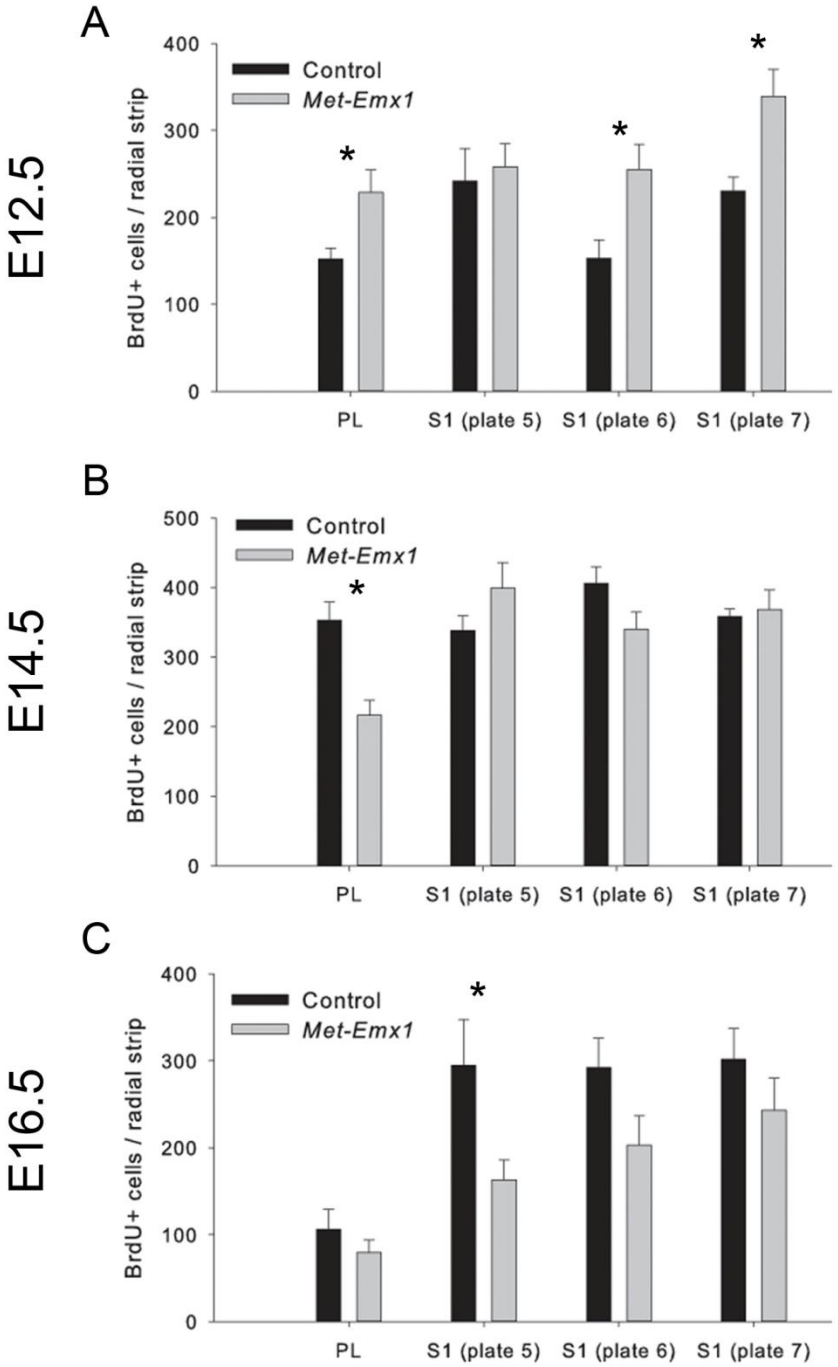

Figure 4.14. Estimated number of BrdU cells per radial strip counted for each injection time and region.

Quantification of the total number of cells counted per radial strip after injections at E12.5 (A), E14.5 (B) and E16.5 (C) are shown for each rostro-caudal level of S1 examined as well as for PL.

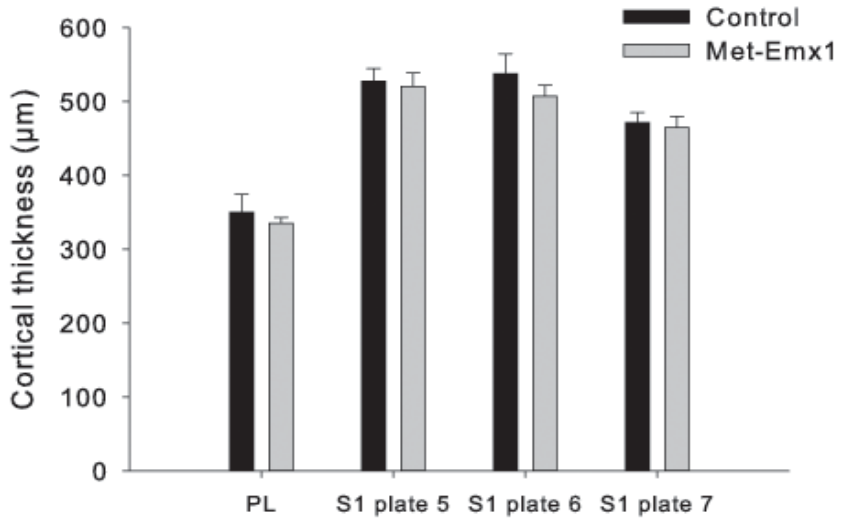

Figure 4.15. Cortical thickness is unaltered at P0.

Quantification of cortical thickness at each level where BrdU density measurements were taken is shown for control and Met-Emx1 mice.

4.3.3 BrdU co-labeling

My BrdU labeling suggests that loss of Met signaling in the cortex in *Met-Emx1* mice results in increased proliferation during early neurogenesis, and decreased proliferation later in neurogenesis. However, I did not find either any increase in the number of deep layer neurons, as would be expected after increased cell birth at E12.5, nor did I find any decrease in the number of $Cux1^+$ cells, as would be expected given decreased BrdU labeling after injections at E16.5. I did, however, find a number of $Cux1^+$ cells residing in abnormally deep layers. This raises the possibility that some of the "extra" early generated cells in *Met-Emx1* mice differentiate as superficial layer neurons, despite their earlier origin, and take up residence in deep layers, possibly because they are unable to migrate to their normal destinations when they are born prior to most other superficial layer cells. To address this possibility, I performed immunohistochemical co-staining for BrdU and Cux1 on P0 or P30 mice after BrdU injections at E12.5. I counted $BrdU^+$ and $Cux1^+/BrdU^+$ cells in 200 µm wide strips of somatosensory cortex in the barrel field. In general I saw very few $Cux1^+/BrdU^+$ double positive cells (Fig. 4.3), and I did not see any significant change in the number of $Cux1^+/BrdU^+$ double-positive cells in *Met-Emx1* mice as compared to control (control, 7.5 ± 2.7; *Met-Emx1* 5.1 ± 2.0; Student's *t* test, p = 0.534). I also did not see any change in the fraction of $BrdU^+$ cells which were also positive for Cux1 (control, 19.5 ± 3.4%; *Met-Emx1* 12.5 ± 2.8%; Student's *t* test, p = 0.194). The lack of any significant number of double-labeled cells in the *Met-Emx1* mice, along with the lack of change from control, suggests that the ectopic $Cux1^+$ cells in *Met-Emx1* mice are not (primarily) born at E12.5. It is therefore unlikely that premature birth of these cells leads to their abnormally deep position in the cortex.

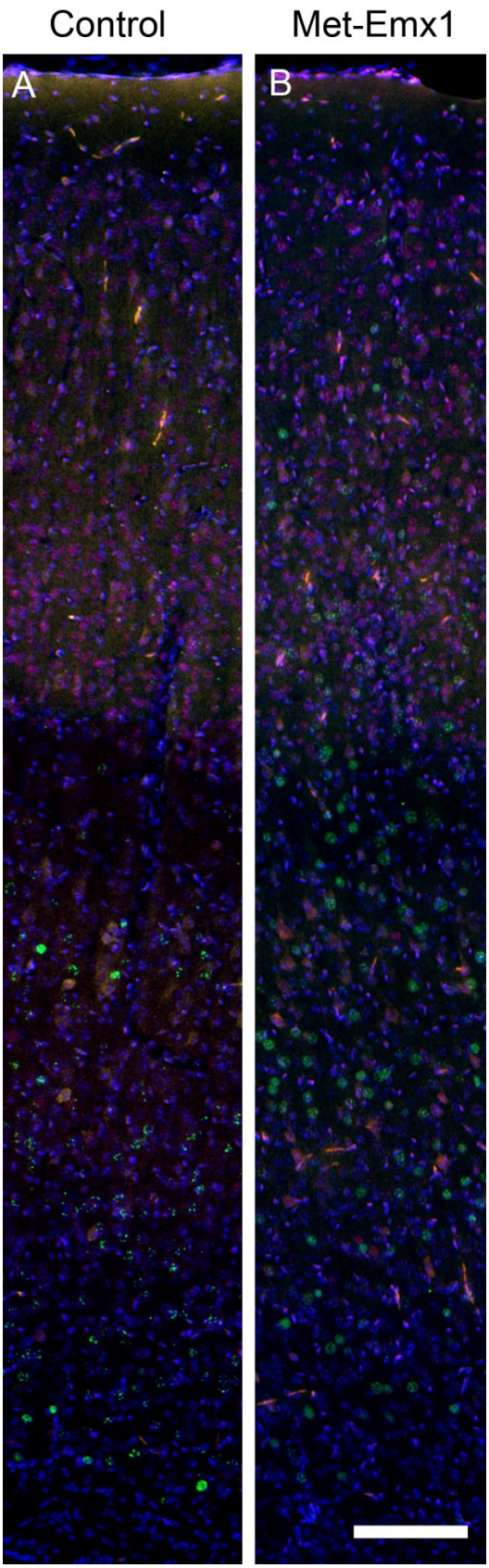

Figure 4.16. Ectopic Cux1^{+} cells are laregly not labeled by E12.5 BrdU injections.

Representative images of the somatosensory cortex in P30 mice showing staining for Cux1 (red) and BrdU (green) after injections at E12.5 from control (A) and *Met-Emx1* (B) mice. Scale bar in (B) represents 100µm

4.4 Discussion

I have previously shown that there is a specific reduction in the thickness of superficial cortical layers in *Met-Emx1* mice. Previous studies have shown that the cortical layers are generated in an inside-out fashion, with deep layers born prior to superficial ones (Angevine and Sidman, 1961; Rakic, 1988; Takahashi et al., 1999). This suggests that there could be a change in the timing of neurogenesis, particularly later in the process when superficial layers are generated. I therefore examined cell birthdates in *Met-Emx1* mice by assessing cell birthdating with BrdU labeling at early (E12.5), middle (E14.5), or late (E16.5) time points during neurogenesis.

In both PL and S1, I found increased overall $BrdU^+$ cell density in *Met-Emx1* mice after injections at E12.5, and decreased $BrdU^+$ cell density after injections at E14.5. I also found decreased overall $BrdU^+$ cell density in S1 after injections at E16.5. I also observed changes in $BrdU^+$ cell density at specific levels through the cortical wall. After injections at E12.5, differences were primarily observed in middle layers, while changes observed after injections at E14.5 tended to be in superficial layers, and those seen after E16.5 injections were in either very deep or superficial bins. Since cells born at E16 typically populate superficial layers, changes in cell density in the deepest bins may represent cells which are still migrating, as it is possible that not all of these cells have reached their final positions by the time the brains were collected at P0. That *Met-Emx1* mice show an increase in cell birth early in neurogenesis is followed by decreased cell birth later on, at E14.5 and E16.5, suggests that the progenitor pool may become depleted in *Met-Emx1*

mice. Extra cells generated at E12.5 may be leaving the cell cycle to differentiate into neurons. Increased cell cycle exit early during neurogenesis would decrease the number of proliferative cells in the progenitor pool at later points in neurogenesis (Caviness et al., 1995; Chenn and Walsh, 2002). Such an early over-production of neurons could help to explain the reduction in thickness of superficial layers. Interestingly, β-catenin, a component of the canonical WNT signaling pathway which has been shown to interact with Met (Hiscox and Jiang, 1999; Zeng et al., 2006), has been shown to influence the timing of neuronal differentiation in cortical progenitors (Chenn and Walsh, 2002; Mutch et al., 2010). It is therefore possible that loss of Met signal in cortical progenitors affects proliferation by altering signaling through β-catenin.

While the overall pattern of changes between *Met-Emx1* and control mice were similar between PL and S1, there were a few notable differences between the areas, and between different rostro-caudal levels within S1. While I saw reductions in $BrdU^+$ cell density in *Met-Emx1* mice after E16.5 injections at multiple levels (plates 5 and 6) within S1, I saw no effect of loss of Met signaling on overall BrdU cell density in PL after E16.5 injections, although density was reduced in a few bins. Conversely, the alterations in the density of $BrdU^+$ cells across the entire thickness of the cortex that were seen in PL were not found at all levels of S1 (plate 5 did not show increased density after E12.5 injections, and plate 7 showed only a marginal decrease after E14.5 injections). Of the different rostro-caudal levels examined within S1, only the middle, plate 6, showed significant effects of the loss of Met signaling on overall $BrdU^+$ cell density after all three injection times. Plate 5 showed a reduction after E16.5 injections, and plate 7 showed an increase

after E12.5 injections. Plates 5 and 7 also showed some evidence of decreased $BrdU^+$ cell density in *Met-Emx1* mice after injections at E14.5 (Student's *t* test, $p < 0.10$). Thus the caudal level showed alterations in early-born cells, while the rostral level showed alterations in late-born cells. The divergence between PL and S1, and between different levels within S1, could be at least partially due to the different developmental time courses followed by these areas. Previous work has shown that cerebral cortical neurogenesis proceeds in a rostro-lateral to caudo-medial gradient (McSherry, 1984; McSherry and Smart, 1986; Takahashi et al., 1999). PL and S1 may therefore be at slightly different points in the process of neurogenesis at any given age.

I have previously shown that superficial layer cells which express Cux1 distribute abnormally in the somatosensory cortex of *Met-Emx1* mice. Furthermore, I found no change in the total number of $Cux1^+$ cells in the somatosensory barrel field, despite the reduced thickness of layer II/III and the reduction in cell birth during later neurogenesis. Combined with the increase in BrdU labeled cells after injections at E12.5, this led me to hypothesize that these mis-localized cells could be born earlier than normal, though in normal numbers, and therefore fail to reach their typical destinations in superficial layers. To test this idea I examined colocalization of BrdU with Cux1 after BrdU injections at E12.5, when I found increased proliferation. I found few $Cux1^+/BrdU^+$ cells in either control or *Met-Emx1* mice, consistent with the normal birth dates of superficial layer neurons. Furthermore, I found no change in the percentage of $BrdU^+$ cells which co-express Cux1, suggesting that the extra cells generated at E12.5 do not differentiate as superficial layer neurons. It remains possible that loss of Met signaling impairs the

migration of these neurons, particularly as HGF-Met signaling has been shown to promote neuronal migration (Powell et al., 2001b; Garzotto et al., 2008).

My results suggest that the role of Met in cortical development may be time specific, particularly centered around early neurogenesis, when I found increased BrdU labeling. However, my data leave open the question of the specific cause underlying the increase in cells born at E12.5. HGF signaling has previously been implicated both in the regulation of cell proliferation as well as neuronal differentiation (Kokuzawa et al., 2003; Kato et al., 2004), and the promotion of either process could potentially explain the increase in labeling after injections at E12. These processes have opposite effects on cortical size, however. An increase in neuronal differentiation of progenitors at E12.5, and therefore their exit from the cell cycle, would lead to a depletion of the progenitor pool, and would likely contribute to a reduction of cortical size, particularly in superficial layers (which are reduced in *Met-Emx1* mice). This would not, however, explain the increase in cortical volume observed in *Met-Emx1* mice. An increase in proliferation, on the other hand, particularly an increase in symmetric divisions of progenitors, would be expected to increase cortical size, and could also be consistent with increased BrdU labeling early in neurogenesis, as an increase in the number of proliferating cells would be expected to generate increased numbers of daughter cells. However, this would not explain the reduction in BrdU labeling during late neurogenesis, nor the reduction in superficial layer thickness. More work is necessary in order to clarify the effects of HGF-Met signaling on the mode of cortical progenitor divisions and Met's possible impact on cell fate.

Chapter 5- Altered social behavior in mice deficient in Met tyrosine kinase

5.1 Introduction:

ASD is characterized by social and communication deficits as well as narrowed interests and repetitive behaviors (Kanner, 1943; Folstein and Rosen-Sheidley, 2001b; Piven, 2001). While ASD is well characterized in humans, experiments in humans are limited by the availability of subjects, as well as by what manipulations can be undertaken. Studies such as this one therefore frequently make use of animal models to examine the effects of genetic or environmental manipulations on behavior.

I have shown that mice in which the Met tyrosine kinase is inactivated within the *Emx1* lineage of the cerebral cortex and hippocampus have larger than normal brains (Smith et al., 2012), and further that cortical lamination is altered in these mice, likely by changes in neuronal proliferation between E12.5 and E1.65. These anatomical changes have little meaning in the context of ASD risk, however, if they do not affect the mouse's behavior. To determine if mice lacking functional Met in the cerebral cortex demonstrate behavior reminiscent of human autism, I examined behavior in the open field, light-dark avoidance, and three-chamber social interaction tasks.

The novel open field task is a paradigm used to asses overall activity levels in rodents (Walsh and Cummins, 1976). The open field is often used as a control to test for gross motor defects in mice which would prevent them from functioning adequately in other

tests which require the animal to move about an arena - such as the three-chamber social interaction test. The ratio of the time a mouse spends in the open center of the arena, relative to the area along the walls is also sometimes used as a measure of anxiety (Carola et al., 2002), as anxiolytic drugs often increase the proportion of time a mouse will spend in the center (Christmas and Maxwell, 1970; Simon et al., 1994; Rex et al., 1998; Kash et al., 1999; Choleris et al., 2001; Prut and Belzung, 2003).

The light-dark preference test is based on the naturalistic conflict between the preference of mice for dark, enclosed areas and the urge to explore well-lit, open areas, which is necessary to find food (Crawley and Goodwin, 1980). An otherwise open field is divided into two chambers, one darkened and one lit. The light-dark preference test can be used to assess anxiety (Crawley and Goodwin, 1980; Crawley, 1981). Anxiolytic drugs, such as benzodiazepines, increase the amount of time mice spend in the lit area (Crawley and Goodwin, 1980; Crawley, 1981; Bourin and Hascoet, 2003), and as such increased time spent in the lit area is used to indicate decreased anxiety. While anxiety is not a feature of ASD itself, it is a prevalent co-morbidity among patients with autism (White et al., 2009). Studies have found co-morbid anxiety disorders in 42% (Simonoff et al., 2008) to 55% (de Bruin et al., 2007) of children with autism, suggesting that anxiety may pose a serious burden in the population of patients with autism.

The three-chamber social interaction test was developed to assess mouse social behavior, with the idea that deficits in these behaviors could parallel the social deficits that, in part, define autism (Moy et al., 2004). The test measures the amount of time a test mouse

spends in a chamber containing either a novel social partner, as compared to an otherwise identical chamber with no mouse. Many mouse strains, such as C57BL/6, have been found to display a strong preference for the chamber containing the other mouse (Moy et al., 2004; Nadler et al., 2004). Mice which are thought to serve as models of ASD, such as the BTBR mouse line (McFarlane et al., 2008), or *Shank3* mutant mice (Peca et al., 2011), do not show this preference for a social partner. Social interaction deficits in these mouse lines are thought to parallel the human deficits seen in ASD, giving the test good face validity for screening mice for autistic-like behavior (Moy et al., 2004; Nadler et al., 2004; McFarlane et al., 2008). I therefore sought to determine if social behavior was altered in *Met-Emx1* mice.

5.2 Methods:

5.2.1. Animals and order of tests

General animal care procedures are described in Appendix 1. All mice used in behavioral testing were adult (at least 90 day old) males. Mice were brought from their housing facility to the behavioral testing room and allowed to acclimate there for at least one hour prior to testing. 3 control, 7 *Met-Emx1*, and 3 heterozygous mice were tested. Tests were performed in order for each mouse, beginning with open field, followed by light-dark exploration, and then three-chamber social interaction test (one test per day).

5.2.2 Open field

Activity in the open field was assessed as previously described (Martins et al., 2011) in a TruScan automated open field (Mouse Truscan Activity Arena; Coulbourn Inst., Allentown, PA). Mice were placed in the center of the arena and left to explore freely for 10 min. Activity in the horizontal and vertical planes was measured by the number of beam breaks in each plane and converted to a distance measurement. Data was collected by TruScan 2.0 software, and analyzed in SigmaPlot 12.0 using a one-way ANOVA.

5.2.3 Light-dark preference

The light-dark preference test was conducted as previously described (Martins et al., 2011), using the same Truscan apparatus as for the open field test, but with partition inserted to darken half of the field. A 4 x 4 cm opening in the partition allowed the mice to move between the dark and light halves of the field. Mice were placed in the center of the light half and allowed to explore the arena for 10 min. Data were again collected by TruScan 2.0 software and analyzed in SigmaPlot 12.0 using a one-way ANOVA.

5.2.4 Three-chamber social interaction

The three-chamber social interaction apparatus consisted of a 56 cm long, 40 cm wide, 20 cm tall plexiglass box, divided into three chambers approximately 18 cm long with 10 x 6 cm openings through which the mice could navigate between chambers (Moy et al., 2004). These openings could be obstructed by sliding plexiglass dividers. On the day

prior to testing, mice were placed in the center chamber without dividers present and allowed to explore the empty apparatus for 5 min, without cages or the partner mouse present. Separately, the partner mice were habituated to the cages for 10 minutes. On the day of testing, the test mice were placed into the center chamber with the barriers in place, and either an empty cage or a cage containing a partner mouse in either side chamber. The barriers were then removed and the test mouse was allowed to explore the apparatus for 10 min before being removed. Sessions were filmed with a digital video camera (Sony DCR-HC40). Films were scored by marking which chamber the test mouse was in every 5 s. The mouse was considered to have entered a new chamber once the head and forelimbs passed the opening. Data were analyzed using a one-way ANOVA.

5.3 Results

5.3.1 Open field

I found that adult male *Met-Emx1* mice show largely normal behavior in the open field. *Met-Emx1* mice moved a similar distance to control mice (Fig. 5.1A, control, 1434.4 ± 132.6 cm; Het, 1789.4 ± 409.6; *Met-Emx1*, 1204.4 ± 105.9 cm; one-way ANOVA, F(2, 20) = 1.38 , p = 0.275) at a similar velocity (Fig. 5.1D, control, 2.27 ± 0.219 cm/s; Het, 2.75 ± 0.546 cm/s; *Met-Emx1*, 1.95 ± 0.144 cm/s; one-way ANOVA, F (2, 20) = 1.38, p = 0.277). *Met-Emx1* mice spent a similar amount of time moving compared to controls (Fig. 5.1B, control, 479.3 ± 16.0 s; Het, 458.3 ± 29.1 s; *Met-Emx1*, 445.5 ± 10.5 s; one-way ANOVA, F (2, 20) = 0.421, p = 0.662), and made a similar number of separate movements (Fig. 5.1C, control, 68.6 ± 5.0; Het, 72.8 ± 8.9; *Met-Emx1*, 88.0 ± 4.7; one-

way ANOVA, F (2, 20) = 1.905, p = 0.178). Lastly, *Met-Emx1* and heterozygous mice did not differ from controls on average distance per movement (Fig. 5.1E, control, 18.8 ± 1.8 cm; Het, 22.5 ± 5.3; *Met-Emx1* 14.7 ± 1.6 cm; one-way ANOVA, F (2, 20) = 1.316, p = 0.293). These results suggest that either complete or partial loss of Met signaling does not impact overall activity levels in mice.

However, there was an effect of genotype on center:margin ratio (control, 1.06 ± 0.25; Het, 0.39 ± 0.09; *Met-Emx1*, 1.06 ± 0.20; one-way ANOVA, F(2,20) = 5.231, p = 0.016), with heterozygous mice spending less of their time in the center of the arena than either control (Holm-Sidak, p = 0.047) or *Met-Emx1* mice (Holm-Sidak, p 0 0.029). This would suggest that mice heterozygous for the *Met* mutation experience elevated levels of anxiety in the open field test.

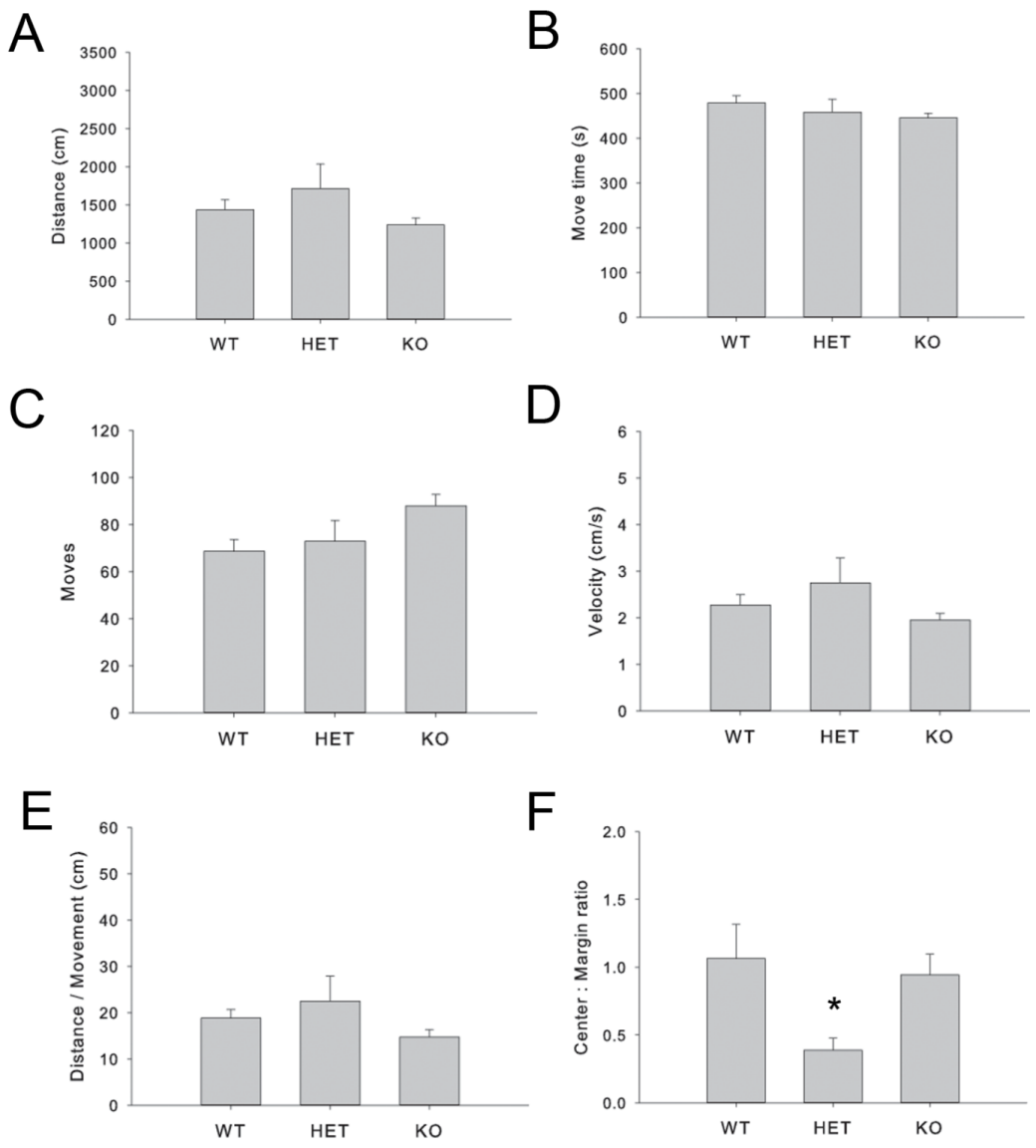

Figure 5.1. Normal motor behavior and altered anxiety-like behavior in *Met* mutants in the open field.

Quantification of the behavior of *Met-Emx1* and control mice in the open field test is shown. Graphs represent (A) total distance traveled over the 10 minute test, (B) time spent mobile, (C) number of separate movements, (D) average velocity, (E) average distance per movement, and (F) ratio of time spent in the center of the arena to time spent around the margins.

5.3.2 Light-dark preference

There were significant differences between genotypes in how much time they spent in either the light (control, 186.0 ± 13.2 s; Het, 332.3 ± 47.5 s; *Met-Emx1*, 294.1 ± 20.1 s; one-way ANOVA, $F(2,10) = 6.14$, $p = 0.024$) or dark (control 414 ± 13.2 s; Het, 267.7 ± 47.5; *Met-Emx1*, 309 ± 20.1 s; one-way ANOVA, $F(2,10) = 6.14$, $p = 0.024$) halves of the arena. Specifically, Het mice spent more time in the light, and less in the dark side of the chamber compared to controls (Holm-Sidak test, p = 0.029). A similar change was seen in *Met-Emx1* mice, but this did not reach significance (Holm-Sidak test, $p = 0.053$). I found no difference in the number of entries to the light side between *Met-Emx1* and control mice (control, 14 ± 3; Het, 22 ± 3; *Met-Emx1*, 21 ± 6; one-way ANOVA, $F(2,10) = 0.602$, $p = 0.571$). These results suggest that mice with reduced Met signaling show reduced anxiety in the light-dark preference test.

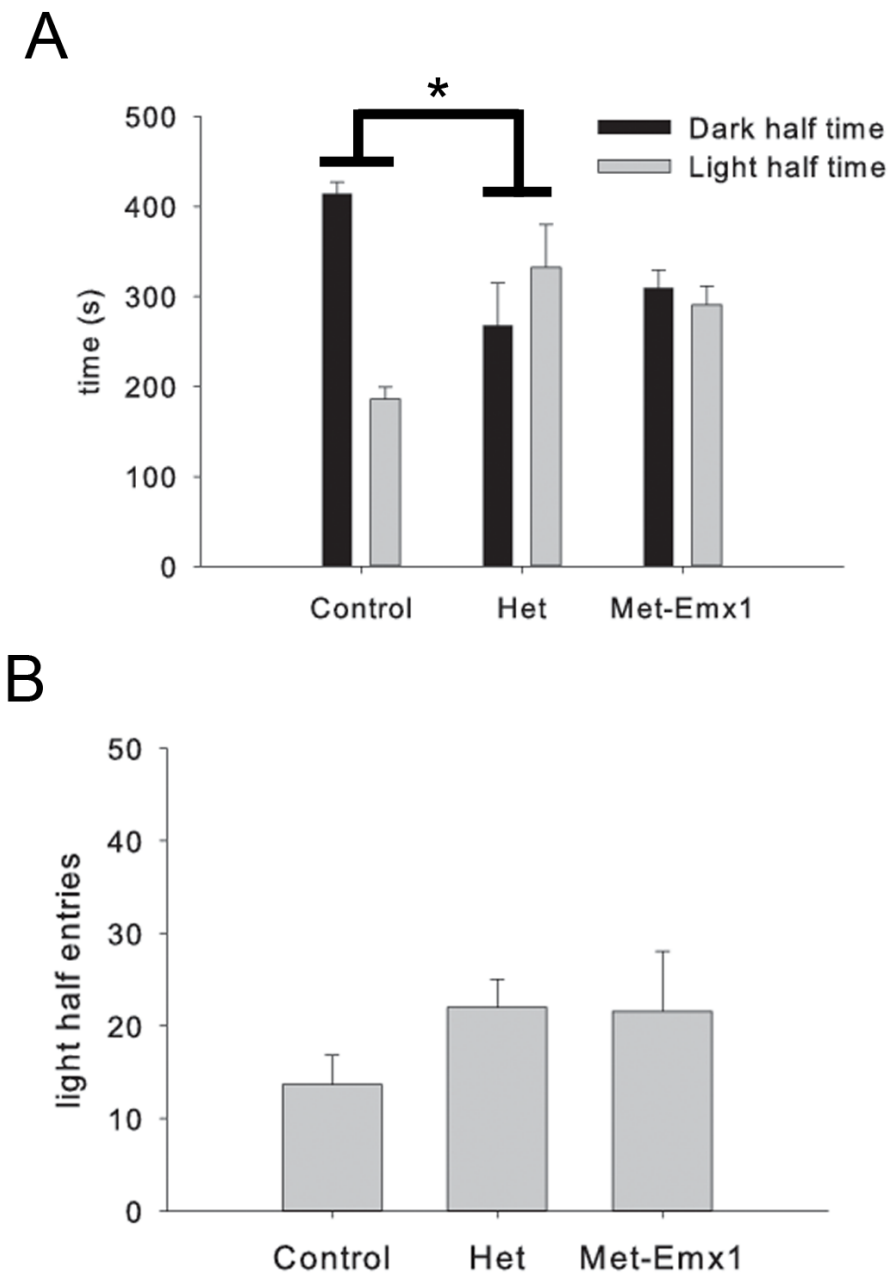

Figure 5.2. Altered anxiety behavior in the light-dark exploration test in *Met* mutant mice.

Quantifications are shown for the amount of time spent in the dark (A) and light (B) chambers, as well as for entries to the light side (C). No significant differences were found between *Met-Emx1* and control mice, suggesting normal anxiety levels in *Met-Emx1* mice.

5.3.3 Three-chamber social interaction

I found no significant difference between genotypes in the percentage of time spent in the social chamber (Control, 53.8 ± 2.4%; Het, 42.7 ± 2.5 %; *Met-Emx1*, 55.75 ± 4.8 % sec; one-way ANOVA,F (2, 12) = 1.745, p = 0.224), nor in the percentage of time spent in the non-social chamber (Control, 46.2 ± 2.4 %; Het, 57.3 ± 2.5 %; *Met-Emx1*, 44.2 ± 4.8 %; one-way ANOVA, F (2, 12) = 1.745, p = 0.224). This suggests that mice with reduced Met signaling do not show deficits in social behavior.

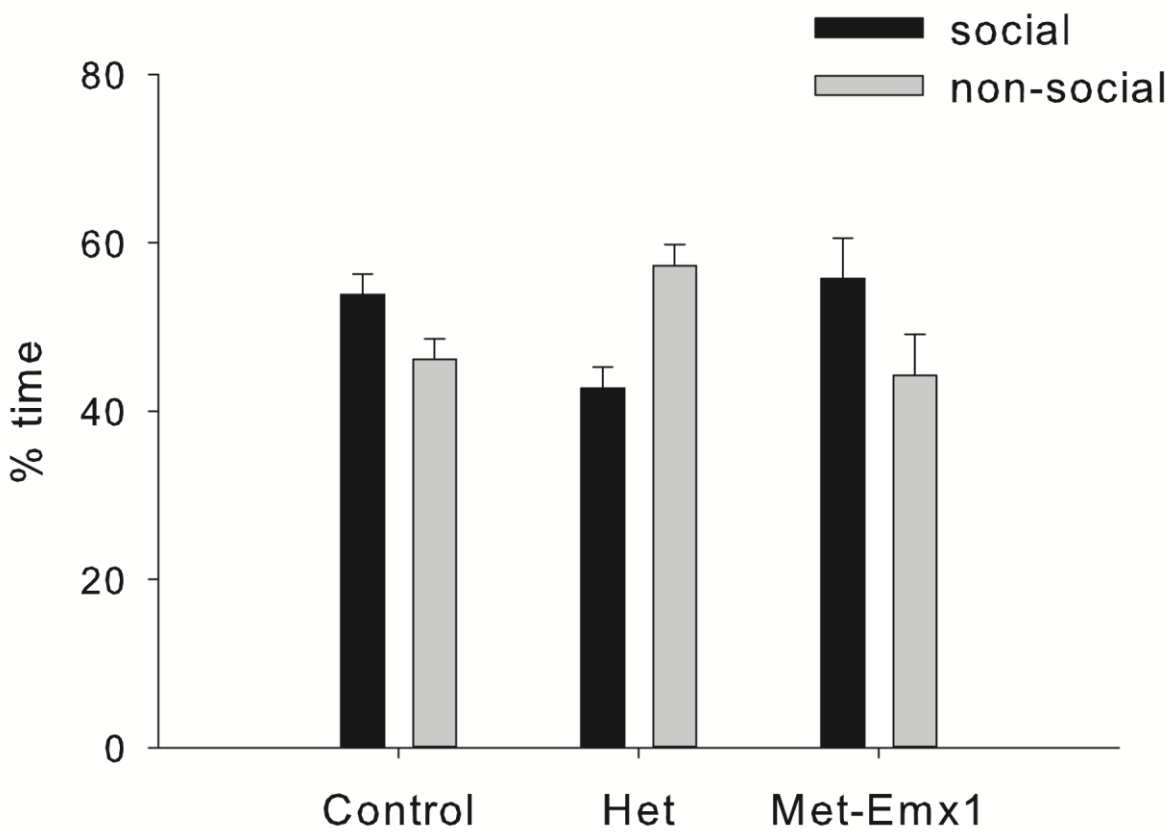

Figure 5.3. Social behavior in mice with reduced Met signaling.

The amount of time spent in the social or non-social chamber, shown as a percentage of time spent outside of the starting middle chamber, are shown for control, homozygous *Met-Emx1*, and heterozygous mice.

5.4 Discussion

I found that *Met-Emx1* and heterozygous mice show normal locomotor behavior in the open field, suggesting that their behavior in the other tests won't be impacted by changes in their overall activity level. However, I did see a change in the amount of time that Het mice spent in the center of the open field. Het mice showed a significantly lower center-to-margin ratio than either control or homozygous *Met-Emx1* mice. This could indicate either increased anxiety in Het mice, or a decreased drive to explore the more exposed center.

In contrast to my findings in the open field, I found an increase in the amount of time Het mice spent in the light side during the light-dark exploration test. In this test, there was a similar, though non-significant change in the homozygous *Met-Emx1* mice. Although I found no significant differences in the number of entries to the light side between genotypes, my results from the light-dark exploration test would indicate that reduced Met signaling in the cortex leads to decreased anxiety. The conflict between this result and my findings in the open field raises the need for future studies to clarify the effect of reduced Met signaling in the cerebral cortex on anxiety behaviors.

Numerous mouse models exist for autism, as well as related monogenic disorders such as Fragile X syndrome and Rett syndrome (Spencer et al., 2005; Gemelli et al., 2006; Moy and Nadler, 2008). While several studies have shown increased anxiety-like behaviors in models of ASD (Moy and Nadler, 2008), not all models, or studies, show the same level

of anxiety-like behaviors in "autistic" mice relative to controls (Mineur et al., 2002; Spencer et al., 2005; Jamain et al., 2008; Mines et al., 2010; Peca et al., 2011). *Fmr1* mutant mice show decreased anxiety-like behavior in the open field and light-dark tests (Spencer et al., 2005), and the elevated plus maze (Mineur et al., 2002), but increased anxiety during tests with a social component (Spencer et al., 2005; Mines et al., 2010). *Shank3* mutants, on the other hand, display increased anxiety in the light-dark emergence and elevated zero maze tests, as well as repetitive grooming (Peca et al., 2011). And *Neuroligin4* mutants show no significant changes in anxiety behavior (Jamain et al., 2008). Notably, mice deficient in *uPAR*, another component of the HGF-Met signaling pathway, show increased anxiety-like behavior (Powell et al., 2003b). However, mice in which Met is inactivated in interneurons of the *Dlx5/6* lineage show normal anxiety levels (Martins et al., 2011). Variation in the effects of different disease-associated mutations on anxiety in mice may be reflective of the variation in anxiety levels among patients with autism, and among different ASD sub-populations (White et al., 2009).

While the changes in anxiety-like behaviors are inconsistent across animal models of autism, social interaction deficits are a consistent feature of these models (Spencer et al., 2005; Jamain et al., 2008; Mines et al., 2010; Peca et al., 2011). Here, I have found no significant differences among genotypes in preference for the social over the non-social chamber. This may be due to our small sample size in this initial examination, and future studies will need to expand on our current sample. However, if true, this could indicate that loss of Met signaling in the cortex, in the absence of other genetic or environmental insults, is not sufficient to produce social deficits in mice. While this would diminish the

usefulness of the *Met-Emx1* line as a model of autism per se, it does not limit their importance as a tool for determining how the developmental effects of reduced Met signaling could contribute to neuropathology.

Notably, I saw the strongest behavioral effects of the conditional *Met* mutation in heterozygous mice. Previous studies examining autism risk genes have shown a role for gene dosage in risk for ASD (Durand et al., 2007; Toro et al., 2010). Heterozygous mutations can produce uneven expression of the affected gene across the brain, either due to mutation or epigenetic silencing of the remaining allele (Schanen, 2006; Toro et al., 2010), or allelic exclusion, as has been observed for protocadherins (Esumi et al., 2005). Notably, the best characterized of the *Met* alleles conferring risk for autism in humans (rs1858830) is not a complete loss-of-function mutation, but rather reduces transcription of *Met* (Campbell et al., 2006). Furthermore, this risk allele has been found to have functional effects in heterozygous carriers (Rudie et al., 2012), showing that not all copies of the *MET* gene need be affected to influence behavior. More work is needed to clarify how partial loss of Met function could impact cerebral cortical development and structure.

Chapter 6: Conclusions and Significance

6.1 Met association with ASD

Met tyrosine kinase has been widely implicated in risk for ASDs by genetic association studies (Campbell et al., 2006; Campbell et al., 2008; Campbell et al., 2009; Sousa et al., 2009b; Thanseem et al., 2010a; Zhou et al., 2011). But perhaps more importantly, autism-associated variants of *MET* have also been shown to have functional significance. Perhaps the best characterized polymorphism, the rs1858830 SNP, is a *G* to *C* polymorphism in the 5' promoter region of *MET*. The *C* allele at this location reduces *MET* transcription in several cell lines (Campbell et al., 2006). The same allele has been associated with social and communication scores on the ADI-R, ADOS, and SRS tests (Campbell et al., 2010), and has been shown to reduce default mode network activity in response to emotional face stimuli (Rudie et al., 2012). Other *MET* polymorphisms have also been associated with altered facial emotion perception (Lin et al., 2012). Together, these findings suggest that impaired MET signaling contributes to some of the symptoms of ASD. In addition to the overall effect of the mutation, the effects of the rs1858830 risk allele appear stronger within subjects diagnosed with autism than in typically developing subjects (Rudie et al., 2012), suggesting an interaction with other risk genes in patients with ASD.

6.2 Structural alterations: grey matter

Our findings suggest that loss of Met signaling in the cerebral cortex and hippocampus leads to brain overgrowth in adult mice. In the cerebral cortex, the increase in size appears to be due to increased surface area, rather than thickness, and is largely confined to rostral levels of the cortex. Indeed, our histological analysis suggests that the cortex is in fact thinner in *Met-Emx1* mice in at least some cortical areas. This reduction is most pronounced in superficial layers II and III. These findings agree with recent work examining cortical thickness in typically developing patients with the rs1858830 *C* allele, which showed reduced cortical thickness in frontal and temporal cortical areas in patients with the risk allele (Hedrick et al., 2012). Increased cortical surface area has also been found in patients with idiopathic autism (Hazlett et al., 2011b; Doyle-Thomas et al., 2013), and numerous studies have shown increased brain size in autism (Piven et al., 1995b; Aylward et al., 2002; Hazlett et al., 2006b; Amaral et al., 2008a; Hazlett et al., 2011b), including in frontal cortical areas (Ecker et al., 2012), where the change in *Met-Emx1* mice is most pronounced.

6.3 Structural alterations: white matter

While numerous studies have examined white matter structure in patients with autism, there is little agreement as to how white matter structure may be altered in ASD. While one study on children between 1.8 and 3.3 years found increased fractional anisotropy in the genu and splenium of the CC (Ben Bashat et al., 2007), others in a slightly older

population have found reduced fractional anisotropy values in the CC and frontal white matter tracts (Barnea-Goraly et al., 2004; Alexander et al., 2007). While some reports have shown decreases in CC size (Piven et al., 1997; Freitag et al., 2009), or no change in autistic subjects (Piven et al., 1997; Herbert et al., 2004), others have found increased white matter volume in autistic individuals (Herbert et al., 2003; Herbert et al., 2004; Freitag et al., 2009). None of these studies were correlated with genetic information, and they likely represent a spectrum of diverse genetic and environmental factors leading to the ASD diagnosis. However, the rs1858830 risk allele has been shown to lead to a dose-dependent reduction in FA in white matter tracts of the temporal, parietal and occipital lobes.(Rudie et al., 2012), suggesting that impaired MET function likely contributes to disorganization of white matter tracts in those areas. This would also suggest that studies which found increases in FA in ASD could represent samples in which *MET* polymorphisms are less prevalent, with other genetic changes leading to most cases of ASD in those studies.

My findings indicate that loss of Met signaling leads to an increase in the thickness of the CC at rostral levels in adult mice, suggesting increased white matter volume in *Met-Emx1* mice. This may help to explain increases in the size of brain areas which do not express *Emx1*, and therefore do not experience Cre recombination and loss of Met function in the *Met-Emx1* line. The dorsal striatum, thalamus, and ventral hippocampus receive extensive input from the cerebral cortex, raising the possibility that changes in the size of these brain regions could be due to changes in axonal projections from the cortex. In the

striatum, I found that loss of Met signaling altered the size of the cortico-striatal bundles, leading to a shift towards larger fascicle sizes in *Met-Emx1* mice.

To try to determine if the increase the size of the CC was due to an increased number of callosal projection neurons in *Met-Emx1* mice, I stained for the transcription factor Satb2, which marks callosal projection neurons and is involved in their specification (Alcamo et al., 2008). I did not find any change in the number of Satb2^{+} cells, either in S1 or in PL, suggesting that the increase in the size of the callosum is not due to an increase in the number of callosal projection neurons. It remains possible that changes in the caliber or branching of callosal projection neurons could account for the increase in the size of the CC. Alternatively, changes in the myelination of crossing fibers could lead to the increase in CC size. Future work could address these possibilities using electron microscopy to examine the size and myelination patterns of callosal projection neurons. Additionally, the branching patterns of callosal projection neurons could be examined using anterograde and retrograde tracers.

6.4 Cell number and proliferation

Oddly, the reduction in the thickness of layers II/III seen in our mice was not mirrored by a change in the number of cells expressing the superficial layer marker Cux1, in either the somatosensory barrel field (S1) or in OFC. Less surprisingly, I also saw no change in the

number of cells expressing the deep layer marker Ctip2, which labels sub-cerebral projection neurons.

We did, however, note a change in the distribution of Cux1$^+$ cells across the thickness of the cortex within cortical barrel field. I found an increase in the number of Cux1$^+$ cells within abnormally deep layers (V-VI) in *Met-Emx1* mice. While Cux1 is expressed in deeper layers in some cortical areas, this is not normally the case in the somatosensory barrel fields. There are several possible explanations for the presence of these ectopic "superficial" neurons in deep layers. One possibility is that loss of Met signaling causes a shift in area identity, such that areas where S1 is found in control mice instead differentiate as more lateral areas in which deep-layer Cux1$^+$ cells are normally found. This is unlikely, as S1 was identified prior to taking cell counts using the presence of barrels, and measurements were confined to this area.

A second possibility is that these ectopic cells are in some way mis-specified. My BrdU labeling studies show increased labeling at P0 after injections at E12.5, when deep layers are being born. This increase is evident particularly in layers somewhat more superficial than are normally populated at E12.5. I also found evidence of decreases in BrdU labeling after injections at E16.5 or E14.5, when superficial or middle layers are born. Particularly after injections at E14.5, the observed decreases in BrdU cell density were prominent in superficial bins. Despite the changes in the timing of cell generation, I saw no increase in Ctip2$^+$ deep layer cells, nor a decrease in Cux1$^+$ superficial layer neurons

in adult *Met-Emx1* mice. This could be explained if the timing of layer generation is altered by loss of Met signaling. In particular, if some of the "extra" cells being generated at E12.5 were differentiating as superficial layer neurons, they could account for the normal overall number of Cux1 cells, as well as possibly explaining the ectopic Cux1 cells in deep layers. As superficial layers have not yet formed early in development, "superficial" layer neurons generated at abnormally early times could become trapped in deeper layers. However, my data suggest that the ectopic $Cux1^+$ cells do not originate from cells born at E12.5, as *Met-Emx1* mice show no increase in co-localization between BrdU and Cux1 relative to controls after BrdU injections at E12.5. Both groups show very low levels of co-localization between Cux1 and BrdU, as is expected for control animals. A third possibility is that loss of Met signaling impairs neuronal migration, resulting in some superficial layer neurons being unable to reach their normal destinations. While I cannot confirm or refute this possibility, it would be consistent with prior work from our lab, showing that loss of Met function impairs migration of interneurons into the cortex from the ganglionic eminence (Martins et al., 2011). Future studies will need to examine the effect of loss of Met signaling on migration in excitatory neurons of the cortex

6.5 Summary

My findings indicate that loss of Met signaling in the cerebral cortex during development results in a larger brain. Specifically, *Met-Emx1* mice have an expanded cortical surface area, but reduced cortical thickness. In addition to this alteration in gray matter volume,

Met-Emx1 mice have an expanded corpus callosum, along with larger cortico-striatal bundles, suggesting that an increase in white matter volume likely contributes to the change in brain size, particularly outside of the cortex and hippocampus - the areas targeted by the *Emx1*-Cre driver.

The reduction in cortical thickness may be at least partially explained by a change in neuronal proliferation. I found more early-born cells in *Met-Emx1* mice, and fewer later-born cells, suggesting that the progenitor pool may become depleted in these animals. This could account both for the reduction in cortical thickness, as well as the specificity of this reduction for superficial layers. An increase in proliferation early during development is also consistent with the expansion of cortical surface area. Lastly, while I found normal numbers of both $Cux1^+$ and $Ctip2^+$ neurons in the cortex, I found that some cells which express the superficial layer marker Cux1 are found in abnormally deep layers in *Met-Emx1* mice. It does not appear as though these cells are related to the early over-proliferation in *Met-Emx1* mice, as they largely do not co-stain for BrdU after early BrdU injections.

6.6 Future work

While reduction or loss of Met function can lead to increased risk for ASD, as well as the host of neuroanatomical abnormalities seen in *Met-Emx1* mice and in individuals with functional *MET* polymorphisms, fundamentally these changes are the result of the

disruption of the normal role of HGF-Met signaling in the developing cerebral cortex. The increase in the volume of the brain in *Met-Emx1* mice, as well as the increase in proliferation I observed after BrdU injections at E12.5, suggest that HGF-Met signaling may play a role in restraining cell division - or possibly in restraining particular kinds of cell divisions. The early increase in BrdU labeling, followed by decreases at later injection times, suggests that the progenitor pool may become depleted in *Met-Emx1* mice. If this is the case, it would indicate that Met signaling contributes to the maintenance of the stem cell pool. This could be either by inhibiting neurogenic and other terminal cell divisions, or by favoring divisions which produce daughter progenitor cells. Future studies could address some of these possibilities. By combining BrdU labeling with markers of proliferating cells, such as Ki67, it would be possible to determine if the loss of Met signaling in *Met-Emx1* mice lead to increased cell cycle exit early in neurogenesis. Co-staining for markers of differentiating neurons or different progenitor subtypes, along with BrdU, would also allow me to determine what kinds of cells are among those "extra" cells born at E12.5.

More work is also needed in order to determine the origin of the increase in white matter I observed in *Met-Emx1* mice. Tract tracing studies can give some indication of whether or not projections from the cerebral cortex are altered by loss of Met signaling, for example if more of the callosal projections are branching in *Met-Emx1* mice. But ultimately, electron microscopic studies will be needed in order to determine if there are changes to axon caliber, fasciculation, or myelination within the corpus callosum. Lastly, future work is needed to clarify the effect of loss of Met signaling in the developing

cortex on behavior. While my data provide some indication that mice with reduced Met signaling show changes in anxiety-like behaviors, and raises the possibility that they may not show a social preference, few conclusions can be drawn from my small sample.

Appendix 1: Common Methods

A.1 Animals

Emx1-Cre (K. Jones, University of Colorado) and *Met-fx* (S. Thorgeirsson, National Cancer Institute, NIH) mice were generous gifts from collaborators and backcrossed onto the C57BL/6^{J} line obtained from the Jackson Laboratory (Bar Harbor, ME). Mice used in these experiments were littermates resulting from matings between non-sibling heterozygotes (*fx/+:Cre*). All mice were genotyped *via* PCR using the following primer sets: *Met-fx* primers 5'-TTA GGC AAT GAG GTG TCC CAC-3' and 5'-CCA GGT GGC TTC AAA TTC TAA GG- 3' (380bp for the *floxed* allele and 300bp for wildtype); *Emx1-Cre* primers 5'-CAC CCT GTT ACG TAT AGC CG-3' and 5'-GAG TCA TCC TTA GCG CCG TA-3' (320bp) (Martins and Powell, 2011).

A.2 Histology and Immunohistochemistry:

Adult mice were transcardially perfused with 0.9% saline followed by 4% buffered paraformaldehyde. Brains were cut at 50µm on either a Leica vibratome VT1000S (Leica, Deerfield, IL) or a Microm HM430 freezing slide microtome (Thermo scientific, Waltham, MA) and processed for immunohistochemistry according to standard laboratory techniques (Martins and Powell, 2011).

Sections were rinsed twice in TBS to remove cryoprotectant, then incubated for five minutes in hydrogen peroxide (0.5% in TBS). For Ctip2 and Cux1 staining, sections were then subjected to heat-mediated antigen retrieval in 10mM sodium citrate buffer (pH 6.0). After boiling in the lab microwave for 1.5 - 2 minutes, the sections were left to incubate for 20 minutes in the hot buffer. For BrdU staining, sections were instead incubated for 15 minutes in 2N HCl. No antigen retrieval step was used for Satb2 staining. After at least five washes, the pH of the wash buffer was checked, and if normal the sections were moved to blocking solution (5% lamb serum in TBS + 0.1% Triton X-100). Sections were incubated overnight with primary antibodies diluted in blocking solution (with 3%, rather than 5% serum): rabbit anti-Cux1 (1:100, Santa Cruz Biotechnology, Inc, Santa Cruz, CA), Rabbit anti-Ctip2 (1:500, abcam), or rat anti-BrdU (1:1000, abcam). Sections were washed and then incubated for 2h in secondary antibody (1:2000 dilution; Cy2 or Cy3-conjugated donkey anti-rabbit or anti-rat; Jackson ImmunoResearch Laboratory, West Grove, PA). For DAB (diaminobenzidine) staining, sections were washed five times in TBS and then incubated for 2h in biotinylated secondary antibody (Jackson ImmunoResearch Laboratory, West Grove, PA) diluted (1:2000) in TBS – 0.1% Triton X-100 (TBST). After brief washes, sections were placed in ABC solution (1:500; Vector Laboratories, Burlingame, CA) for 1h, rinsed, and placed in DAB solution (Sigma, D4418) with nickel enhancement for visualization. Sections were counterstained with DAPI (142 nM, Sigma) or nuclear fast red (Vector Laboratories, Burlingame, CA) to visualize cell nuclei and mounted onto slides. Images were obtained using a PowerPhase digital camera (Phase-one, Coppenhagen, Denmark) or Fluoview v.5.0 software as part of

a Confocal Olympus BX61 imaging system (Melville, NY). Images were saved as *tiff* files and processed in Photoshop CS2.

Cresyl violet staining was performed as previously described (Bae et al., 2010). Sections were mounted on subbed slides and allowed to dry for a minimum of one hour. Slides were then incubated briefly in water, followed by five minutes in cresyl violet staining solution. Following staining, slides were incubated in 70% ethanol with acetic acid (3-4 drops in 250mL ethanol) for 5 minutes, then dehydrated through graded ethanol, cleared in xylenes, and cover-slipped with DPX mounting medium.

References

Abrahams BS, Geschwind DH (2008) Advances in autism genetics: on the threshold of a new neurobiology. Nature reviews Genetics 9:341-355.

Abrahams BS, Geschwind DH (2010) Connecting genes to brain in the autism spectrum disorders. Archives of Neurology 67:395-399.

Achim CL, Katyal S, Wiley CA, Shiratori M, Wang G, Oshika E, Petersen BE, Li JM, Michalopoulos GK (1997) Expression of HGF and cMet in the developing and adult brain. Brain research Developmental brain research 102:299-303.

Alcamo EA, Chirivella L, Dautzenberg M, Dobreva G, Farinas I, Grosschedl R, McConnell SK (2008) Satb2 regulates callosal projection neuron identity in the developing cerebral cortex. Neuron 57:364-377.

Alexander AL, Lee JE, Lazar M, Boudos R, DuBray MB, Oakes TR, Miller JN, Lu J, Jeong EK, McMahon WM, Bigler ED, Lainhart JE (2007) Diffusion tensor imaging of the corpus callosum in Autism. NeuroImage 34:61-73.

Amaral DG, Schumann CM, Nordahl CW (2008a) Neuroanatomy of autism. Trends in neurosciences 31:137-145.

Amaral DG, Schumann CM, Nordahl CW (2008b) Neuroanatomy of autism. Trends Neurosci 31:137-145.

Angevine JB, Jr., Sidman RL (1961) Autoradiographic study of cell migration during histogenesis of cerebral cortex in the mouse. Nature 192:766-768.

Anney R et al. (2012) Individual common variants exert weak effects on risk for Autism Spectrum Disorders. Hum Mol Genet.

APA (2000) Diagnostic and statistical manual of mental disorders DSM-IV-TR. Washington, DC: American Pyschiatric Association.

Arlotta P, Molyneaux BJ, Chen J, Inoue J, Kominami R, Macklis JD (2005) Neuronal subtype-specific genes that control corticospinal motor neuron development in vivo. Neuron 45:207-221.

Aylward EH, Minshew NJ, Field K, Sparks BF, Singh N (2002) Effects of age on brain volume and head circumference in autism. Neurology 59:175-183.

Aylward EH, Minshew NJ, Goldstein G, Honeycutt NA, Augustine AM, Yates KO, Barta PE, Pearlson GD (1999) MRI volumes of amygdala and hippocampus in non-mentally retarded autistic adolescents and adults. Neurology 53:2145-2150.

Bae MH, Bissonette GB, Mars WM, Michalopoulos GK, Achim CL, Depireux DA, Powell EM (2010) Hepatocyte growth factor (HGF) modulates GABAergic inhibition and seizure susceptibility. Experimental neurology 221:129-135.

Bailey A, Le Couteur A, Gottesman I, Bolton P, Simonoff E, Yuzda E, Rutter M (1995) Autism as a strongly genetic disorder: evidence from a British twin study. Psychological medicine 25:63-77.

Bailey DB, Jr., Hatton DD, Skinner M, Mesibov G (2001) Autistic behavior, FMR1 protein, and developmental trajectories in young males with fragile X syndrome. J Autism Dev Disord 31:165-174.

Bailey DB, Jr., Mesibov GB, Hatton DD, Clark RD, Roberts JE, Mayhew L (1998) Autistic behavior in young boys with fragile X syndrome. Journal of autism and developmental disorders 28:499-508.

Barnea-Goraly N, Kwon H, Menon V, Eliez S, Lotspeich L, Reiss AL (2004) White matter structure in autism: preliminary evidence from diffusion tensor imaging. Biol Psychiatry 55:323-326.

Bauman M, Kemper TL (1985) Histoanatomic observations of the brain in early infantile autism. Neurology 35:866-874.

Bauman ML (1991) Microscopic neuroanatomic abnormalities in autism. Pediatrics 87:791-796.

Ben Bashat D, Kronfeld-Duenias V, Zachor DA, Ekstein PM, Hendler T, Tarrasch R, Even A, Levy Y, Ben Sira L (2007) Accelerated maturation of white matter in young children with autism: a high b value DWI study. NeuroImage 37:40-47.

Benayed R, Gharani N, Rossman I, Mancuso V, Lazar G, Kamdar S, Bruse SE, Tischfield S, Smith BJ, Zimmerman RA, Dicicco-Bloom E, Brzustowicz LM, Millonig JH (2005) Support for the homeobox transcription factor gene ENGRAILED 2 as an autism spectrum disorder susceptibility locus. American journal of human genetics 77:851-868.

Birchmeier C, Gherardi E (1998) Developmental roles of HGF/SF and its receptor, the c-Met tyrosine kinase. Trends in cell biology 8:404-410.

Bissonette GB, Powell EM (2012) Reversal learning and attentional set-shifting in mice. Neuropharmacology 62:1168-1174.

Bissonette GB, Bae MH, Suresh T, Jaffe DE, Powell EM (2010) Astrocyte-mediated hepatocyte growth factor/scatter factor supplementation restores GABAergic interneurons and corrects reversal learning deficits in mice. The Journal of neuroscience : the official journal of the Society for Neuroscience 30:2918-2923.

Bissonette GB, Bae MH, Suresh T, Jaffe DE, Powell EM (2014) Prefrontal cognitive deficits in mice with altered cerebral cortical GABAergic interneurons. Behavioural brain research 259:143-151.

Bissonette GB, Martins GJ, Franz TM, Harper ES, Schoenbaum G, Powell EM (2008) Double dissociation of the effects of medial and orbital prefrontal cortical lesions on attentional and affective shifts in mice. The Journal of neuroscience : the official journal of the Society for Neuroscience 28:11124-11130.

Bladt F, Riethmacher D, Isenmann S, Aguzzi A, Birchmeier C (1995) Essential role for the c-met receptor in the migration of myogenic precursor cells into the limb bud. Nature 376:768-771.

Bonni A, Sun Y, Nadal-Vicens M, Bhatt A, Frank DA, Rozovsky I, Stahl N, Yancopoulos GD, Greenberg ME (1997) Regulation of gliogenesis in the central nervous system by the JAK-STAT signaling pathway. Science 278:477-483.

Borglum AD, Byskov A, Ragno P, Roldan AL, Tripputi P, Cassani G, Dano K, Blasi F, Bolund L, Kruse TA (1992) Assignment of the urokinase-type plasminogen activator receptor gene (PLAUR) to chromosome 19q13.1-q13.2. American journal of human genetics 50:492-497.

Bourin M, Hascoet M (2003) The mouse light/dark box test. European journal of pharmacology 463:55-65.

Brembeck FH, Schwarz-Romond T, Bakkers J, Wilhelm S, Hammerschmidt M, Birchmeier W (2004) Essential role of BCL9-2 in the switch between beta-catenin's adhesive and transcriptional functions. Genes & development 18:2225-2230.

Brown WT, Jenkins EC, Friedman E, Brooks J, Wisniewski K, Raguthu S, French J (1982) Autism is associated with the fragile-X syndrome. Journal of autism and developmental disorders 12:303-308.

Campbell DB, Li C, Sutcliffe JS, Persico AM, Levitt P (2008) Genetic evidence implicating multiple genes in the MET receptor tyrosine kinase pathway in autism spectrum disorder. Autism research : official journal of the International Society for Autism Research 1:159-168.

Campbell DB, Warren D, Sutcliffe JS, Lee EB, Levitt P (2010) Association of MET with social and communication phenotypes in individuals with autism spectrum disorder. American journal of medical genetics Part B, Neuropsychiatric genetics : the official publication of the International Society of Psychiatric Genetics 153B:438-446.

Campbell DB, D'Oronzio R, Garbett K, Ebert PJ, Mirnics K, Levitt P, Persico AM (2007a) Disruption of cerebral cortex MET signaling in autism spectrum disorder. Annals of neurology 62:243-250.

Campbell DB, D'Oronzio R, Garbett K, Ebert PJ, Mirnics K, Levitt P, Persico AM (2007b) Disruption of cerebral cortex MET signaling in autism spectrum disorder. Ann Neurol 62:243-250.

Campbell DB, Buie TM, Winter H, Bauman M, Sutcliffe JS, Perrin JM, Levitt P (2009) Distinct genetic risk based on association of MET in families with co-occurring autism and gastrointestinal conditions. Pediatrics 123:1018-1024.

Campbell DB, Sutcliffe JS, Ebert PJ, Militerni R, Bravaccio C, Trillo S, Elia M, Schneider C, Melmed R, Sacco R, Persico AM, Levitt P (2006) A genetic variant that disrupts MET transcription is associated with autism. Proceedings of the National Academy of Sciences of the United States of America 103:16834-16839.

Carola V, D'Olimpio F, Brunamonti E, Mangia F, Renzi P (2002) Evaluation of the elevated plus-maze and open-field tests for the assessment of anxiety-related behaviour in inbred mice. Behavioural brain research 134:49-57.

Carper RA, Moses P, Tigue ZD, Courchesne E (2002) Cerebral lobes in autism: early hyperplasia and abnormal age effects. NeuroImage 16:1038-1051.

Caton A, Hacker A, Naeem A, Livet J, Maina F, Bladt F, Klein R, Birchmeier C, Guthrie S (2000) The branchial arches and HGF are growth-promoting and chemoattractant for cranial motor axons. Development 127:1751-1766.

Caviness VS, Jr., Takahashi T, Nowakowski RS (1995) Numbers, time and neocortical neuronogenesis: a general developmental and evolutionary model. Trends in neurosciences 18:379-383.

Chenn A, Walsh CA (2002) Regulation of cerebral cortical size by control of cell cycle exit in neural precursors. Science 297:365-369.

Cheung C, Chua SE, Cheung V, Khong PL, Tai KS, Wong TK, Ho TP, McAlonan GM (2009) White matter fractional anisotrophy differences and correlates of diagnostic symptoms in autism. Journal of child psychology and psychiatry, and allied disciplines 50:1102-1112.

Choleris E, Thomas AW, Kavaliers M, Prato FS (2001) A detailed ethological analysis of the mouse open field test: effects of diazepam, chlordiazepoxide and an extremely low frequency pulsed magnetic field. Neuroscience and biobehavioral reviews 25:235-260.

Christmas AJ, Maxwell DR (1970) A comparison of the effects of some benzodiazepines and other drugs on aggressive and exploratory behaviour in mice and rats. Neuropharmacology 9:17-29.

Colasante G, Simonet JC, Calogero R, Crispi S, Sessa A, Cho G, Golden JA, Broccoli V (2013) ARX Regulates Cortical Intermediate Progenitor Cell Expansion and Upper Layer Neuron Formation Through Repression of Cdkn1c. Cerebral cortex.

Comi AM, Zimmerman AW, Frye VH, Law PA, Peeden JN (1999) Familial clustering of autoimmune disorders and evaluation of medical risk factors in autism. Journal of child neurology 14:388-394.

Connors SL, Crowell DE, Eberhart CG, Copeland J, Newschaffer CJ, Spence SJ, Zimmerman AW (2005) beta2-adrenergic receptor activation and genetic polymorphisms in autism: data from dizygotic twins. Journal of child neurology 20:876-884.

Courchesne E, Pierce K (2005) Why the frontal cortex in autism might be talking only to itself: local over-connectivity but long-distance disconnection. Current opinion in neurobiology 15:225-230.

Courchesne E, Campbell K, Solso S (2011) Brain growth across the life span in autism: age-specific changes in anatomical pathology. Brain Res 1380:138-145.

Crawley J, Goodwin FK (1980) Preliminary report of a simple animal behavior model for the anxiolytic effects of benzodiazepines. Pharmacology, biochemistry, and behavior 13:167-170.

Crawley JN (1981) Neuropharmacologic specificity of a simple animal model for the behavioral actions of benzodiazepines. Pharmacology, biochemistry, and behavior 15:695-699.

Croen LA, Connors SL, Matevia M, Qian Y, Newschaffer C, Zimmerman AW (2011) Prenatal exposure to beta2-adrenergic receptor agonists and risk of autism spectrum disorders. Journal of neurodevelopmental disorders 3:307-315.

David MD, Yeramian A, Dunach M, Llovera M, Canti C, de Herreros AG, Comella JX, Herreros J (2008) Signalling by neurotrophins and hepatocyte growth factor regulates axon morphogenesis by differential beta-catenin phosphorylation. Journal of cell science 121:2718-2730.

de Bruin EI, Ferdinand RF, Meester S, de Nijs PF, Verheij F (2007) High rates of psychiatric co-morbidity in PDD-NOS. Journal of autism and developmental disorders 37:877-886.

Dean M, Park M, Le Beau MM, Robins TS, Diaz MO, Rowley JD, Blair DG, Vande Woude GF (1985) The human met oncogene is related to the tyrosine kinase oncogenes. Nature 318:385-388.

Defrances MC, Wolf HK, Michalopoulos GK, Zarnegar R (1992) The presence of hepatocyte growth factor in the developing rat. Development 116:387-395.

Devan BD, Goad EH, Petri HL (1996) Dissociation of hippocampal and striatal contributions to spatial navigation in the water maze. Neurobiology of learning and memory 66:305-323.

Dewerchin M, Nuffelen AV, Wallays G, Bouche A, Moons L, Carmeliet P, Mulligan RC, Collen D (1996) Generation and characterization of urokinase receptor-deficient mice. J Clin Invest 97:870-878.

Di Martino A, Kelly C, Grzadzinski R, Zuo XN, Mennes M, Mairena MA, Lord C, Castellanos FX, Milham MP (2011) Aberrant Striatal Functional Connectivity in Children with Autism. Biological psychiatry 69:847-856.

Doyle-Thomas KA, Kushki A, Duerden EG, Taylor MJ, Lerch JP, Soorya LV, Wang AT, Fan J, Anagnostou E (2013) The effect of diagnosis, age, and symptom severity on cortical surface area in the cingulate cortex and insula in autism spectrum disorders. Journal of child neurology 28:732-739.

Duerden EG, Mak-Fan KM, Taylor MJ, Roberts SW (2012) Regional differences in grey and white matter in children and adults with autism spectrum disorders: an activation likelihood estimate (ALE) meta-analysis. Autism Res 5:49-66.

Durand CM et al. (2007) Mutations in the gene encoding the synaptic scaffolding protein SHANK3 are associated with autism spectrum disorders. Nature genetics 39:25-27.

Eagleson KL, Bonnin A, Levitt P (2005) Region- and age-specific deficits in gamma-aminobutyric acidergic neuron development in the telencephalon of the uPAR(-/-) mouse. The Journal of comparative neurology 489:449-466.

Ecker C, Suckling J, Deoni SC, Lombardo MV, Bullmore ET, Baron-Cohen S, Catani M, Jezzard P, Barnes A, Bailey AJ, Williams SC, Murphy DG, Consortium MA (2012) Brain anatomy and its relationship to behavior in adults with autism spectrum disorder: a multicenter magnetic resonance imaging study. Archives of general psychiatry 69:195-209.

Ellis V, Behrendt N, Dano K (1991) Plasminogen activation by receptor-bound urokinase. A kinetic study with both cell-associated and isolated receptor. The Journal of biological chemistry 266:12752-12758.

Esumi S, Kakazu N, Taguchi Y, Hirayama T, Sasaki A, Hirabayashi T, Koide T, Kitsukawa T, Hamada S, Yagi T (2005) Monoallelic yet combinatorial expression of variable exons of the protocadherin-alpha gene cluster in single neurons. Nature genetics 37:171-176.

Fame RM, MacDonald JL, Macklis JD (2011) Development, specification, and diversity of callosal projection neurons. Trends in neurosciences 34:41-50.

Fanselow MS, Dong HW (2010) Are the dorsal and ventral hippocampus functionally distinct structures? Neuron 65:7-19.

Ferland RJ, Cherry TJ, Preware PO, Morrisey EE, Walsh CA (2003) Characterization of Foxp2 and Foxp1 mRNA and protein in the developing and mature brain. The Journal of comparative neurology 460:266-279.

Folstein S, Rutter M (1977) Infantile autism: a genetic study of 21 twin pairs. Journal of child psychology and psychiatry, and allied disciplines 18:297-321.

Folstein SE, Rosen-Sheidley B (2001a) Genetics of autism: complex aetiology for a heterogeneous disorder. Nat Rev Genet 2:943-955.

Folstein SE, Rosen-Sheidley B (2001b) Genetics of autism: complex aetiology for a heterogeneous disorder. Nature reviews Genetics 2:943-955.

Freitag CM, Luders E, Hulst HE, Narr KL, Thompson PM, Toga AW, Krick C, Konrad C (2009) Total brain volume and corpus callosum size in medication-naive adolescents and young adults with autism spectrum disorder. Biol Psychiatry 66:316-319.

Fukuyama R, Ichijoh Y, Minoshima S, Kitamura N, Shimizu N (1991) Regional localization of the hepatocyte growth factor (HGF) gene to human chromosome 7 band q21.1. Genomics 11:410-415.

Garzotto D, Giacobini P, Crepaldi T, Fasolo A, De Marchis S (2008) Hepatocyte growth factor regulates migration of olfactory interneuron precursors in the rostral migratory stream through Met-Grb2 coupling. The Journal of neuroscience : the official journal of the Society for Neuroscience 28:5901-5909.

Geisert EE, Jr., Williams RW, Geisert GR, Fan L, Asbury AM, Maecker HT, Deng J, Levy S (2002) Increased brain size and glial cell number in CD81-null mice. The Journal of comparative neurology 453:22-32.

Gemelli T, Berton O, Nelson ED, Perrotti LI, Jaenisch R, Monteggia LM (2006) Postnatal loss of methyl-CpG binding protein 2 in the forebrain is sufficient to mediate behavioral aspects of Rett syndrome in mice. Biological psychiatry 59:468-476.

Giacobini P, Messina A, Wray S, Giampietro C, Crepaldi T, Carmeliet P, Fasolo A (2007) Hepatocyte growth factor acts as a motogen and guidance signal for gonadotropin hormone-releasing hormone-1 neuronal migration. The Journal of neuroscience : the official journal of the Society for Neuroscience 27:431-445.

Gibbard CR, Ren J, Seunarine KK, Clayden JD, Skuse DH, Clark CA (2013) White matter microstructure correlates with autism trait severity in a combined clinical-control sample of high-functioning adults. NeuroImage Clinical 3:106-114.

Girgis RR, Minshew NJ, Melhem NM, Nutche JJ, Keshavan MS, Hardan AY (2007) Volumetric alterations of the orbitofrontal cortex in autism. Progress in neuro-psychopharmacology & biological psychiatry 31:41-45.

Gorski JA, Balogh SA, Wehner JM, Jones KR (2003) Learning deficits in forebrain-restricted brain-derived neurotrophic factor mutant mice. Neuroscience 121:341-354.

Gorski JA, Talley T, Qiu M, Puelles L, Rubenstein JL, Jones KR (2002a) Cortical excitatory neurons and glia, but not GABAergic neurons, are produced in the Emx1-expressing lineage. The Journal of neuroscience : the official journal of the Society for Neuroscience 22:6309-6314.

Gorski JA, Talley T, Qiu M, Puelles L, Rubenstein JL, Jones KR (2002b) Cortical excitatory neurons and glia, but not GABAergic neurons, are produced in the Emx1-expressing lineage. The Journal of neuroscience : the official journal of the Society for Neuroscience 22:6309-6314.

Griswold AJ, Ma D, Cukier HN, Nations LD, Schmidt MA, Chung RH, Jaworski JM, Salyakina D, Konidari I, Whitehead PL, Wright HH, Abramson RK, Williams SM, Menon R, Martin ER, Haines JL, Gilbert JR, Cuccaro ML, Pericak-Vance MA (2012) Evaluation of copy number variations reveals novel candidate genes in autism spectrum disorder-associated pathways. Hum Mol Genet 21:3513-3523.

Groszer M, Erickson R, Scripture-Adams DD, Lesche R, Trumpp A, Zack JA, Kornblum HI, Liu X, Wu H (2001) Negative regulation of neural stem/progenitor cell proliferation by the Pten tumor suppressor gene in vivo. Science 294:2186-2189.

Guo H, Hong S, Jin XL, Chen RS, Avasthi PP, Tu YT, Ivanco TL, Li Y (2000a) Specificity and efficiency of Cre-mediated recombination in Emx1-Cre knock-in mice. Biochem Biophys Res Commun 273:661-665.

Guo HL, Hong SS, Jin XL, Chen RS, Avasthi PP, Tu YT, Ivanco TL, Li YQ (2000b) Specificity and efficiency of cre-mediated recombination in Emx1-Cre knock-in mice. Biochemical and biophysical research communications 273:661-665.

Gutierrez H, Dolcet X, Tolcos M, Davies A (2004) HGF regulates the development of cortical pyramidal dendrites. Development 131:3717-3726.

Gutknecht L (2001) Full-genome scans with autistic disorder: a review. Behav Genet 31:113-123.

Hallmayer J, Cleveland S, Torres A, Phillips J, Cohen B, Torigoe T, Miller J, Fedele A, Collins J, Smith K, Lotspeich L, Croen LA, Ozonoff S, Lajonchere C, Grether JK, Risch N (2011) Genetic heritability and shared environmental factors among twin pairs with autism. Arch Gen Psychiatry 68:1095-1102.

Hamanoue M, Takemoto N, Matsumoto K, Nakamura T, Nakajima K, Kohsaka S (1996a) Neurotrophic effect of hepatocyte growth factor on central nervous system neurons in vitro. Journal of neuroscience research 43:554-564.

Hamanoue M, Takemoto N, Matsumoto K, Nakamura T, Nakajima K, Kohsaka S (1996b) Neurotrophic effect of hepatocyte growth factor on central nervous system neurons in vitro. Journal of neuroscience research 43:554-564.

Hardan AY, Muddasani S, Vemulapalli M, Keshavan MS, Minshew NJ (2006) An MRI study of increased cortical thickness in autism. The American journal of psychiatry 163:1290-1292.

Hazlett HC, Poe MD, Gerig G, Smith RG, Piven J (2006a) Cortical gray and white brain tissue volume in adolescents and adults with autism. Biol Psychiatry 59:1-6.

Hazlett HC, Poe MD, Gerig G, Smith RG, Piven J (2006b) Cortical gray and white brain tissue volume in adolescents and adults with autism. Biological psychiatry 59:1-6.

Hazlett HC, Poe MD, Gerig G, Styner M, Chappell C, Smith RG, Vachet C, Piven J (2011a) Early brain overgrowth in autism associated with an increase in cortical surface area before age 2 years. Arch Gen Psychiatry 68:467-476.

Hazlett HC, Poe MD, Gerig G, Styner M, Chappell C, Smith RG, Vachet C, Piven J (2011b) Early brain overgrowth in autism associated with an increase in cortical surface area before age 2 years. Archives of general psychiatry 68:467-476.

Hedrick A, Lee Y, Wallace GL, Greenstein D, Clasen L, Giedd JN, Raznahan A (2012) Autism risk gene MET variation and cortical thickness in typically developing children and adolescents. Autism research : official journal of the International Society for Autism Research 5:434-439.

Herbert MR, Ziegler DA, Makris N, Filipek PA, Kemper TL, Normandin JJ, Sanders HA, Kennedy DN, Caviness VS, Jr. (2004) Localization of white matter volume increase in autism and developmental language disorder. Ann Neurol 55:530-540.

Herbert MR, Ziegler DA, Deutsch CK, O'Brien LM, Lange N, Bakardjiev A, Hodgson J, Adrien KT, Steele S, Makris N, Kennedy D, Harris GJ, Caviness VS, Jr. (2003) Dissociations of cerebral cortex, subcortical and cerebral white matter volumes in autistic boys. Brain : a journal of neurology 126:1182-1192.

Hiscox S, Jiang WG (1999) Hepatocyte growth factor/scatter factor disrupts epithelial tumour cell-cell adhesion: involvement of beta-catenin. Anticancer research 19:509-517.

Hogart A, Wu D, LaSalle JM, Schanen NC (2010) The comorbidity of autism with the genomic disorders of chromosome 15q11.2-q13. Neurobiology of disease 38:181-191.

Hollander E, Anagnostou E, Chaplin W, Esposito K, Haznedar MM, Licalzi E, Wasserman S, Soorya L, Buchsbaum M (2005) Striatal volume on magnetic resonance imaging and repetitive behaviors in autism. Biol Psychiatry 58:226-232.

Honda S, Kagoshima M, Wanaka A, Tohyama M, Matsumoto K, Nakamura T (1995) Localization and functional coupling of HGF and c-Met/HGF receptor in rat brain: implication as neurotrophic factor. Brain research Molecular brain research 32:197-210.

Huh CG, Factor VM, Sanchez A, Uchida K, Conner EA, Thorgeirsson SS (2004) Hepatocyte growth factor/c-met signaling pathway is required for efficient liver regeneration and repair. Proceedings of the National Academy of Sciences of the United States of America 101:4477-4482.

Hutcheson HB, Olson LM, Bradford Y, Folstein SE, Santangelo SL, Sutcliffe JS, Haines JL (2004) Examination of NRCAM, LRRN3, KIAA0716, and LAMB1 as autism candidate genes. BMC medical genetics 5:12.

IMGSAC (1998) A Full Genome Screen for Autism with Evidence for Linkage to a Region on Chromosome 7q. Human Molecular Genetics 7:571-578.

Ingram JL, Stodgell CJ, Hyman SL, Figlewicz DA, Weitkamp LR, Rodier PM (2000) Discovery of allelic variants of HOXA1 and HOXB1: genetic susceptibility to autism spectrum disorders. Teratology 62:393-405.

Iyer A, Kmiecik TE, Park M, Daar I, Blair D, Dunn KJ, Sutrave P, Ihle JN, Bodescot M, Vande Woude GF (1990) Structure, tissue-specific expression, and transforming activity of the mouse met protooncogene. Cell growth & differentiation : the molecular biology journal of the American Association for Cancer Research 1:87-95.

Jackson PB, Boccuto L, Skinner C, Collins JS, Neri G, Gurrieri F, Schwartz CE (2009) Further Evidence that the rs1858830 C Variant in the Promoter Region of the MET Gene is Associated with Autistic Disorder. Autism Research 2:232-236.

Jacobowitz DM, Abbott LC (1998) Chemoarchitectonic atlas of the developing mouse brain. Boca Raton: CRC Press.

Jamain S, Radyushkin K, Hammerschmidt K, Granon S, Boretius S, Varoqueaux F, Ramanantsoa N, Gallego J, Ronnenberg A, Winter D, Frahm J, Fischer J, Bourgeron T, Ehrenreich H, Brose N (2008) Reduced social interaction and ultrasonic communication in a mouse model of monogenic heritable autism. Proceedings of the National Academy of Sciences of the United States of America 105:1710-1715.

Judson MC, Amaral DG, Levitt P (2011) Conserved subcortical and divergent cortical expression of proteins encoded by orthologs of the autism risk gene MET. Cerebral cortex 21:1613-1626.

Judson MC, Eagleson KL, Wang L, Levitt P (2010a) Evidence of cell-nonautonomous changes in dendrite and dendritic spine morphology in the met-signaling-deficient mouse forebrain. The Journal of comparative neurology 518:4463-4478.

Judson MC, Eagleson KL, Wang L, Levitt P (2010b) Evidence of cell-nonautonomous changes in dendrite and dendritic spine morphology in the met-signaling-deficient mouse forebrain. The Journal of comparative neurology 518:4463-4478.

Judson MC, Bergman MY, Campbell DB, Eagleson KL, Levitt P (2009a) Dynamic gene and protein expression patterns of the autism-associated met receptor tyrosine kinase in the developing mouse forebrain. The Journal of comparative neurology 513:511-531.

Judson MC, Bergman MY, Campbell DB, Eagleson KL, Levitt P (2009b) Dynamic gene and protein expression patterns of the autism-associated met receptor tyrosine kinase in the developing mouse forebrain. J Comp Neurol 513:511-531.

Jung W, Castren E, Odenthal M, Vande Woude GF, Ishii T, Dienes HP, Lindholm D, Schirmacher P (1994) Expression and functional interaction of hepatocyte growth factor-scatter factor and its receptor c-met in mammalian brain. The Journal of cell biology 126:485-494.

Kanner L (1943) Autistic distrubances of affective contact. Nervous Child 2:217 - 250.

Kasai H, Matsuzaki M, Noguchi J, Yasumatsu N, Nakahara H (2003) Structure-stability-function relationships of dendritic spines. Trends in neurosciences 26:360-368.

Kash SF, Tecott LH, Hodge C, Baekkeskov S (1999) Increased anxiety and altered responses to anxiolytics in mice deficient in the 65-kDa isoform of glutamic acid decarboxylase. Proceedings of the National Academy of Sciences of the United States of America 96:1698-1703.

Kato M, Yoshimura S, Kokuzawa J, Kitajima H, Kaku Y, Iwama T, Shinoda J, Kunisada T, Sakai N (2004) Hepatocyte growth factor promotes neuronal differentiation of neural stem cells derived from embryonic stem cells. Neuroreport 15:5-8.

Kelly AM, Hester R, Murphy K, Javitt DC, Foxe JJ, Garavan H (2004) Prefrontal-subcortical dissociations underlying inhibitory control revealed by event-related fMRI. The European journal of neuroscience 19:3105-3112.

Kokuzawa J, Yoshimura S, Kitajima H, Shinoda J, Kaku Y, Iwama T, Morishita R, Shimazaki T, Okano H, Kunisada T, Sakai N (2003) Hepatocyte growth factor promotes proliferation and neuronal differentiation of neural stem cells from mouse embryos. Molecular and cellular neurosciences 24:190-197.

Land PW, Monaghan AP (2003) Expression of the transcription factor, tailless, is required for formation of superficial cortical layers. Cerebral cortex 13:921-931.

Langen M, Leemans A, Johnston P, Ecker C, Daly E, Murphy CM, Dell'Acqua F, Durston S, Murphy DGM, Consortium A (2012) Fronto-striatal circuitry and inhibitory control in autism: Findings from diffusion tensor imaging tractography. Cortex 48:183-193.

Lee SL, Dickson RB, Lin CY (2000) Activation of hepatocyte growth factor and urokinase/plasminogen activator by matriptase, an epithelial membrane serine protease. J Biol Chem 275:36720-36725.

Levitt P, Eagleson KL, Powell EM (2004) Regulation of neocortical interneuron development and the implications for neurodevelopmental disorders. Trends in neurosciences 27:400-406.

Lewis WW, Sahin M, Scherrer B, Peters JM, Suarez RO, Vogel-Farley VK, Jeste SS, Gregas MC, Prabhu SP, Nelson CA, 3rd, Warfield SK (2012a) Impaired Language Pathways in Tuberous Sclerosis Complex Patients with Autism Spectrum Disorders. In: Cerebral cortex, 2012/06/05 Edition.

Lewis WW, Sahin M, Scherrer B, Peters JM, Suarez RO, Vogel-Farley VK, Jeste SS, Gregas MC, Prabhu SP, Nelson CA, 3rd, Warfield SK (2012b) Impaired Language Pathways in Tuberous Sclerosis Complex Patients with Autism Spectrum Disorders. Cereb Cortex.

Lin MT, Huang KH, Huang CL, Huang YJ, Tsai GE, Lane HY (2012) MET and AKT genetic influence on facial emotion perception. PloS one 7:e36143.

Liou GI, Matragoon S, Samuel S, Behzadian MA, Tsai NT, Gu X, Roon P, Hunt DM, Hunt RC, Caldwell RB, Marcus DM (2002) MAP kinase and beta-catenin signaling in HGF induced RPE migration. Molecular vision 8:483-493.

Maina F, Klein R (1999) Hepatocyte growth factor, a versatile signal for developing neurons. Nature neuroscience 2:213-217.

Maina F, Hilton MC, Ponzetto C, Davies AM, Klein R (1997) Met receptor signaling is required for sensory nerve development and HGF promotes axonal growth and survival of sensory neurons. Genes & development 11:3341-3350.

Maina F, Hilton MC, Andres R, Wyatt S, Klein R, Davies AM (1998) Multiple roles for hepatocyte growth factor in sympathetic neuron development. Neuron 20:835-846.

Mairet-Coello G, Tury A, Van Buskirk E, Robinson K, Genestine M, DiCicco-Bloom E (2012) p57(KIP2) regulates radial glia and intermediate precursor cell cycle dynamics and lower layer neurogenesis in developing cerebral cortex. Development 139:475-487.

Marin O, Rubenstein JL (2003) Cell migration in the forebrain. Annual review of neuroscience 26:441-483.

Mars WM, Zarnegar R, Michalopoulos GK (1993) Activation of hepatocyte growth factor by the plasminogen activators uPA and tPA. Am J Pathol 143:949-958.

Martins GJ, Powell EM (2011) Genetic disruption of Met signaling impairs GABAergic striatal development and cognition. Neuroscience 176:199-209.

Martins GJ, Plachez C, Powell EM (2007) Loss of embryonic MET signaling alters profiles of hippocampal interneurons. Developmental neuroscience 29:143-158.

Martins GJ, Shahrokh M, Powell EM (2011) Genetic disruption of Met signaling impairs GABAergic striatal development and cognition. Neuroscience 176:199-209.

McFarlane HG, Kusek GK, Yang M, Phoenix JL, Bolivar VJ, Crawley JN (2008) Autism-like behavioral phenotypes in BTBR T+tf/J mice. Genes, brain, and behavior 7:152-163.

McSherry GM (1984) Mapping of cortical histogenesis in the ferret. Journal of embryology and experimental morphology 81:239-252.

McSherry GM, Smart IH (1986) Cell production gradients in the developing ferret isocortex. Journal of anatomy 144:1-14.

Menard C, Hein P, Paquin A, Savelson A, Yang XM, Lederfein D, Barnabe-Heider F, Mir AA, Sterneck E, Peterson AC, Johnson PF, Vinson C, Miller FD (2002) An essential role for a MEK-C/EBP pathway during growth factor-regulated cortical neurogenesis. Neuron 36:597-610.

Mines MA, Yuskaitis CJ, King MK, Beurel E, Jope RS (2010) GSK3 influences social preference and anxiety-related behaviors during social interaction in a mouse model of fragile X syndrome and autism. PloS one 5:e9706.

Mineur YS, Sluyter F, de Wit S, Oostra BA, Crusio WE (2002) Behavioral and neuroanatomical characterization of the Fmr1 knockout mouse. Hippocampus 12:39-46.

Mosconi MW, Kay M, D'Cruz AM, Seidenfeld A, Guter S, Stanford LD, Sweeney JA (2009) Impaired inhibitory control is associated with higher-order repetitive behaviors in autism spectrum disorders. Psychological medicine 39:1559-1566.

Mount RH, Charman T, Hastings RP, Reilly S, Cass H (2003) Features of autism in Rett syndrome and severe mental retardation. Journal of autism and developmental disorders 33:435-442.

Moy SS, Nadler JJ (2008) Advances in behavioral genetics: mouse models of autism. Molecular psychiatry 13:4-26.

Moy SS, Nadler JJ, Perez A, Barbaro RP, Johns JM, Magnuson TR, Piven J, Crawley JN (2004) Sociability and preference for social novelty in five inbred strains: an approach to assess autistic-like behavior in mice. Genes, brain, and behavior 3:287-302.

Mundy P (2003) Annotation: the neural basis of social impairments in autism: the role of the dorsal medial-frontal cortex and anterior cingulate system. Journal of child psychology and psychiatry, and allied disciplines 44:793-809.

Mutch CA, Schulte JD, Olson E, Chenn A (2010) Beta-catenin signaling negatively regulates intermediate progenitor population numbers in the developing cortex. PloS one 5:e12376.

Nadler JJ, Moy SS, Dold G, Trang D, Simmons N, Perez A, Young NB, Barbaro RP, Piven J, Magnuson TR, Crawley JN (2004) Automated apparatus for quantitation of social approach behaviors in mice. Genes, brain, and behavior 3:303-314.

Naldini L, Tamagnone L, Vigna E, Sachs M, Hartmann G, Birchmeier W, Daikuhara Y, Tsubouchi H, Blasi F, Comoglio PM (1992) Extracellular proteolytic cleavage by urokinase is required for activation of hepatocyte growth factor/scatter factor. The EMBO journal 11:4825-4833.

Naldini L, Weidner KM, Vigna E, Gaudino G, Bardelli A, Ponzetto C, Narsimhan RP, Hartmann G, Zarnegar R, Michalopoulos GK, et al. (1991) Scatter factor and hepatocyte growth factor are indistinguishable ligands for the MET receptor. EMBO J 10:2867-2878.

Nieto M, Monuki ES, Tang H, Imitola J, Haubst N, Khoury SJ, Cunningham J, Gotz M, Walsh CA (2004) Expression of Cux-1 and Cux-2 in the subventricular zone and upper layers II-IV of the cerebral cortex. The Journal of comparative neurology 479:168-180.

Niimura M, Takagi N, Takagi K, Funakoshi H, Nakamura T, Takeo S (2006) Effects of hepatocyte growth factor on phosphorylation of extracellular signal-regulated kinase and hippocampal cell death in rats with transient forebrain ischemia. Eur J Pharmacol 535:114-124.

Nowakowski RS, Lewin SB, Miller MW (1989) Bromodeoxyuridine immunohistochemical determination of the lengths of the cell cycle and the DNA-synthetic phase for an anatomically defined population. Journal of neurocytology 18:311-318.

Packard MG, Teather LA (1997) Double dissociation of hippocampal and dorsal-striatal memory systems by posttraining intracerebral injections of 2-amino-5-phosphonopentanoic acid. Behavioral neuroscience 111:543-551.

Paxinos G, Franklin KBJ (2001) The mouse brain in stereotaxic coordinates, 2nd Edition. San Diego: Academic Press.

Peca J, Feliciano C, Ting JT, Wang W, Wells MF, Venkatraman TN, Lascola CD, Fu Z, Feng G (2011) Shank3 mutant mice display autistic-like behaviours and striatal dysfunction. Nature 472:437-442.

Percy AK (2011) Rett syndrome: exploring the autism link. Arch Neurol 68:985-989.

Persico AM, Bourgeron T (2006) Searching for ways out of the autism maze: genetic, epigenetic and environmental clues. Trends in neurosciences 29:349-358.

Petit E, Herault J, Martineau J, Perrot A, Barthelemy C, Hameury L, Sauvage D, Lelord G, Muh JP (1995) Association study with two markers of a human homeogene in infantile autism. Journal of medical genetics 32:269-274.

Piven J (2001) The broad autism phenotype: a complementary strategy for molecular genetic studies of autism. American journal of medical genetics 105:34-35.

Piven J, Bailey J, Ranson BJ, Arndt S (1997) An MRI study of the corpus callosum in autism. The American journal of psychiatry 154:1051-1056.

Piven J, Arndt S, Bailey J, Havercamp S, Andreasen NC, Palmer P (1995a) An MRI study of brain size in autism. The American journal of psychiatry 152:1145-1149.

Piven J, Arndt S, Bailey J, Havercamp S, Andreasen NC, Palmer P (1995b) An MRI study of brain size in autism. The American journal of psychiatry 152:1145-1149.

Ponzetto C, Bardelli A, Zhen Z, Maina F, dalla Zonca P, Giordano S, Graziani A, Panayotou G, Comoglio PM (1994) A multifunctional docking site mediates signaling and transformation by the hepatocyte growth factor/scatter factor receptor family. Cell 77:261-271.

Powell EM, Mars WM, Levitt P (2001a) Hepatocyte growth factor/scatter factor is a motogen for interneurons migrating from the ventral to dorsal telencephalon. Neuron 30:79-89.

Powell EM, Mars WM, Levitt P (2001b) Hepatocyte growth factor/scatter factor is a motogen for interneurons migrating from the ventral to dorsal telencephalon. Neuron 30:79-89.

Powell EM, Muhlfriedel S, Bolz J, Levitt P (2003a) Differential regulation of thalamic and cortical axonal growth by hepatocyte growth factor/scatter factor. Developmental neuroscience 25:197-206.

Powell EM, Campbell DB, Stanwood GD, Davis C, Noebels JL, Levitt P (2003b) Genetic disruption of cortical interneuron development causes region- and GABA cell type-specific deficits, epilepsy, and behavioral dysfunction. The Journal of neuroscience : the official journal of the Society for Neuroscience 23:622-631.

Powell EM, Campbell DB, Stanwood GD, C. D, Noebels JL, Levitt P (2003c) Genetic disruption of cortical interneuron development causes region- and GABA cell type-specific deficits, epilepsy, and behavioral dysfunction. Journal of Neuroscience 23:622-631.

Prut L, Belzung C (2003) The open field as a paradigm to measure the effects of drugs on anxiety-like behaviors: a review. European journal of pharmacology 463:3-33.

Qian X, Shen Q, Goderie SK, He W, Capela A, Davis AA, Temple S (2000) Timing of CNS cell generation: a programmed sequence of neuron and glial cell production from isolated murine cortical stem cells. Neuron 28:69-80.

Qiu S, Anderson CT, Levitt P, Shepherd GM (2011a) Circuit-specific intracortical hyperconnectivity in mice with deletion of the autism-associated Met receptor tyrosine kinase. The Journal of neuroscience : the official journal of the Society for Neuroscience 31:5855-5864.

Qiu S, Anderson CT, Levitt P, Shepherd GM (2011b) Circuit-specific intracortical hyperconnectivity in mice with deletion of the autism-associated Met receptor tyrosine kinase. The Journal of neuroscience : the official journal of the Society for Neuroscience 31:5855-5864.

Raballo R, Rhee J, Lyn-Cook R, Leckman JF, Schwartz ML, Vaccarino FM (2000) Basic fibroblast growth factor (Fgf2) is necessary for cell proliferation and neurogenesis in the developing cerebral cortex. The Journal of neuroscience : the official journal of the Society for Neuroscience 20:5012-5023.

Rajan P, McKay RD (1998) Multiple routes to astrocytic differentiation in the CNS. The Journal of neuroscience : the official journal of the Society for Neuroscience 18:3620-3629.

Rakic P (1972) Mode of cell migration to the superficial layers of fetal monkey neocortex. The Journal of comparative neurology 145:61-83.

Rakic P (1988) Specification of cerebral cortical areas. Science 241:170-176.

Rash BG, Lim HD, Breunig JJ, Vaccarino FM (2011) FGF signaling expands embryonic cortical surface area by regulating Notch-dependent neurogenesis. The Journal of neuroscience : the official journal of the Society for Neuroscience 31:15604-15617.

Rash BG, Tomasi S, Lim HD, Suh CY, Vaccarino FM (2013) Cortical gyrification induced by fibroblast growth factor 2 in the mouse brain. The Journal of neuroscience : the official journal of the Society for Neuroscience 33:10802-10814.

Redcay E, Courchesne E (2005) When is the brain enlarged in autism? A meta-analysis of all brain size reports. Biol Psychiatry 58:1-9.

Regeur L, Pakkenberg B (1989) Optimizing sampling designs for volume measurements of components of human brain using a stereological method. J Microsc 155:113-121.

Rex A, Voigt JP, Voits M, Fink H (1998) Pharmacological evaluation of a modified open-field test sensitive to anxiolytic drugs. Pharmacology, biochemistry, and behavior 59:677-683.

Rojas DC, Peterson E, Winterrowd E, Reite ML, Rogers SJ, Tregellas JR (2006) Regional gray matter volumetric changes in autism associated with social and repetitive behavior symptoms. BMC psychiatry 6:56.

Roy K, Kuznicki K, Wu Q, Sun Z, Bock D, Schutz G, Vranich N, Monaghan AP (2004) The Tlx gene regulates the timing of neurogenesis in the cortex. The Journal of neuroscience : the official journal of the Society for Neuroscience 24:8333-8345.

Rubia K, Smith AB, Taylor E, Brammer M (2007) Linear age-correlated functional development of right inferior fronto-striato-cerebellar networks during response inhibition and anterior cingulate during error-related processes. Human brain mapping 28:1163-1177.

Rudie JD, Hernandez LM, Brown JA, Beck-Pancer D, Colich NL, Gorrindo P, Thompson PM, Geschwind DH, Bookheimer SY, Levitt P, Dapretto M (2012) Autism-associated promoter variant in MET impacts functional and structural brain networks. Neuron 75:904-915.

Sauvageot CM, Stiles CD (2002) Molecular mechanisms controlling cortical gliogenesis. Current opinion in neurobiology 12:244-249.

Schanen NC (2006) Epigenetics of autism spectrum disorders. Hum Mol Genet 15 Spec No 2:R138-150.

Schmidt C, Bladt F, Goedecke S, Brinkmann V, Zschiesche W, Sharpe M, Gherardi E, Birchmeier C (1995) Scatter factor/hepatocyte growth factor is essential for liver development. Nature 373:699-702.

Schumann CM, Hamstra J, Goodlin-Jones BL, Lotspeich LJ, Kwon H, Buonocore MH, Lammers CR, Reiss AL, Amaral DG (2004a) The amygdala is enlarged in children but not adolescents with autism; the hippocampus is enlarged at all ages. The Journal of neuroscience : the official journal of the Society for Neuroscience 24:6392-6401.

Schumann CM, Hamstra J, Goodlin-Jones BL, Lotspeich LJ, Kwon H, Buonocore MH, Lammers CR, Reiss AL, Amaral DG (2004b) The amygdala is enlarged in children but not adolescents with autism; the hippocampus is enlarged at all ages. The Journal of neuroscience : the official journal of the Society for Neuroscience 24:6392-6401.

Sears LL, Vest C, Mohamed S, Bailey J, Ranson BJ, Piven J (1999a) An MRI study of the basal ganglia in autism. Progress in neuro-psychopharmacology & biological psychiatry 23:613-624.

Sears LL, Vest C, Mohamed S, Bailey J, Ranson BJ, Piven J (1999b) An MRI study of the basal ganglia in autism. Progress in neuro-psychopharmacology & biological psychiatry 23:613-624.

Seeds NW, Basham ME, Haffke SP (1999) Neuronal migration is retarded in mice lacking the tissue plasminogen activator gene. Proc Natl Acad Sci U S A 96:14118-14123.

Segarra J, Balenci L, Drenth T, Maina F, Lamballe F (2006) Combined signaling through ERK, PI3K/AKT, and RAC1/p38 is required for met-triggered cortical neuron migration. The Journal of biological chemistry 281:4771-4778.

Shimomura T, Miyazawa K, Komiyama Y, Hiraoka H, Naka D, Morimoto Y, Kitamura N (1995) Activation of hepatocyte growth factor by two homologous proteases, blood-coagulation factor XIIa and hepatocyte growth factor activator. Eur J Biochem 229:257-261.

Simon P, Dupuis R, Costentin J (1994) Thigmotaxis as an index of anxiety in mice. Influence of dopaminergic transmissions. Behavioural brain research 61:59-64.

Simonoff E, Pickles A, Charman T, Chandler S, Loucas T, Baird G (2008) Psychiatric disorders in children with autism spectrum disorders: prevalence, comorbidity, and associated factors in a population-derived sample. Journal of the American Academy of Child and Adolescent Psychiatry 47:921-929.

Smalley SL, Tanguay PE, Smith M, Gutierrez G (1992) Autism and tuberous sclerosis. J Autism Dev Disord 22:339-355.

Smith JM, Xu J, Powell EM (2012) Age dependent forebrain structural changes in mice deficient in the autism associated gene Met tyrosine kinase. Neuroimage: Clinical 1:66 - 74.

Sousa I, Clark TG, Toma C, Kobayashi K, Choma M, Holt R, Sykes NH, Lamb JA, Bailey AJ, Battaglia A, Maestrini E, Monaco AP (2009a) MET and autism susceptibility: family and case-control studies. European journal of human genetics : EJHG 17:749-758.

Sousa I, Clark TG, Toma C, Kobayashi K, Choma M, Holt R, Sykes NH, Lamb JA, Bailey AJ, Battaglia A, Maestrini E, Monaco AP, International Molecular Genetic Study of Autism C (2009b) MET and autism susceptibility: family and case-control studies. European journal of human genetics : EJHG 17:749-758.

Spencer CM, Alekseyenko O, Serysheva E, Yuva-Paylor LA, Paylor R (2005) Altered anxiety-related and social behaviors in the Fmr1 knockout mouse model of fragile X syndrome. Genes, brain, and behavior 4:420-430.

Spruston N (2008) Pyramidal neurons: dendritic structure and synaptic integration. Nature reviews Neuroscience 9:206-221.

Stigler KA, McDonald BC, Anand A, Saykin AJ, McDougle CJ (2011) Structural and functional magnetic resonance imaging of autism spectrum disorders. Brain Res 1380:146-161.

Stoltenberg C, Schjolberg S, Bresnahan M, Hornig M, Hirtz D, Dahl C, Lie KK, Reichborn-Kjennerud T, Schreuder P, Alsaker E, Oyen AS, Magnus P, Suren P, Susser E, Lipkin WI (2010) The Autism Birth Cohort: a paradigm for gene-environment-timing research. Mol Psychiatry 15:676-680.

Straussman R, Morikawa T, Shee K, Barzily-Rokni M, Qian ZR, Du J, Davis A, Mongare MM, Gould J, Frederick DT, Cooper ZA, Chapman PB, Solit DB, Ribas A, Lo RS, Flaherty KT, Ogino S, Wargo JA, Golub TR (2012) Tumour micro-environment elicits innate resistance to RAF inhibitors through HGF secretion. Nature 487:500-504.

Sun W, Funakoshi H, Nakamura T (2002) Localization and functional role of hepatocyte growth factor (HGF) and its receptor c-met in the rat developing cerebral cortex. Brain research Molecular brain research 103:36-48.

Takahashi T, Goto T, Miyama S, Nowakowski RS, Caviness VS, Jr. (1999) Sequence of neuron origin and neocortical laminar fate: relation to cell cycle of origin in the developing murine cerebral wall. The Journal of neuroscience : the official journal of the Society for Neuroscience 19:10357-10371.

Tassone F, Qi L, Zhang W, Hansen RL, Pessah IN, Hertz-Picciotto I (2011) MAOA, DBH, and SLC6A4 variants in CHARGE: a case-control study of autism spectrum disorders. Autism Res 4:250-261.

Thanseem I et al. (2010a) Further evidence for the role of MET in autism susceptibility. Neuroscience research 68:137-141.

Thanseem I et al. (2010b) Further evidence for the role of MET in autism susceptibility. Neurosci Res 68:137-141.

Tiberi L, Vanderhaeghen P, van den Ameele J (2012) Cortical neurogenesis and morphogens: diversity of cues, sources and functions. Current opinion in cell biology 24:269-276.

Toro R, Konyukh M, Delorme R, Leblond C, Chaste P, Fauchereau F, Coleman M, Leboyer M, Gillberg C, Bourgeron T (2010) Key role for gene dosage and synaptic homeostasis in autism spectrum disorders. Trends in genetics : TIG 26:363-372.

Trusolino L, Comoglio PM (2002) Scatter-factor and semaphorin receptors: cell signalling for invasive growth. Nat Rev Cancer 2:289-300.

Tsatsanis KD, Rourke BP, Klin A, Volkmar FR, Cicchetti D, Schultz RT (2003a) Reduced thalamic volume in high-functioning individuals with autism. Biol Psychiatry 53:121-129.

Tsatsanis KD, Rourke BP, Klin A, Volkmar FR, Cicchetti D, Schultz RT (2003b) Reduced thalamic volume in high-functioning individuals with autism. Biological psychiatry 53:121-129.

Turner KC, Frost L, Linsenbardt D, McIlroy JR, Muller RA (2006) Atypically diffuse functional connectivity between caudate nuclei and cerebral cortex in autism. Behavioral and brain functions : BBF 2:34.

Turner M (1999) Annotation: Repetitive behaviour in autism: a review of psychological research. Journal of child psychology and psychiatry, and allied disciplines 40:839-849.

Uehara Y, Minowa O, Mori C, Shiota K, Kuno J, Noda T, Kitamura N (1995) Placental defect and embryonic lethality in mice lacking hepatocyte growth factor/scatter factor. Nature 373:702-705.

Vaccarino FM, Schwartz ML, Raballo R, Nilsen J, Rhee J, Zhou M, Doetschman T, Coffin JD, Wyland JJ, Hung YT (1999) Changes in cerebral cortex size are governed by fibroblast growth factor during embryogenesis. Nature neuroscience 2:848.

Veltman MW, Craig EE, Bolton PF (2005) Autism spectrum disorders in Prader-Willi and Angelman syndromes: a systematic review. Psychiatric genetics 15:243-254.

Vorhees CV, Williams MT (2006) Morris water maze: procedures for assessing spatial and related forms of learning and memory. Nature protocols 1:848-858.

Walsh RN, Cummins RA (1976) The Open-Field Test: a critical review. Psychological bulletin 83:482-504.

Wassink TH, Piven J, Vieland VJ, Huang J, Swiderski RE, Pietila J, Braun T, Beck G, Folstein SE, Haines JL, Sheffield VC (2001) Evidence supporting WNT2 as an autism susceptibility gene. American journal of medical genetics 105:406-413.

White SW, Oswald D, Ollendick T, Scahill L (2009) Anxiety in children and adolescents with autism spectrum disorders. Clinical psychology review 29:216-229.

Williams EL, Casanova MF (2011) Above genetics: lessons from cerebral development in autism. Transl Neurosci 2:106-120.

Wu SX, Goebbels S, Nakamura K, Nakamura K, Kometani K, Minato N, Kaneko T, Nave KA, Tamamaki N (2005) Pyramidal neurons of upper cortical layers generated by NEX-positive progenitor cells in the subventricular zone.

Proceedings of the National Academy of Sciences of the United States of America 102:17172-17177.

Yamada T, Yoshiyama Y, Tsuboi Y, Shimomura T (1997) Astroglial expression of hepatocyte growth factor and hepatocyte growth factor activator in human brain tissues. Brain Res 762:251-255.

Zeng G, Apte U, Micsenyi A, Bell A, Monga SP (2006) Tyrosine residues 654 and 670 in beta-catenin are crucial in regulation of Met-beta-catenin interactions. Experimental cell research 312:3620-3630.

Zhou X, Xu Y, Wang J, Zhou H, Liu X, Ayub Q, Wang X, Tyler-Smith C, Wu L, Xue Y (2011) Replication of the association of a MET variant with autism in a Chinese Han population. PloS one 6:e27428.

Zimmer C, Tiveron MC, Bodmer R, Cremer H (2004) Dynamics of Cux2 expression suggests that an early pool of SVZ precursors is fated to become upper cortical layer neurons. Cerebral cortex 14:1408-1420.